4-15-2014

Operational Actual Wetland Evapotranspiration Estimation for South Florida Using MODIS Imagery

Cristobal N. Ceron
Florida International University, ccero001@fiu.edu

DOI: 10.25148/etd.FI14071129

FLORIDA INTERNATIONAL UNIVERSITY

Miami, Florida

OPERATIONAL ACTUAL WETLAND EVAPOTRANSPIRATION ESTIMATION FOR SOUTH FLORIDA USING MODIS IMAGERY

A thesis submitted in partial fulfillment of

the requirements for the degree of

MASTER OF SCIENCE

in

GEOSCIENCE

by

Cristobal Ceron

2014

To: Dean Kenneth G. Furton
College of Arts and Sciences

This thesis, written by Cristobal Ceron, and entitled OPERATIONAL ACTUAL WETLAND EVAPOTRANSPIRATION ESTIMATION FOR SOUTH FLORIDA USING MODIS IMAGERY, having been approved in respect to style and intellectual content, is referred to you for judgment.

We have read this thesis and recommend that it be approved.

Pete Markowitz

Dean Whitman

René Price, Co-Major Professor

Assefa Melesse, Co-Major Professor

Date of Defense: April 15, 2014

The thesis of Cristobal Ceron is approved.

Dean Kenneth G. Furton
College of Arts and Sciences

Dean Lakshmi N. Reddi
University Graduate School

Florida International University, 2014

DEDICATION

To my Mom, Sister, Brother, and Father. Love you guys.

ACKNOWLEDGMENTS

I would like to thank Dr. Assefa Melesse for giving me the opportunity to explore a new area of science and for his valuable advice and guidance. I would also like to thank Dr. René Price and Dr. Dean Whitman for taking the time to be part of my committee and for the support and advice they have provided. Also, thanks go out to Dr. Pete Markowitz for his many years of help and support.

I would also like to include my lab mates Hari Kandel and Shimelis Behailu for the many tips and tricks they shared which saved me days of work. Finally, I benefited from the help and support of Priscilla Pamela, Luis Lebolo, Vashti Sawtell, and Seth Manthey. Thank you guys for being so smart.

ABSTRACT OF THE THESIS

OPERATIONAL ACTUAL WETLAND EVAPOTRANSPIRATION ESTIMATION FOR SOUTH FLORIDA USING MODIS IMAGERY

by

Cristobal Ceron

Florida International University, 2014

Miami, Florida

Professor Assefa Melesse, Major Professor

The purpose of this study is to validate the ability of the Simplified Surface Energy Balance (SSEB) approach and the Simple Method to provide AET estimates for wetland recovery efforts. The study utilizes the MODIS sensor aboard NASA's Terra satellite and SFWMD solar radiation data to derive AET values for South Florida. The SSEB/Simple-Method approach provided mixed results with good agreement with control values during dry season (r_{ave} (59) = 0.700, $p_{ave} < 0.0005$) and poor agreement during wet season (r_{ave}(46) = 0.137, $p_{ave} = 0.304$). Further refinement is needed to make this method viable for yearly estimates due to the poor performance during wet season months. This approach can prove useful for short term wetland recovery assessment projects that occur during the dry season and/or long term projects that compare AET rates from a site from dry season to dry season.

TABLE OF CONTENTS

LIST OF TABLES

LIST OF FIGURES

FIGURE PAGE

ABBREVIATIONS AND ACRONYMS

AET	Actual Evapotranspiration
EC	Eddy Covariance
ET	Evapotranspiration
Et_f	Evapotranpiration fraction
EC	Eddy Covariance
GIS	Geographic Information System
LST	Land Surface Temperature
MODIS	Moderate Resolution Imaging Spectroradiometer
PET	Potential Evapotranspiration
SF	South Florida
SFWMD	South Florida Water Management District
SSEB	Simplified Surface Energy Balance
WRD	Water Resource Development Act

CHAPTER 1: INTRODUCTION

1.1. Motivation and Background

Wetlands provide a wide range of services and benefits to a region. They provide erosion protection to coastlines and sediment control for large areas (Maltby, 2009). They provide extensive habitat for a wide range of wildlife including nursery habitats for numerous fish and shellfish species and breeding, nursing, and migratory habitat for large number of waterbirds (Aber, 2012). Furthermore, wetlands provide a welcoming environment for many species of reptiles, amphibians, some mammals, and a myriad of insect and plant species (Lepage, 2009; Maltby, 2009, Aber, 2012). Wetlands act as a giant filter cleaning both natural and man-made waste from the local water supply, help recharge aquifers, and provide drinking water for many communities across the world (Aber, 2012; Lepage, 2011). Finally, wetlands can be ideal sites for recreational activities such as camping, fishing, and hunting and for educational and scientific study (Abtew, 2013).

Unfortunately, some of the very characteristics that make wetlands so unique, diverse, and beneficial have also contributed to the destruction of many wetland areas. By their very nature, wetlands have a propensity to flood. Over the years, many wetlands have been drained or seen their water sources diverted in order to stop or control the flooding of developed (or soon to be developed) areas (Abtew, 2013; Maltby, 2009). Similarly, many wetlands have been drained in order to take advantage of the rich soils created in a wetland environment. The drained areas are replaced with agricultural fields or grazing land for livestock (Mitsch, 2000; Abtew, 2013). Wetlands that are not directly developed still suffer from effects of urban and agricultural development. Polluted runoff from agricultural and urban areas can “poison” wetlands, affecting the natural chemistry of these areas (Maltby, 2009). Many of these problems currently affect one of the largest wetland environments in the world: South Florida's Everglades National Park.

Figure 1.1. Average annual net loss and gain of wetland acreage for U.S. from 1950 to 2009. Source: U.S Fish and Wildlife Service. Image taken from Dahl, 2009.

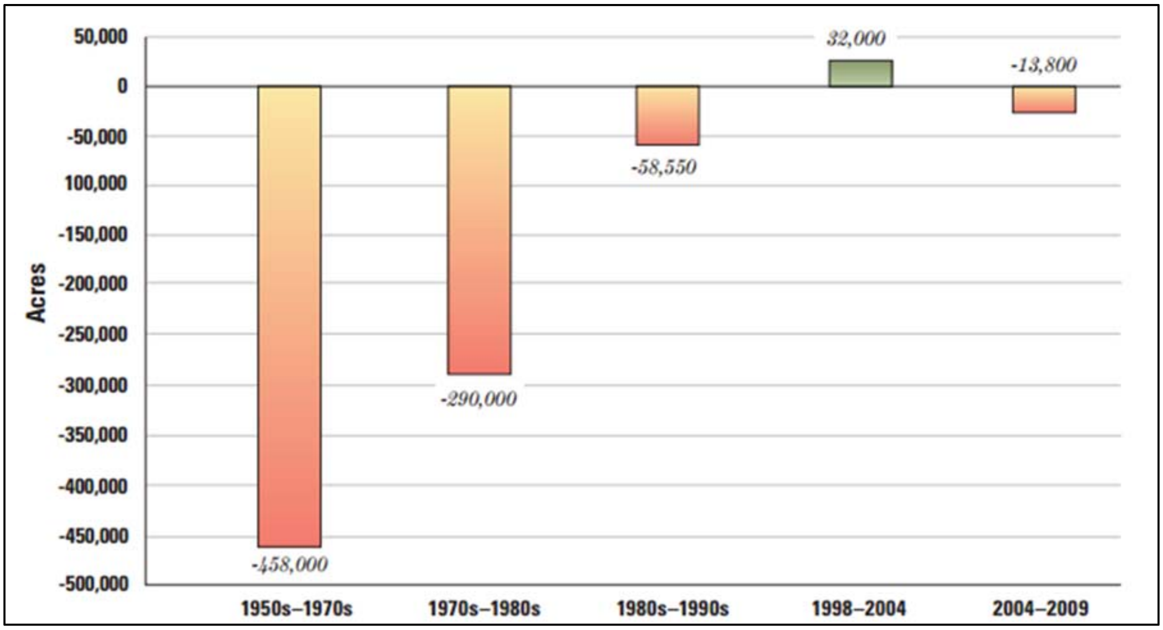

1.2. Study Area: South Florida

Loss of wetlands is a worldwide problem and the U.S. has experienced major losses in recent history (Figure 1.1). It is estimated that during the late part of the 20^{th} century, the US was losing wetlands at the rate of 60,000 acres per year (Davis, 2013). Fortunately, concerted conservation and remediation efforts have helped slow down the loss of wetland environments. South Florida offers a perfect microcosm of the threats faced by the world's wetlands and the efforts being made to protect these unique ecosystems from disappearing. The South Florida area is dominated by three major ecosystems: natural, agricultural, and urban (Fig. 1.2). The eastern edge of South Florida is covered mostly by urban sprawl

Figure 1.2. Map of the South Florida Region. Wikimedia Commons, http://en.wikipedia.org/wiki/File:Evergladesareamap.png

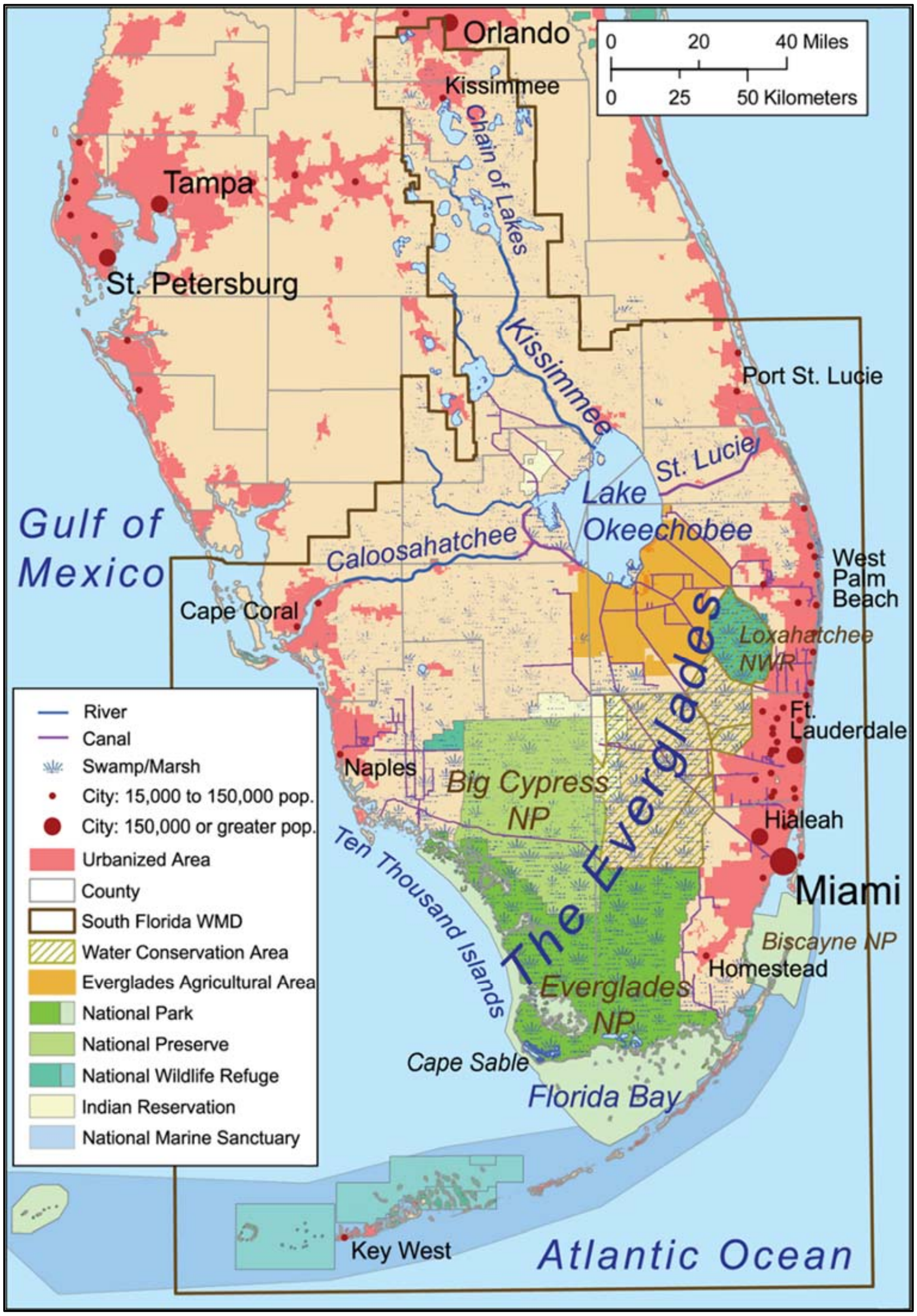

which is in close proximity to extensive natural areas to the west and south. These natural areas include Everglades National Park, Big Cypress National Preserve, Biscayne National Park, and many smaller wild wetland areas. Also, agricultural lands are scattered across the South Florida landscape, the most significant of which is the Everglades agricultural areas near and around the southern edge of Lake Okeechobee. The interactions between these three closely linked ecological systems are of major interest to scientists and researchers looking to better understand the nature of wetlands and looking to design wetland restoration and conservation plans that balance the needs of people with those of nature. South Florida offers the perfect natural laboratory to explore wetland science and wetland restoration methods.

Unsurprisingly, decades of urban and agricultural development have severely altered the hydrology and ecology of the South Florida region, including those of the aforementioned Florida Everglades, one of the largest wetland ecosystems in the world (Abtew, 1996). Canals and other waterways divert most of the natural water flow for the sake of flood control, crop irrigation, and urbanization projects. To combat the negative effects this development has had on this wetland ecosystem, Florida approved the Water Resource Development Act (WRDA) in 2000. The act contains within it the Comprehensive Everglades Restoration Plan (CERP), which aims to capture water that now flows unused to the ocean and to redirect it to wetland areas in need of new water flow (U.S. Army Corps of Engineers, 2013).

The CERP is a massive restoration undertaking covering 16 Central and South Florida counties. It is composed of more than 60 individual elements, it is expected to take

30 years to complete, and has an estimated price tag of about 9.5 billion dollars (U.S. Army Corps of Engineers, 2013). The CERP aims to enhance both the ecologic and economic values of the South Florida area by increasing the size of natural areas, improving the habitat, abundance, and diversity of native plant and animal species, and improving the hydrological regime of wetland areas. Although this large and complex project often demands complex and nuanced solutions from many scientific and non-scientific disciplines, the driving idea of the whole restoration program is a simple one: Restore the historic water flow (Fig. 1.3). So, as the CERP outlines, the first step to wetland restoration is to add water. In fact, hydrology is the most important factor influencing the success of a wetland restoration (Clewell, 1989) and understanding hydrologic processes of wetlands is key in their effective restoration (Mitsch, 2000).

Figure 1.3. Past, Present, and Future Water Flow through the South Florida Region.

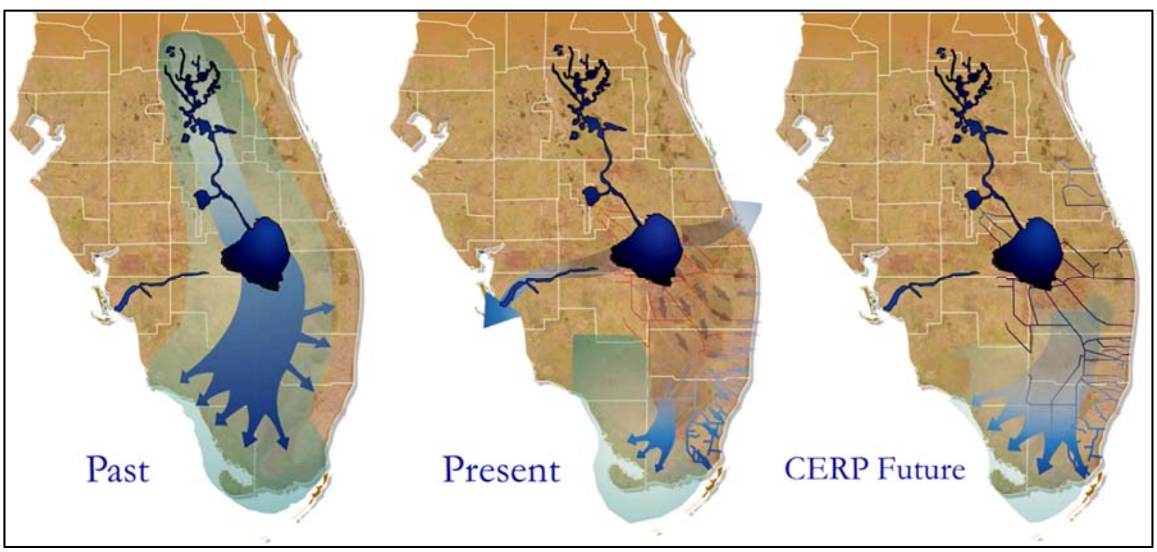

Figure 1.4. The Water Cycle. Evapotranspiration is just one of many ways water is transported. U.S. Geological Survey http://ga.water.usgs.gov/edu/watercycle.html

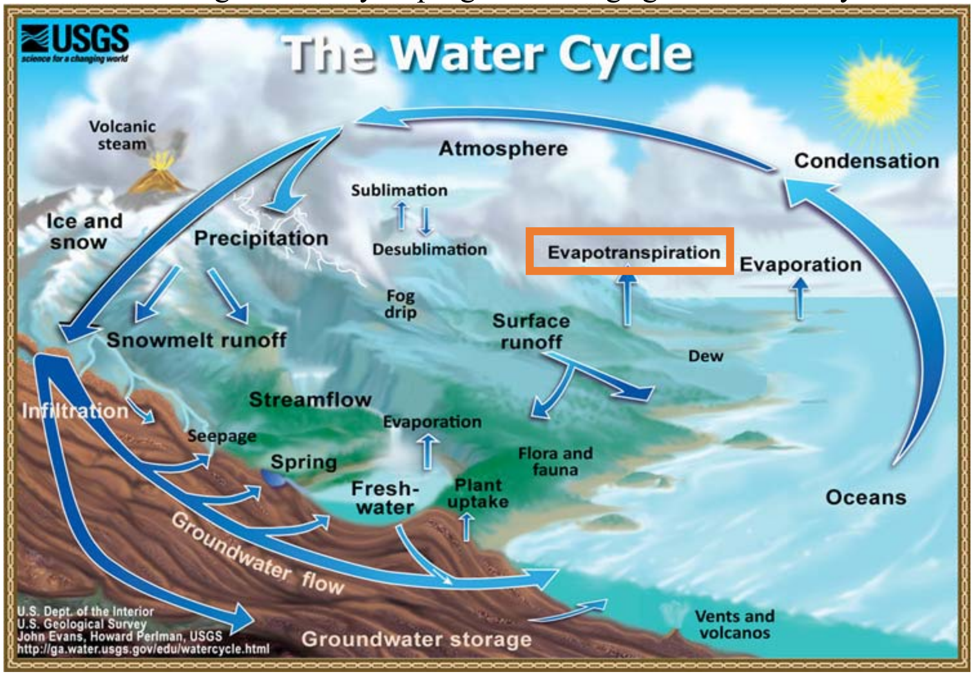

1.3. Evapotranspiration as an Indicator of Wetland Recovery.

With many restoration efforts now underway, the question becomes how to assess the success of the restoration methods being used. Again, water provides a solution. Water has a direct impact on the ecosystem dynamics of wetlands and hydrologic variables such as hydroperiod, flow velocity, flow duration, flow variability, and evapotranspiration provide a glimpse at the wetland's health (Gurnell et al., 2000; Price et al., 2000; Jansen, 2004). Of these hydrological "vital signs", evapotranspiration (ET) proves an important indicator of hydrological recovery (Oberg, 2005). Evapotranspiration is the combined measurement of water being lost to the atmosphere as a result of evaporation from open water sources and transpiration from plants. In general ET is only one of many components of the water cycle (Fig. 1.4) but it is one of the principle methods of water transport in

South Florida wetlands. For example, the Everglades experiences a yearly rainfall of around 50 inches and an estimated yearly ET total of about 40 inches (German, 2000). So, a large portion of the water received by the Everglades through precipitation is returned to the atmosphere through evapotranspiration and measuring these rates can provide a glimpse at the workings of healthy wetland ecosystems.

The reasoning behind how ET can serve as an indicator of wetland recovery is relatively simple. A healthy wetland area will be fully or partially inundated for most of the year. The water will provide the necessary conditions for wetland flora to grow and thrive. The combination of above-surface water and healthy plant population will result in high rates of both evaporation and transpiration (high ET). Now, an unhealthy wetland area will be dry for most, if not all, of the year. The lack of the necessary flooding needed to maintain a healthy wetland ecosystem will prevent the growth of native flora. The lack of above-surface water and healthy plant population results in low evaporation and transpiration rates (low ET). Hence, measuring the ET rates of a treated wetland and comparing them to the ET rates of healthy wetlands can provide a measure of how well the treated wetland is recovering. Furthermore, studying ET rates over prolonged periods of time can give information on the speed and efficiency of the restoration techniques applied at a given site. So, ET can be an important measure of wetland health, the question now becomes what technique is best suited for measuring ET rates for the South Florida region.

1.4. Measuring ET.

The two most basic methods for finding ET are based on mass conservation and energy conservation. The mass conservation approach,-more commonly referred to as the "water balance" approach in the literature, uses the terrestrial water cycle to derive a water conservation equation. The equation states that water coming into the system as precipitation can leave the system through rivers, evapotranspiration, or remain in the system stored underground or in above ground reservoirs.

$$P - E - Q - \frac{dw}{dt} = 0 \tag{1.1}$$

Where P is precipitation, E is evapotranspiration, Q is surface runoff, and dw/dt is the change of terrestrial water storage (Wang and Dickingson, 2012). Precipitation includes both rain and snow and can be measured using rain gauges or satellite imagery. Surface runoff refers to the water flowing into rivers and/or streams and then out of the system. Q can be measured using stream gauges. Water storage refers to water that seeps into the ground and it is stored in aquifers or stays above ground stored in lakes and/or reservoirs. Water storage change is difficult to measure and for an annual time scale dw/dt is often assumed to equal 0. For shorter time scales, measuring slight variations of the Earth's gravitational field can provide estimates of dw/dt (Tapley et al., 2004a, 2004b). With values for P, Q, and dw/dt the equation is solved to obtain an estimate of evapotranspiration.

The energy conservation method defines the source of incoming energy into a natural system and how this energy is used within the system. Evaporation (as well as transpiration) is the phase change of water from liquid to gas, which takes a certain amount of energy to occur. It stands to reason then that the amount of evapotranspiration will depend on the amount of energy available to transform water to water vapor. The question then becomes what are the sources of energy and how is this energy used by a natural (wetland, prairie, grassland, etc…) system. The answer comes in the form of the following energy conservation equation:

$$R_n - H - G - \lambda E = 0 \tag{1.2}$$

Where Rn is net radiation, H is sensible heat flux, G is soil heat flux, and λE is latent heat flux (Abtew, 2013). The variable Rn is the only source of incoming energy and it is the difference between incoming and outgoing shortwave radiation added to the difference between the incoming and outgoing long-wave radiation. The sensible heat flux, H, is the energy that goes into heating up the atmosphere above the land surface. Soil heat flux, G, is the energy that is absorbed by the ground causing the soil to warm up. Lastly, sensible heat flux, λE, is the energy that powers the phase change of water from liquid to gas. This phase change occurs without a temperature change, so sensible heat does not contribute to atmospheric temperature changes above the land surface. The sensible heat flux term consists of two values: The latent heat of vaporization (λ) and evapotranspiration (E). Hence, evapotranspiration can be calculated using eq. 2, if Rn, H, and G are known. What distinguishes many energy-balance methods from one another is how these three variables are computed.

Aside from the two major methods described above, there are more direct methods that rely on specialized equipment to provide an estimate of ET. These methods include Lysimetry, pan-evaporation, scintillometry,and eddy covariance (EC) (Abtew, 2013). Detailed descriptions of these methods are discussed further in the Literature Review section of this thesis. The aforementioned techniques work best for relatively small study areas. The equipment used for these methods is expensive and work best with regular upkeep and maintenance, hence, they quickly become inconvenient when studying large areas (i.e., South Florida). Similarly, mass and energy conservation techniques also become less convenient as the size of the study area increases since larger sets of data (i.e., more sensors) are needed to account for the inputs and outputs of each conservation equation. Fortunately, Et can also be effectively calculated through satellite imaging techniques (Melesse et al., 2006, 2007). The importance and value of satellite imagery lies in its accessibility, which allows for ET studies of large and/or inaccessible areas. The purpose of the present study is to evaluate an ET measuring method that relies on satellite imagery to cover a large study area. The methodology is described in detail in the next section.

1.5. The Simple Method and the Simplified Surface Energy Balance Equation.

The study will calculate weekly Actual Evapotranspiration (AET) values using a combination of methodologies that have not been used in tandem before. Actual evapotranspiration (AET) is a measurement of the true amount of water being evapotranspirated by an area of land (the term evapotranspiration often refers to AET, although it can also refer to potential and/or reference evapotranspiration). It is given by the following equation:

$$AET = (Et_f)(PET) \tag{1.3}$$

Where PET stands for Potential Evapotranspiration and Et_f is the evapotranspiration fraction. Potential evapotranspiration is an estimate of the maximum possible amount of water that can evapotranspirate from an area (similar to what potential energy represents in an energy system). Evapotranspiration fraction (Etf) is a factor which estimates what portion of the total available water will actually evapotranspire. The variable Etf can be calculated in many ways, and can include factors such as surface temperature, atmospheric pressure, wind speed, and humidity as inputs.

For the current study, two methods -one for calculating PET and the other for calculating Etf- will be used together for the first time to provide AET estimates for the South Florida region. Potential evapotranspiration (PET) is calculated using the Simple Abtew model (Abtew, 1996), also called the "Simple Method". The Abtew model was developed using lysimeter measurements of open water evaporation and of wetland evapotranspiration in the South Florida region. Through his study Abtew found that, in South Florida, evaporation from shallow lakes, evapotranspiration from wetlands, and potential evaporation occur at very similar rates (Abtew, 1996). This means most of the available water is being evapotranspirated as opposed to leaving the system through other means. With this in mind, Abtew proposed a simple equation relating the potential Et (which in this case would be close to actual Et) to solar radiation, Rn. The equations is as follows:

$$PET = K_1 \frac{R_s}{\lambda} \tag{1.4}$$

Where Rs is solar radiation, λ is the latent heat of vaporization, and K_1 is a calibration coefficient equal to 0.53 for the South Florida region.

The value of Etf is calculated using the Simplified Surface Energy Balance Method (SSEB) equation (Senay et al. 2007). The SSEB is derived from a more complex model called SEBAL (Bastiaanssen et al. 1998a, b, 2005) which uses energy conservation arguments to estimate evapotranspiration rates. Although the technical aspects of the model are complex, the underlying ideas guiding the SSEB model are not. The SSEB model utilizes surface temperature measurements to calculate the ET fraction. It assumes that areas with high surface temperature will have low ET rates (low ET fraction value), and that areas with low surface temperature will experience high ET rates (high ET fraction values). The idea here is that when incoming solar radiation energy hits a dry, poorly vegetated area most of that energy goes into heating up the ground and atmospheric layer right above the ground (the H and G terms in the energy conservation equation). The energy then raises the overall temperature of that area. On the other hand, when incoming solar radiation hits a wet, vegetated area, a large portion of the energy goes into latent heat, that is, powering the phase change from water to water vapor (the λE term in the energy conservation equation). Since phase changes occur without an increase in temperature, these wet areas remain relatively cool. The SSEB uses remotely sensed temperature values (i.e. temperatures gathered by satellite sensors) to calculate ET fraction. The SSEB equation states:

$$Et_f = \frac{(T_h - T_x)}{(T_h - T_c)} \tag{1.5}$$

Where T_h and T_c are the average hottest and average coldest temperatures, respectively, of a land surface temperature (LST) image provided by satellite mounted spectroradiometer. The value of T_x is the LST value for an area of interest within the satellite image ("scene").

The SSEB model equation for ETf relies on satellite LST data which for this study is provided by the Moderate Resolution Imaging Spectroradiometer (MODIS) onboard NASA's TERRA satellite (Fig. 1.5). The TERRA satellite circles the Earth on a sun synchronous polar orbit that travels from North Pole to South Pole every 99 minutes. This allows MODIS to image Earth's entire surface every one to two days. The MODIS instrument uses 36 spectral bands to image the Earth at resolutions of 250, 500, and 1000 meters, providing information on cloud/aerosol properties, ocean phytoplankton densities, surface and cloud temperature, among other atmospheric, land, and ocean surface phenomena. The preset study, MODIS provides the necessary spatial and temporal dimensions needed to estimate weekly evapotranspiration rates across the expansive South Florida Region.

1.6. Research Questions, Hypothesis, and Goals.

The main goal of my Master's project is to validate a model that will provide weekly Actual Evapotranspiration estimates for the South Florida region using the "Simple Method" technique in combination with an SSEB remote sensing methodology. In the process, my study will produce actual evapotranspiration estimates and maps for the South Florida region with a focus on wetland areas in and around Everglades National Park and Big Cypress National Preserve.

Hence, the current project aims to aid future restoration assessment studies by providing a simple and accessible method of calculating Et values. More specifically, this Master's project will attempt to answer the following research questions:

Question 1. Is the SSEB/Simple Method approach applicable for the Everglades study area?

By “applicable” it is meant that this procedure is not severely limited by the geography or any other variable associated to the study site that is not yet accounted for.

Question 2. Is the SSEB/Simple Method approach useful for the Everglades study area? By “useful”, it is meant that the procedure will provide comparable results to those obtained by more standard methods (Florida Water Management Data) while still maintaining its simplicity and ease of use.

Question 3. How many meteorological stations are sufficient to provide accurate evapotranspiration values for the Everglades study area?

Hypothesis 1. Surface Temperature and solar radiation are sufficient variables to accurately calculate Actual Et values for the Everglades study area.

Hypothesis 2. The Actual Et values derived from the SSEB approach will have a significant correlation to the values provided by the South Florida Water Management district, with a correlation coefficient (R) above 0.7.

Hypothesis 3. A total of nine weather stations will provide enough solar radiation data to calculate accurate Actual Et values for the Everglades study site.

Goal 1. Create actual spatial ET maps for the study area on a weekly timeframe.

Ideally, this procedure will be automated as much as possible, hence providing a reliable and easily accessible source for obtaining ET maps.

Goal 2. Create a template for applications to similar study sites.

The template will include procedural information as well as the GIS tools needed to carry out the analysis. Because of the remote sensing aspect of this method, this template may prove of great benefit for remote study areas that, unlike the Everglades study area, do not have the benefit of weather stations located nearby.

CHAPTER 2: LITERATURE REVIEW

2.1. Wetlands Dynamics and Hydrology

A broad review of wetland ecosystem dynamics, wetland hydrology, and wetland restoration and managing techniques was carried out to attain a good foundation of the overlying science and themes inspiring this study (Maltby, 2009; Lepage, 2011; Abers, 2012). These general overviews on wetland properties provide various definitions of what characterizes a wetland. Definitions may change from country to country and even from region to region and institution to institution. Although varied, all definitions share a similarity succinctly expressed by the American Environmental Protection Agency definition of a wetland (Wetland Definitions, 2013):

“[wetlands are] those areas that are inundated or saturated by surface or groundwater at a frequency and duration sufficient to support, and that under normal circumstances do support, a prevalence of vegetation typically adapted for life in saturated soil conditions. Wetlands generally include swamps, marshes, bogs and similar areas."

Wetlands can be further categorized by factors such as climate, hydrogeomorphology, hydroperiod, and water chemistry, among other factors (Arthington, 2012), but in general they share the quality of being covered by water for prolonged periods of time. Stating the importance of water to the well-being of wetlands seems obvious (and it is), yet the ways hydrological variables affect wetland ecology are varied and sometimes much more nuanced than assumed. It is known that hydrological variables such as water flow velocity, flow duration, flow variability, hydroperiod, and evapotranspiration play important roles in the ecosystem dynamics of wetlands (Cole and Brooks, 2000; Gurnell et al., 2000; Price et al., 2000; Melesse et al. 2006, 2007). Water impacts several major aspects of wetland health including soil composition (Faulkner, 1989; Venterink, 2002), vegetation cover (van der Valk, 1994; Todd, 2010; Cooper, 2012), and wildlife diversity (Bunn, 2002; Davidson, 2012; Konar, 2013). Clearly, hydrological factors affect every major ecological aspect of wetlands.

The great influence that hydrology has on wetland ecosystems makes it one of the most important factors influencing wetland restoration (Clewell, 1989; Mitsch, 2000). Although wetland restoration must include expertise from many different fields and consider numerous factors (Maltby, 2009; Abers, 2012; Zedler, 2000), examples of the importance of hydrological factors on wetland recovery are numerous (Bendix, 2000; Wassen, 2006; Money, 2009) and apply to wetlands across the world (Turner, 1997; Bedford, 1999; Acreman, 2007; Cowdery 2008). The importance of hydrological variables to wetland health makes the ability to accurately measure these variables crucial to restoration efforts. As mentioned before, many different hydrological variables contribute to the overall hydrological scheme of a wetland. My study focuses on one of these variables, evapotranspiration (ET), which is the amount of water lost to the atmosphere as a result of both evaporation from open water sources and transpiration from plants. Evapotranspiration has shown to be an important indicator of wetland hydrological and vegetation recovery (Oberg, 2005; Melesse et al. 2006, 2007; Abtew, 2013). Furthering evapotranspiration's appeal as a measure of wetland health and recovery, satellite imagery techniques allow for ET collection of large wetland areas (Melesse et al. 2006, 2007). The inclusion of remote sensing tools means that ET can be used to provide a picture of how well large scale wetland recovery efforts are progressing without the need for large networks of ground-based sensors collecting the necessary data.

2.2. ET Calculation Methods

Having established evapotranspiration as the variable of interest of the present study, a concerted effort to understand past and present methods of calculating ET was carried out. It is an understatement to say that there are many ways to calculate ET. Good overviews of the many methods for finding evapotranspiration are provided in Allen (2011), Fisher (2011), and Abtew (2013). Evapotranspiration can be measured directly or indirectly. Pan evaporation, lysimetry, and eddy covariance (EC) were the most common and most often utilized direct methods of finding ET. Pan evaporation, which consists of measuring the water level in a standard sized container over a set period of time (i.e., daily) and calculating how much of the depth change is due to evaporation (Abtew et al. 2011; Shuttleworth, 1993). Lysimetry, which uses an instrument (i.e., lysimeter) that recreates a small section of the surrounding environment and measures the water mass-balance of that section. Mass changes of the tank are attributed to gains from precipitation, losses from infiltration (water flowing out the bottom of the tank), and evapotranspiration. Precipitation and infiltration are measured and used to solve for ET (Abtew, 2013). Lysimeters have been used for calibrating and validating other ET models (Makkink, 1957; Allen et al., 1989) as well as developing new models (Abtew, 1996). Eddy Covariance (EC) is a technique that relies on the correlation between the vertical motion of vapor and the circular motion of wind above the land surface (Abtew, 2013). The wind's circular motion, referred to as eddies, transports vapor towards or away from the land surface, impeding of facilitating the ET rate from the ground (Wang and Dickingson, 2012). Eddy covarience has been used to test, validate, and develop ET models (Mu, 2011; Glenn, 2011; Douglas, 2009), over large study areas (Jia, 2012; Liu, 2012) including global models (Miralles, 2010; Mu, 2007).

Although pan evaporation, lysimmetry, and EC systems are routinely used to validate and develop ET models, these methods utilize ground-sited instrumentation that is often expensive and difficult to use for large scale studies at the regional level. These limitations can be overcome by utilizing models that rely on empirical, measured, or modeled data to indirectly calculate ET (Courault, 2005; Taconet, 1985, Enku, 2011). The models can be loosely placed in three categories: Temperature-based models, radiation-based models, and energy-balance models. Temperature-based models assume mean air temperature in the most influential variable affecting ET. The relative ease by which temperature can be measured is one of the main reasons for utilizing these models (Xu and Sighn, 2001). Solar radiation models assume that ET is most influenced by solar radiation. Much like temperature, solar radiation data are easy to collect and widely available, making solar radiation models an attractive option for finding ET. Energy balance models estimate ET by solving the energy-balance equation (Eq. 1.2). The models attempt to account for all the physical factors that influence evapotranspiration. These factors include solar radiation, temperature, wind speed and direction, vapor pressure, atmospheric density, aerodynamic resistance, canopy resistance, stomatal conductance of plants, leaf area index, soil moisture, soil composition, among many others (Abtew, 2013; Allen, 2011). What usually differentiates one model from the next is the choice of factors used to solve for Rn, G, and H (Eq. 1.2). Examples of these models include SEBAL (Bastiaanssen, 1998a,b), METRIC (Allen, 2007), and the Penman Method (Abtew, 2013). The models have been tested over a wide range of ecosystems and been validated using more direct ET measuring techniques such as EC measurements (Bastiaanssen, 1998b; Douglas, 2009; Serrat-Capdevila, 2011; Timmermans, 2007). Out of the myriad of methods available for calculating ET, two are of special interest in this study: Abtew's "Simple" Method and the Simplified Surface Energy (SSEB) method.

2.3. Abtew's Simple Model and the SSEB

Abtew's "Simple" Method is a radiation-based model. The Abtew method had been tested against other solar-radiation models (Xiu and Singh, 2000), compared to evaporation methods (Delclaux and Coudrain, 2005), and used in rainfall-runoff models (i.e., mass conservation) (Oudin et al., 2005). Throughout these studies the Abtew model has shown comparable results to more standard methods. More recently, the model has been used to estimate evaporation from Lake Ziway in the Ethiopian Rift valley, providing estimates close to those produced through energy conservation models (Melesse et al., 2009). The Abtew model has also been used to estimate ET for the Ganzu Province in Northwest China (Zhai, 2010) and the Fogera flood plain in Ethiopia (Enku, 2011). For both these sites, the Abtew method provided satisfactory results when the constant coefficient was calibrated for each study site.

The SSEB method was developed to monitor and assess the performance of irrigated agriculture in Afghanistan (Senay et al., 2007). The model assumes that the temperature difference between land surface and near-surface air varies linearly with land surface temperature, an idea first used by the SEBAL model and also applied to the METRIC model (Senay et al., 2007). The SSEB model further assumes that this difference between land surface temperature and near-surface air temperature is linearly related to soil moisture (Senay et al., 2007). Soil moisture is linearly related to evapotranspiration (Senay, 2003; Allen, 1998), hence ET can be estimated using the near-surface temperature difference between land and air. The SSEB method has been tested against METRIC and shown to be applicable on a wide range of topographical regions (Senay, 2011). Furthermore, the SSEB method has been used as a base for more refined models (Savoca, 2013; Senay, 2013) that compare well to eddy covariance measurements.

One of the key elements that make the SSEB method so useful for this study is its utilization of satellite image for data input. Utilizing land surface temperature (LST) data from satellite sensors allows for coverage of large study areas like the South Florida region. Remote sensing techniques, such as LST imaging by satellite sensors, have been widely used to calculate ET rates (Courault, 2005; Immerzeel, 2007; Kustas, 1997). Regional scale ET studies (Glenn, 2011; Price, 1990; Jia, 2012) and global scale ET studies (Miralles, 2010; Wang, 2008) have been carried out using various satellite based measurements. The current study uses the Moderate Resolution Imaging Spectroradiometer (MODIS) onboard NASA's Terra satellite to collect LST data. MODIS LST products have been used for both regional studies (Cammalleri, 2012; Enku 2011) as well as global (Mu, 2007) ET studies. The MODIS LST data have also been validated using ground truthing (Tang, 2010; Wan, 2008; Coll, 2009). NASA's Land Processes Distributed Active Archive Center (LP DAAC) processes, archives, and distributes all MODIS data and provided all LST data used in this study. The LP DAAC's website, https://lpdaac.usgs.gov/, contains further technical information on the technical aspects of MODIS data.

CHAPTER 3: METHODOLOGY

3.1. Evapotranspiration Fraction (Etf) Calculation.

The Etf calculation process begins with the acquisition of MODIS Land Surface temperature (LST) and emissivity 8-day data. The MODIS data can be downloaded from several sources available through: https://lpdaac.usgs.gov/data_access. The MODIS sensor collects raw digital signals which are used to calculate reflectance and Earth-exiting radiance (Various, 2012). LST data is calculated using the radiance data (MOD021KM) in combination with, geolocation data (MOD03), atmospheric temperature and water profile data (MOD07_L2), cloud mask data (MOD35_L2), and land-cover ((MOD12Q1) and snow cover data (MOD10_L2) (Wan, 2006). The MOD11A2 products use 8 daily 1-km LST products (MOD11A1) to create the average of clear sky LST's for 8-day periods. In order to be classified as "clear sky" an image or pixel must pass several tests which look for signs of cloud cover. The details of the "clear sky" validation process are given by Ackerman, 2010. The data outputted by the MODIS sensor are projected onto a sinusoidal grid of "tiles" composed of 36 columns and 18 rows. The study area is located on tile (10, 6), where the first number corresponds to the column and the second to the row of the grid. Figure 3.1 shows the grid system and a sample unedited LST image if the study area. Images from January 1, 2008 to December 31, 2010 were downloaded using the bulk download tool provided by the USGS site (http://earthexplorer.usgs.gov/bulk/help). There are 46 images per year, bringing the total number of images to 138.

The MODIS MOD11A2 data sets provide an 8-day clear day/night average of LST and emissivity values as well as several quality assurance layers. A single product (i.e. image) consists of 12 layers.

Figure 3.1. SIN Grid and MOD11A2 Image.

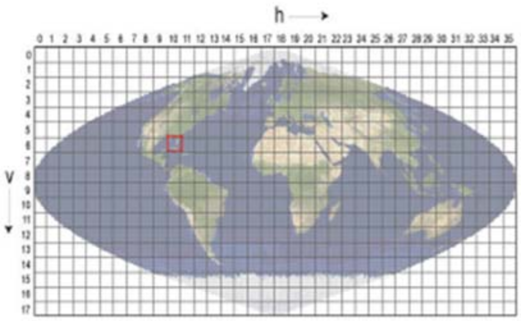

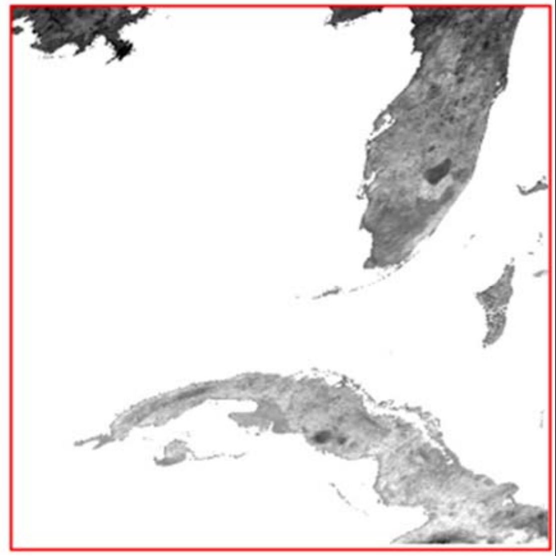

Above: Sinusoidal grid used by for MOD11A2 LST data. The grid is made up of 36 columns numbered 0-35 on the horizontal (h) axis and 18 rows numbered 0-17 on the vertical (v) axis. The tile used for this study is highlighted in red and has the coordinates (10,6). Right: Unedited MOD11A2 LST image product (also referred to as a "granule"). The image contains parts of Cuba, the Caribbean Islands, Louisiana, Northern Florida, and all of Central and South Florida.

Sinusoidal Grid image courtesy of the Land Processes Distributed Active Archive Center (LP DAAC).

Each layer is made up by 0.93 km x 0.93 km pixels and each pixel contains a single number value whose meaning depends on the layer being studied. For example, each pixel in layer 1 provides a temperature in Kelvin and each pixel in layer 3 provides a time in hours. A detailed description of each layer's content is depicted in Table 3.1. Once downloaded, the images are then loaded into ArcGis10 software for processing. The process that follows is all done within ArcMap 10 and uses the tools and resources provided by this program.

Obtaining a workable image of the study area takes several steps. First, the 8-day daytime 1km LST layer (layer 1) is extracted from the full product using the "Extract Subdataset" tool in ArcToolbox. The LST layer is then re-projected to the more useful geographical coordinate system

Table 3.1. MOD11A2 Image Layer Information. LP DAAC, https://lpdaac.usgs.gov/products/modis_products_table/mod11a2

Data Layer Name	Units	Value Range	Scale Factor
LST_Day_1km: 8-Day daytime 1km grid land surface temperature	Kelvin	7500–65535	0.02
QC_Day: Quality control for daytime LST and emissivity	Bit Field	0–255	na
Day_view_time: Average time of daytime land surface temperature observation	Hours	0–240	0.1
Day_view_angle: Average view zenith angle of daytime land surface temperature	Degree	0–130	1 (-65)
LST_Night_1km: 8-Day nighttime 1km grid land surface temperature	Kelvin	7500–65535	0.02
QC_Night: Quality control for nighttime LST and emissivity	Bit Field	0–255	na
Night_view_time: Average time of nighttime land surface temperature observation	Hours	0 – 240	0.1
Night_view_angle: Average view zenith angle of nighttime land surface temperature	Degree	0–130	1 (-65)
Emis_31: Band 31 Emissivity	none	1–255	0.0020 (+0.49)
Emis_32: Band 32 Emissivity	none	1–255	0.0020 (+0.49)
Clear_sky_days: the days in clear sky conditions and with valid LSTs	None	1–255	na
Clear_sky_nights: the nights in clear sky conditions and with valid LSTs	None	1–255	na

"NAD_1983_HARN_StatePlane_Florida_East_FIPS_0901" from its original sinusoidal projection using the "Project Raster" tool on ArcToolbox. The new projection uses units of meters, keeps the original pixel size of 926.63 m by 926.63 m, and it is used for all of the maps created in this study. A more detailed look at the projection is given in Table 3.2.

Once projected, the image is clipped to include only the South Florida region using the "Extract by Mask" tool on ArcToolbox. At this point, the pixel values can be converted from degrees Kelvin to degrees Fahrenheit using the following equation:

$$^{o}F = [\tfrac{9}{5}(.02 * {}^{o}K_s - 273) + 32] \tag{3.1}$$

Where Ks is the temperature in Kelvin given in each pixel and 0.02 is a scale factor needed to convert the pixel temperature to true surface temperature in Kelvin.

Table 3.2. Analysis Projection Details.

Spatial Reference	NAD_1983_HARN_StatePlane_Florida_East_FIPS_0901
Linear Unit	Meter (1.0)
Angular Unit	Degree (0.0175)
False Easting	200,000
False Northing	0
Central Meridian	-81
Scale Factor	0.999941
Latitude of Origin	24.3
Datum	D_North_American_1983_HARN

The unit conversion process is not necessary since only the ratio of temperatures is needed to create the Etf maps for each 8-day period.

The image is now ready to be used for the Etf calculation using the SSEB equation. High temperature (T_h) and low temperature (T_c) benchmarks are needed for the calculation but extreme temperature values that may not be representative of the average highest or average lowest temperatures must be avoided (i.e., outliers). To minimize the effect of these extreme values on the Etf calculation, each pixel temperature value is averaged with the values of the surrounding 8 pixels (a 3x3 pixel area) using the "Focal Statistics" tool in ArcToolbox. Fig. 3.2 shows a visual representation of the "focal statistics" averaging procedure.

Figure 3.2: Focal Statistics Averaging Method.

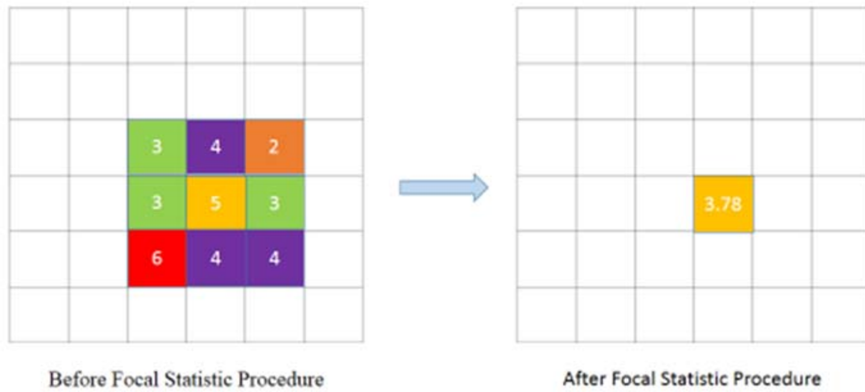

The "Focal Statistics" tool in ArcMap takes the average of a 3x3 pixel area and replaces the value of the center pixel with the calculated value. The calculation for the example above is: (3+3+6+4+5+4+2+3+4)/9 = 3.78. The process goes pixel by pixel, ensuring that each pixel in the image will be averaged with its surrounding 8 pixels.

A new layer is created where the new, average temperatures replace the original temperature values. A corresponding T_h and T_c value is extracted from this new image layer using the "Get Raster Properties" tool from ArcToolbox. The SSEB equation is now applied to the previous un-averaged image pixel by pixel using the "Map Algebra" tool in ArcToolbox:

$$Etf_x = \frac{T_h - T_x}{T_h - T_c} \tag{3.2}$$

Where T_h and T_c are extracted from the average temperature layer and T_x represents each individual pixel on the temperature layer created previous to the averaging step. The resulting temperature layer may have values greater than one or less than zero, which correspond to temperature values higher than the average high temperature and lower than the average low temperature. These values usually correspond to outlier pixels and are dealt with by converting negative values to Etf = 0 (no evapotranspiration from that pixel) and converting values over one to Etf = 1 (Pixels evapotranspirate at PET rates). The process of replacing outlier values is also done with the “Map Algebra” tool. The final layer is composed of individual pixels that contain Etf values between 0 and 1. A diagram showing the process of creating Etf maps is given in Figure 3.3 and a list of ArcMap tools used in the analysis (with directions on how to find them in the ArcMap program) is given in Table 3.3. Etf maps were created for all 130 8-day periods.

3.2. Potential Evapotranspiration (PET) Calculation.

Solar radiation data were downloaded from the South Florida Water Management DBHYDRO online database (http://xportal.sfwmd.gov/dbhydroplsql/show_dbkey_info.main_menu). The data are located under the “Hydrological and Physical” data section of the database and categorized as part of the “meteorological” datasets. The data were found using the “data type” search parameter “Total Solar Radiation” and ordered by “station”. A total of 15 stations were chosen for this study (Table 3.4). The stations were chosen in order to cover a significant portion of the study site and to provide a long enough data record to extend from 2008 to 2010, the time period for which control data is available. Solar radiation data for these stations are available as instant (30 min interval) values or as a daily mean solar radiation value in units of KW/m^2. For the current study, the mean values were used. Daily mean solar radiation data were downloaded for the 15 sites for the period of January 1, 2008 to December 31, 2010.

Figure 3.3. Diagram of the Etf Map Creation Process..

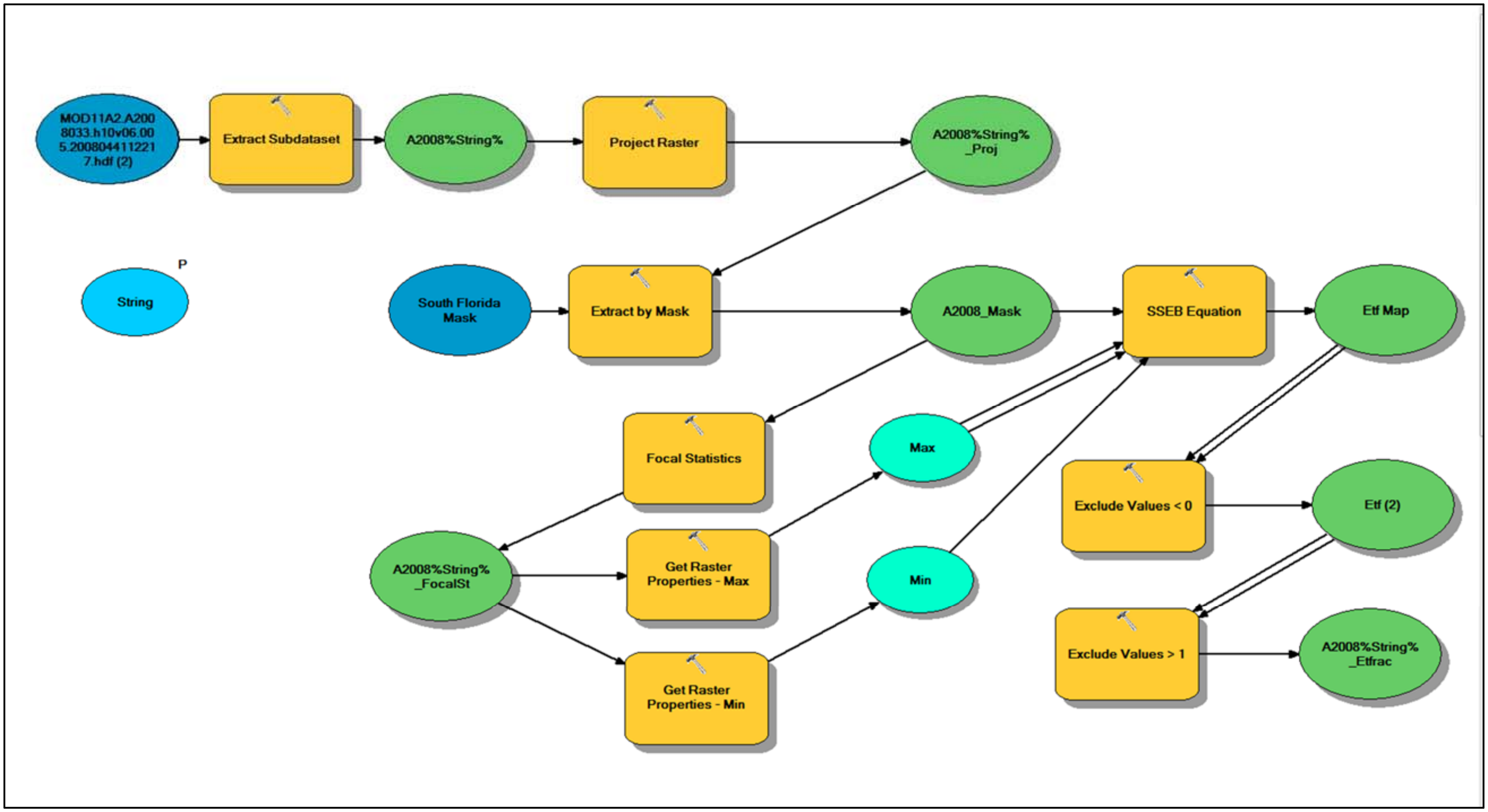

Table 3.3. ArcMap 10 Tools List.

Tool Name	Location Path in ArcToolbox	Inputs	Outputs
Extract Subdataset	Data Management Tools – Raster – Raster Processing.	MOD11A2 LST Image	Layer 1 of MOD11A2 LST image
Project Raster	Data Management Tools – Projections and Transformations – Raster.	Layer 1 of MOD11A2 LST Image.	MOD11A2 Layer 1 LST image projected to NAD_1983_HARN_StatePlane_Florida_East_FIPS_0901
Extract by Mask	Spatial Analyst Tools – Extraction.	Projected LST layer, Polygon layer of South Florida boundary.	LST image of South Florida region
Focal Statistics	Spatial Analyst Tools – Neighborhood.	Masked LST layer from previous step.	Averaged LST map of South Florida region.
Get Raster Properties	Data Management Tools – Raster – Raster Properties.	Averaged LST layer from Focal Statistics output.	Max and Min LST values of the averaged LST map.
Map Algebra	Spatial Analyst Tools	Masked LST layer, extracted min and max LST values from Get Raster Properties tool.	Final Etf Map of the South Florida region.

The daily mean solar radiation values were loaded into an excel spreadsheet. These values provide an estimate of the average solar radiation a 1m x 1m square of land received in one second on a particular day. In order to estimate the total amount of solar radiation that square of land received in one day, the following equation is used:

$$\varphi_d = \frac{(24*3600*\varphi_i)}{1000} \tag{3.3}$$

Where φ_d is the mean daily solar radiation in MJ/m^2*day and φ_i is the mean solar radiation in KW/m^2. The factor of 1000 is used to convert KW to MW and the (24*3600) term corresponds to the number of seconds in one day.

The converted values are then used to calculate PET values for each day using the Simple Method:

$$PET = k_1 \frac{\varphi_d}{\lambda} \tag{3.4}$$

Where k_1 is an empirical factor equal to 0.53 and λ is the latent heat of vaporization of water, taken to be 2.45 MJ/kg. The PET values calculated from this formula are represented in units of mm/day (often expressed only with mm next to the number since the daily rate is assumed) by using the fact that 1 kg is equal to 1 x 10^6 mm^3 and 1 m^2 is equal to 1 x 10^6 mm^2. The daily PET values were averaged into 8 day periods to match the MODIS satellite data. Each year (2008-2010) is averaged separately, that is, the first period for 2008 is from January 1st to January 8th and the last period is from December 26th to December 31st (note that the last period contains less than 8 days). This pattern begins again in 2009, with the first period starting on January 1st and ending on January 8th.

Table 3.4. Weather Stations Information.

Station	Basin	Lat.	Long.	County	Description
3AS3WX	Conservation area 3a	25°51’6.2”	80°45’58.5”	Miami-Dade	Water Conservation Area 3 (WCA3) weather station, tree islands.
Ave Maria	Faka Union.	26°18’6.09”	81°25’52.9”	Collier	Town of Ave Maria weather station.
BELLE GL	S-2_6_7	26o39’24.6”	80°37’48.09”	Palm Beach	Belle Glade Weather Station
BIG CY SIR	Feeder Canal	26°19’17.3”	3’81°4’4.24”	Hendry	Big Cypress at Seminole Indian reservation.
CFSW	S-4	26°44’6.23”	80°53’43.2”	Hendry	Clewinston field station weather station.
ENR308	STA-1W	26°37’21.2”	80°26’20.2”	Palm Beach	Weather station near interior levee in cell 3.
FPWX	Estero Bay	26°25’57.3”	81°43’24.3”	Lee	Flint Pen Strand weather station.
JBTS	C-111 Coastal	25°13’28.4”	80°32’24.2”	Miami-Dade	Joe Bay, approx., 9.5 km from Gilbert’s Res. Overseas Hwy boat ramp, Key Largo.
L006	Lake Okeechobee	26°49’21.2”	80°46’58.2”	Palm Beach	Lake Okeechobee tower South (#6).
LOXWS	Conservation Area 1	26°29’56.3”	80°13’20.2”	Palm Beach	Loxahatchee weather station at CA1-8C and L-40.
ROTNWX	STA-5/6	26°19’56.8”	80°52’53.1”	Broward	Rotenberger tract weather station.
S140W	Conservation Area 3A	26°10’16.7”	80°49’33.6”	Broward	S140 weather station on levee L28 near Alligator Alley.
S331W	L-31NS	25°36’37.5”	80°30’34.6”	Miami-Dade	S-331 weather station on L-31N
S78W	East Caloosahatche e	26°47’23.2”	81°18’10.3”	Glades	S-78 weather station on Caloosahatchee River at Ortona.
SGGEWX	Faka Union	26°8’43.3”	81°34’32.3”	Collier	Southern Golden Gate Estates weather station.

A GIS layer containing the large majority of monitoring sites located in the South Florida region was obtained from the SFWMD GIS database (http://my.sfwmd.gov/gisapps/sfwmdxwebdc/dataview.asp?query=unq_id=1588). It was from this vast layer that the 15 relevant monitoring station point features were acquired and placed onto a separate layer (Fig. 3.4). The 8 day average PET values were loaded onto this new 15 point layer as data table elements of the corresponding monitoring station.

Next, the "Geostatistical Tool" provided by ArcMap 10 was used to create interpolated PET value surfaces for each 8 day period using the corresponding 15 data points for each period. The Baysian-Krigging method was used with an iteration value of 100, and a smoothing factor of 0.4. Baysian-Krigging provided the most consistent results of any of the available interpolation methods and was recommended because of the small number of data values available for the interpolation. Furthermore, iterations over 100 (500 to 1000) showed no significant improvement in the interpolation results but noticeably increased the processing time. Similarly, smoothing factors over 0.4 did not produce visible improvement on the interpolation results. Once the interpolated PET layer was created, it was expanded to cover the whole South Florida region and saved to a new raster layer in order to match the format of the Etf layer. This process was conducted for all 138 8-day periods stretching from January 1, 2008 to December 31, 2010.

3.3. Actual Evapotranspiration (AET) Calculation and Validation

To create the final AET layer, the Etf layer and PET layer are multiplied together using the "Map Algebra" tool in ArcToolbox:

Figure 3.4. Map of Weather Stations that Provided Solar Radiation Data.

$$AET = Et_f * PET \quad (3.5)$$

The calculation is carried out pixel by pixel, meaning that the program matches up the Etf pixel with the PET pixel that represents the same geographical location and multiplies the values in those pixels together. The output of the multiplication process is the modeled AET map of the study area. The final output is AET in units of mm and each pixel has dimensions of 0.96 km by 0.96 km.

The USGS eddy covariance AET data were used to test the validity of the modeled AET data. The USGS data were part of an earlier study (Shoemaker, 2011) which collected data from 5 sites located inside Big Cypress National Preserve (Fig. 3.5). Each site is distinguished by the type of land cover the ET measuring equipment was installed upon. A description of the sites can be seen in Table 3.5. The latitude and longitude of each of these stations were used to code a point layer in ArcMap. The point layer was then used to extract the pixel values of Etf, PET, and AET from the corresponding layers. The values extracted correspond to the pixels atop which the control stations lay. These values were then compared to the 8 day averaged AET values from the control sites.

The statistical comparison and analysis of the data were carried out using SPSS software and the majority of the graphs were created in excel software. Basic statistics including the calculation of the mean, standard deviation of the mean, standard error, median, kurtosis and skewness of the data were calculated for the control data and experimental data. The control AET, experimental AET, and PET data sets were checked for normality using both histogram analysis and the Shapiro-Wilk normality test. The test was done for all five control sites separately.

Figure 3.5. AET Control Site Locations.

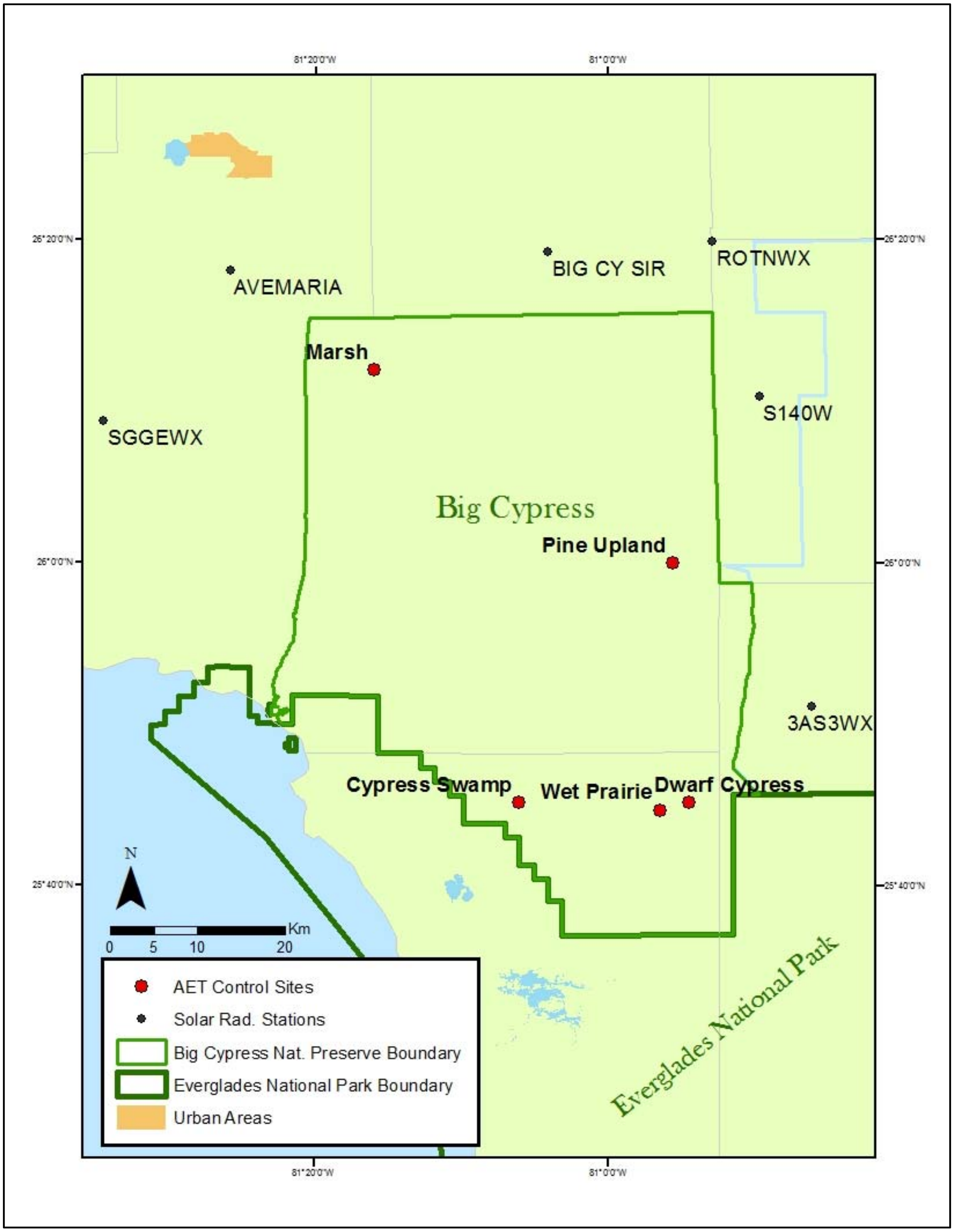

Table 3.5. AET Control Sites.

Site Name	Latitude	Longitude	Height of EC Tower (m)	Land Cover Description
Dwarf Cypress	25º45’45”	80º54’27”	16.5	Dwarf cypress and sawgrass (herbaceous vegetation).
Cypress Swamp	25º45’10”	81º06’01”	38	Tall cypress strand.
Pine Upland	25º59’59”	80º55’29’	38	Pine upland and cypress domes
Wet Prairie	25º44’41”	80º56’24”	3.6	Wet prairie with short (<1 m) sawgrass (herbaceous vegetation)
Marsh	26º11’57”	81º15’58”	3.6	Deep-water marsh with tall (1-2 m) sawgrass (herbaceous vegetation).

The correlation between the control and experimental AET, and PET data sets were checked for normality using both histogram analysis and the Shapiro-Wilk normality test. The test was done for all five control sites separately. The correlation between the control and experimental AET data was tested using several different techniques. These techniques include several nonparametric “rank tests” (Related-Samples Sign Test, related samples Wilcoxon Signed Rank Test, the related samples Friedman’s Two-Way Analysis of Variance by Ranks), the related samples Kendall’s Coefficient of Concordance, the Pearson’s correlation coefficient and the Spearman’s correlation coefficient.

Upon inspection of the data, it was decided to separate the full data set into dry and wet season subsets. The dry set includes values from November to April of each year and the wet set includes values from May to October of each year. Once separated, both the dry season and wet season datasets were subjected to the same tests for normality and correlation carried out for the full set. The correlation between the calculated PET data and the control data was also explored using the correlation tools described previously.

Figure 3.6. Validation Analysis Workflow.

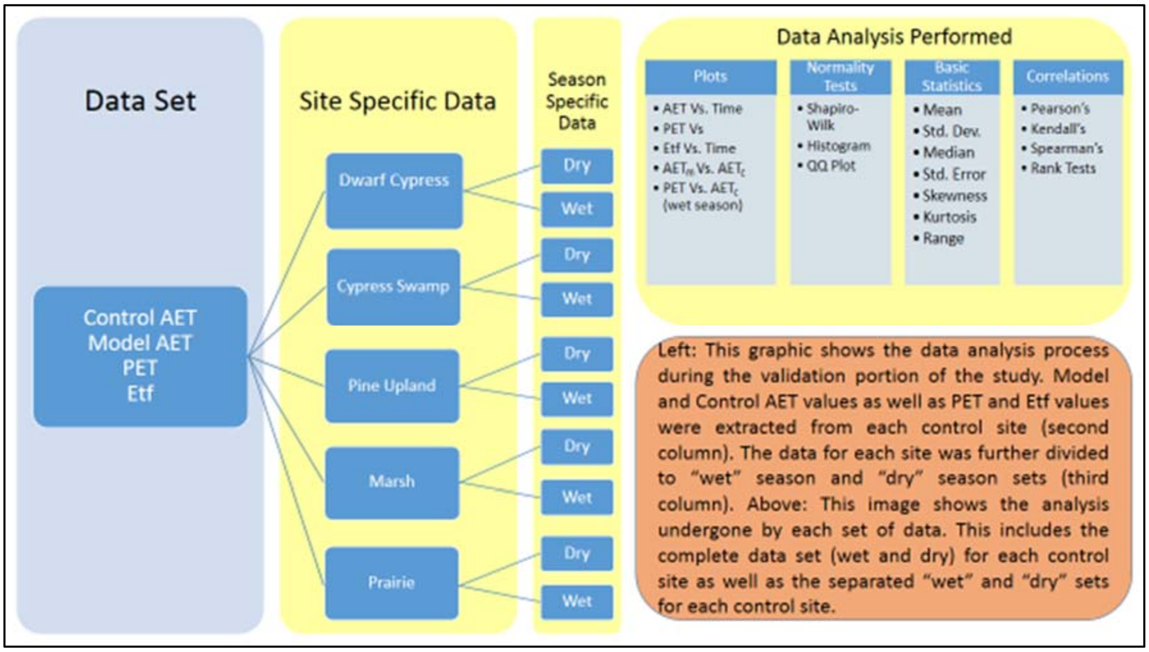

CHAPTER 4: RESULTS

Evapotranspiration fraction (Etf), potential evapotranspiration (PET), and actual evapotranspiration (AET) maps were created for the period from January 1, 2008 to December 31, 2010. Each map contains the average data of 8-day observation periods and are labeled using the Julian date of the first day of observation within the corresponding 8 day period. For example, the map from 2008001 (January 1, 2008) was created using the average values of data collected from January 1, 2008 to January 9, 2008. All maps use the "NAD_1983_HARN_StatePlane_Florida_East_FIPS_0901" projection, use units of meters for distance, and are composed of 926 m x 926 m pixels. Fig. 4.1 shows samples of Etf, PET, and AET maps created for a single 8 day period. Etf, PET, and AET data can be extracted for any pixel within a corresponding map, but for the analysis and validation of the model, only the values of five sites (pixels) were extracted from the maps. Results from each of the major components of the model (i.e. Etf calculation, PET calculation, and final AET calculation) are first considered separately and then considered as a complete model during the validation analysis.

4.1. PET Calculation Results.

Solar radiation data from 15 stations were used for the majority of the PET calculation. The major exception was the period between January 1, 2008 and May 20, 2008 where data from "Ave Maria" station were not available. During this period only 14 data points were used to create the interpolated PET surface. Other periods of missing data are listed on Table 4.1. There were a total of 84 missing days of solar radiation, which translates to about 5.6 days per station, and about 0.51% of all days with available data.

There was no station (aside from AVE MARIA) where data were missing for an entire 8-day averaging period. The “Bayesian-Kriging” interpolation method used to create the.

PET surfaces provided workable results but the accuracy of the interpolated values suffered from the lack of data points available. In general, the interpolated surfaces can vary noticeably from one time period to the next (fig. 4.2). The lack of consistency among the created PET surfaces seems to extend from the lack of data points used to create the surfaces (15 points, one from each solar radiation station) since Kriging interpolation works best with a larger set of normally distributed data (Clark, 1987). Unfortunately, the data available for each interpolation is rarely normally distributed due to the relatively small number of data points. Furthermore, the Bayesian-Kriging method could not consistently accommodate for extreme values. The method consistently underestimated high values and overestimated low values. This had the effect of “narrowing” the range of PET values of the interpolated surface. This effect can be seen when comparing the PET calculated from data at the solar radiation stations with the PET extracted from the interpolated PET surfaces at the control sites (fig. 4.3). PET vs. time plots for each individual control site are given in appendix A.

The most noticeable feature of the first plot is the strong seasonal trend experienced by PET values over the study period. High PET values occur during summer (wet) months while low PET values occur during winter (dry) months. The interpolated values at the control sites also show this seasonal trend, which bodes well for the utility of the of the interpolation method chosen. That said, the calculated PET values do show higher maximums and lower minimums of PET when compared to the extracted values, with the

Figure 4.1. PET, Etf, and AET maps for observation period 2008025. This period includes data from January 25th to February 1st of 2008.

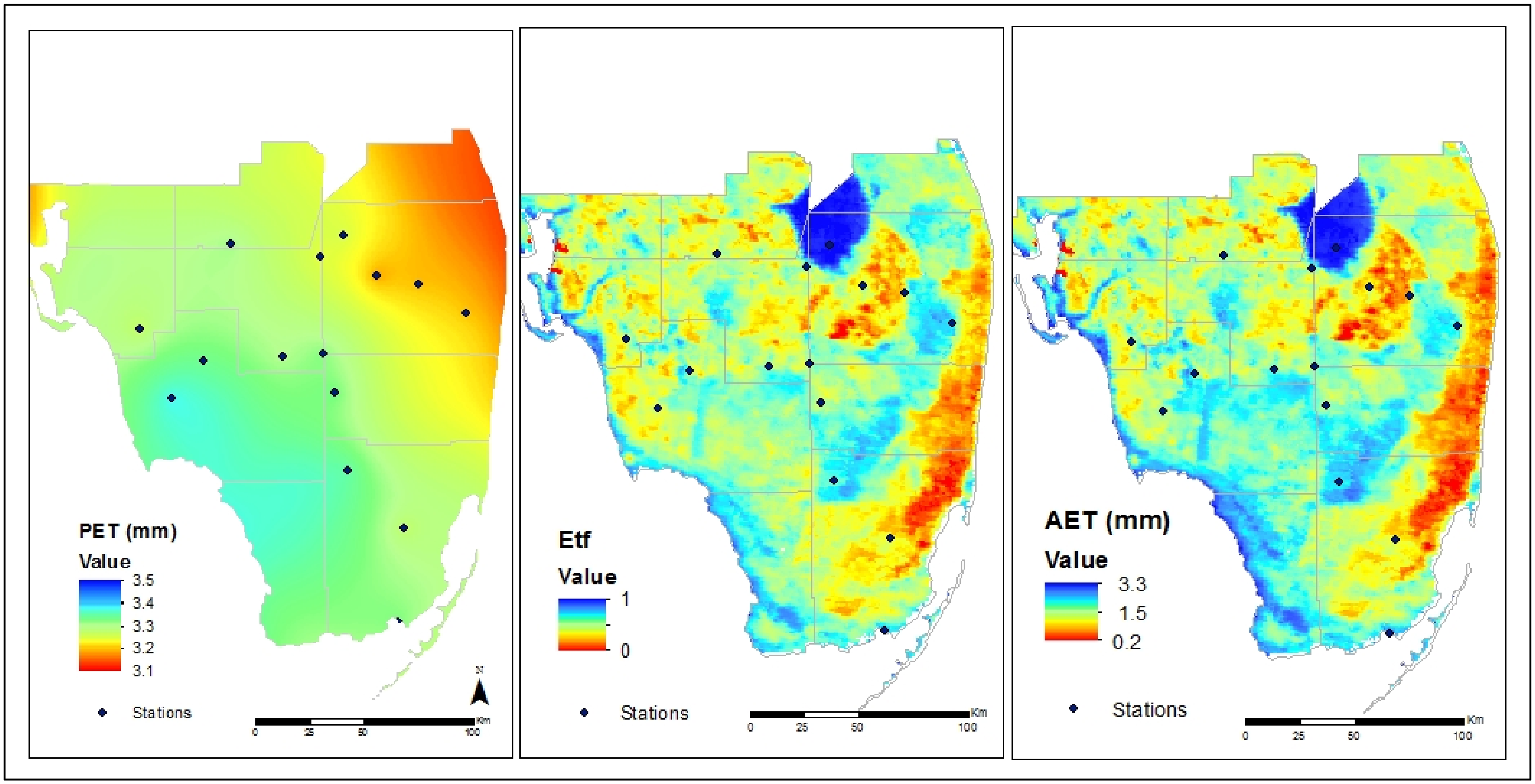

Table 4.1. Dates of missing solar radiation data.

Station	Year	Dates
Ave Maria	2008	Jan. 1 to May 20
ENR308	2008	Apr. 10
JBTS	2008	Nov. 15
S140W	2008	Apr. 27 to Apr. 29
S331W	2008	Mar. 14 to Mar. 16
Ave Maria	2009	Aug. 28 to Aug. 30
ENR308	2009	Jan. 17
JBTS	2009	Jun. 12 to Jun. 17
L006	2009	Jul. 16 to Jul. 23
S140W	2009	Apr. 2 to Apr. 8
S140W	2009	Jun. 10 to Jun. 15
SGGEWX	2009	Aug. 6
3AS3WX	2010	Aug. 28
Ave Maria	2010	Jun. 5-9, and 12-17
Ave Maria	2010	Oct. 6
Ave Maria	2010	Dec. 13-16, 18, 21, and 30-31
ENR308	2010	Jun. 10 to Jun. 13
S140W	2010	Jul. 6 to Jul. 13
SGGEWX	2010	Dec. 15, 16, 22-31

Figure 4.2. Sample Interpolated PET Surfaces.

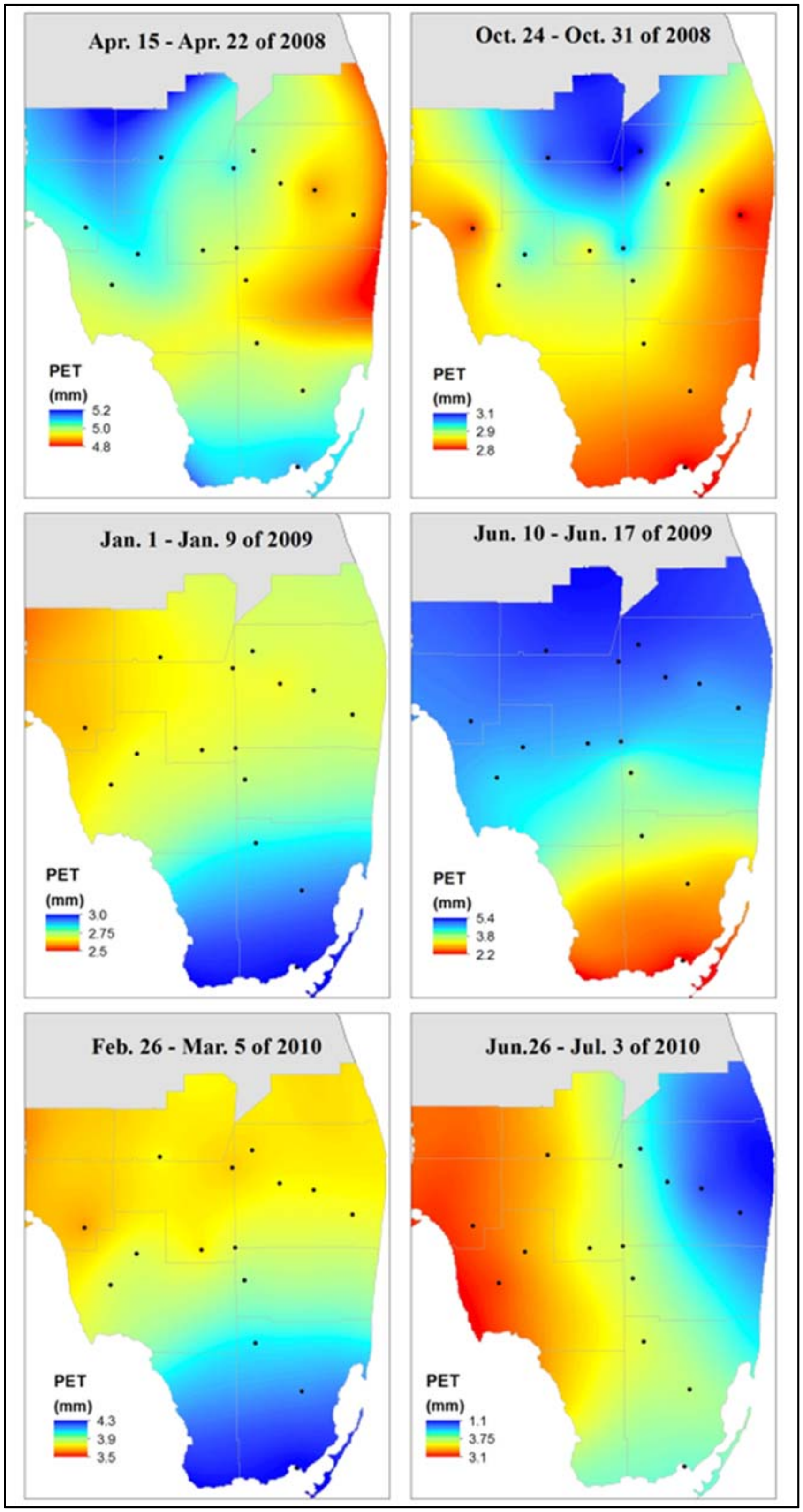

calculated high and low being around 6 mm and 1.1 mm respectively while the interpolated maximum and minimum being around 5.5 mm and 1.8 mm, respectively. This again shows the tendency of the interpolation to “narrow” the PET values.

4.2. Etf Calculation Results.

A total of 138 Etf maps were created covering the study period starting on Jan. 1, 2008 and culminating on Dec 31, 2010. A visual survey of the maps shows constant areas of low Etf values across the urban area of South Florida, as well as the agricultural zones located south of Lake Okeechobee. Wetland regions inside Big Cypress national preserve and Everglades National Park, as well as the water conservation areas show higher Etf values throughout the study period. As expected, wetter (cooler) areas produce higher Etf values than dryer (hotter) areas.

Unfortunately, a number of Etf maps contained missing pixels due to the original MOD11A2 satellite image having missing temperature data (figure 4.4). The majority of these incomplete maps occur during the wetter summer months and are due to prolonged cloud cover over the majority or entirety of an 8 day observation period. This cloud effect not only produces missing data, but also seems to underestimate Etf values for all pixels within an affected map. This can be seen in Figure 4.5, which plots the Etf values at the control sites from 2008 to 2010. The plot shows how Etf values fall to values around 0.2 during wet season, a time of year where Etf is expected to be at its highest (Shoemaker, 2011). This pattern repeats for all five sites and it is a direct effect of the missing temperature data due to extended periods of cloud cover.

Figure 4.3 Comparison between PET values calculated at solar radiation monitoring stations and the interpolated PET values calculated at the 5 control sites. Low outlier numbers are due to missing data. The single high outlier point occurred at station JBTS on November 16-23 of 2008 (JD 2008321) and is accredited to equipment malfunction.

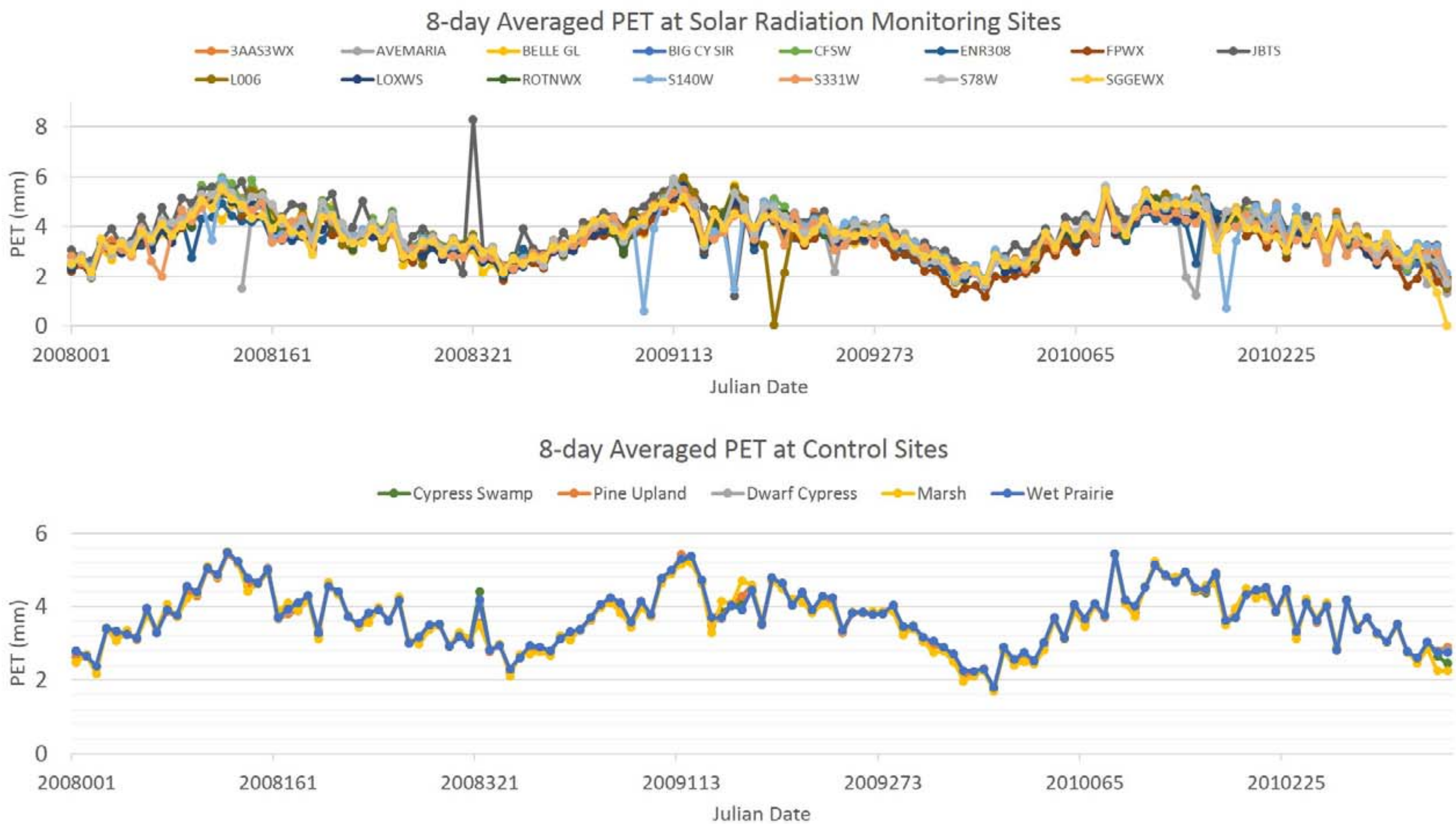

Table 4.2 shows the mean Etf value for the dry months, wet months, and the whole study period for the five control sites. Mean Etf is higher during dry season (0.559) than wet season (0.473) yet both seasons have comparable maximum values (0.878). It is clear that that the wet season data is being critically underestimated and bringing the total mean down to a lower value than expected (0.518).

Table 4.2. Means and Standard Deviations of Etf for Control Sites.

Site	Mean Etf	Std Etf	Mean Dry Etf	Std Dry Etf	Mean Wet Etf	Std Wet Etf
Cypress Swamp	0.516	0.161	0.558	0.119	0.470	0.188
Pine Upland	0.487	0.153	0.518	0.112	0.453	0.183
Dwarf Cypress	0.531	0.171	0.574	0.119	0.484	0.205
Marsh	0.537	0.170	0.587	0.122	0.482	0.199
Wet Prairie	0.519	0.170	0.557	0.129	0.477	0.199
Average	0.518	0.165	0.559	0.120	0.473	0.195

4.3. AET Calculation Results

A total of 138 AET maps were created for the study period starting on Jan. 1, 2008 and Dec. 31, 2010. The AET maps mirror patterns seen in the PET maps, with higher AET areas within wetlands (Everglades, Big Cypress) and the water conservation areas (Fig. 4.6). The urban area and the agricultural zones consistently show lower AET values throughout the study period. Several AET maps contain missing pixels due to the effect carried over from the Etf maps. Again, these missing pixels due to cloud cover effects occur mostly during the wet part of the year. This effect can be readily seen on all five control sites (Fig. 4.7) where the model data brakes down during the wet months of each year. It can also be seen that during the dry portions of the year the model performs much better,

Figure 4.4. Sample 8-day averaged Etf Maps. Areas with missing data are shown in grey.

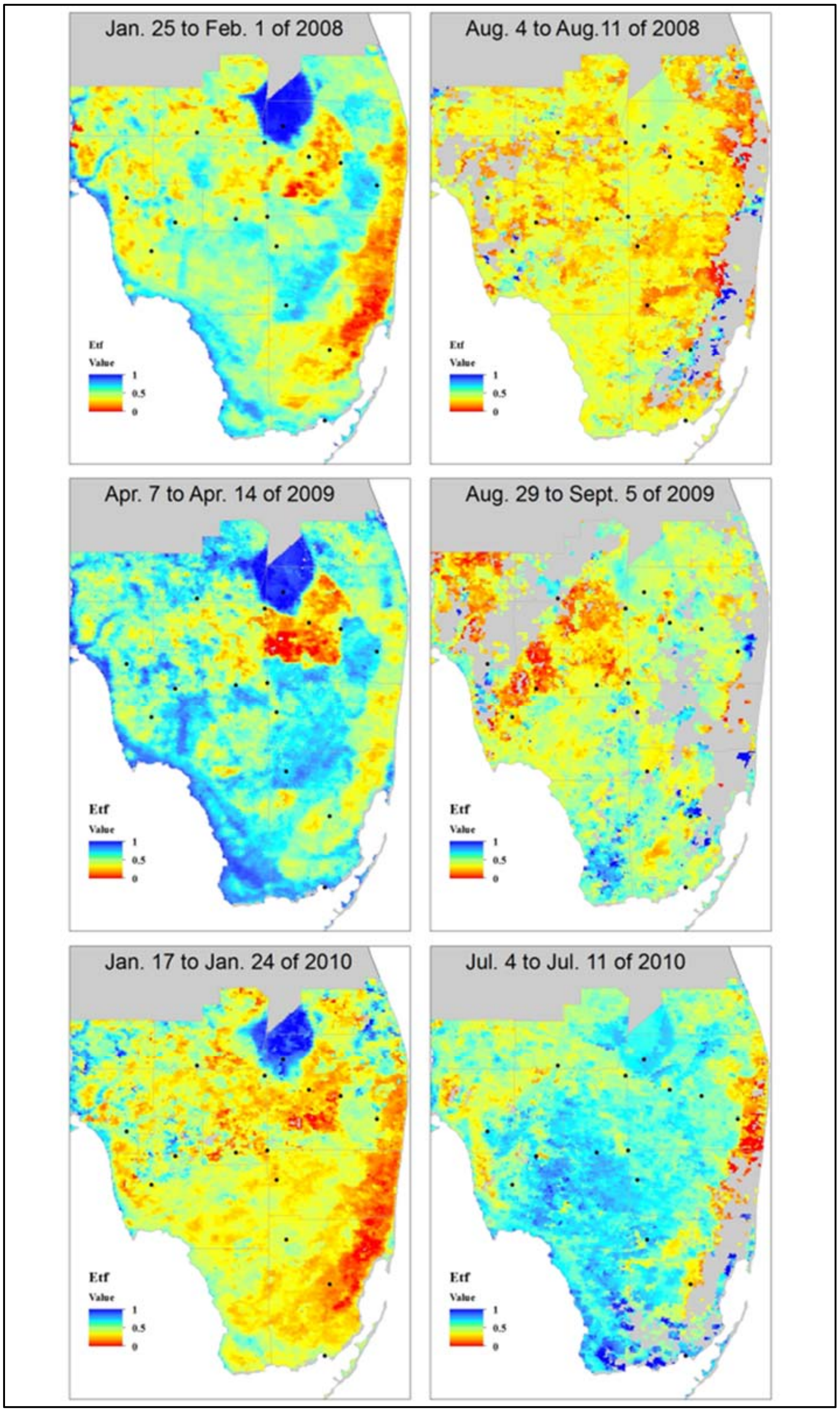

Figure 4.5. Averaged 8-day Etf Values for the Five Control Sites in Big Cypress..

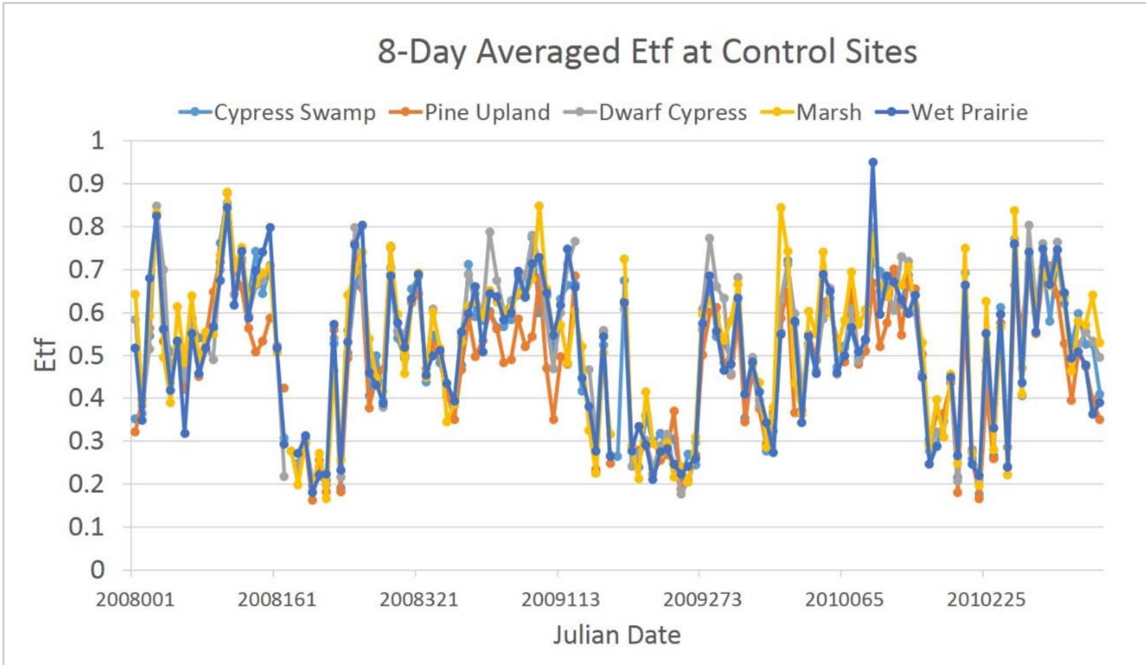

matching the trends seen in the control data. Figure 4.8 shows Model AET plotted against Control AET. The plots show that the model underestimates AET values for all five sites.

Basic statistical information for each site's AET data is given in Appendix B and comparison statistics between control AET and model AET are given in Table 4.3. The average control AET across the five sites has an average mean value of 2.61 mm while the average mean for the modeled values is 1.92 mm. The average bias (difference between model mean and control mean) is -0.696 mm which is 26.0% of the average control mean. The marsh sites show the lowest bias value with -0.406 mm while the Wet Prairie site has the largest bias at -0.938 mm. The average RMSE across the five control sites is 1.25 mm, constituting 46.3% of the average control mean. The Pine upland site shows the lowest

Figure 4.6. Sample 8-day Averaged AET Maps. Grey areas represent missing data.

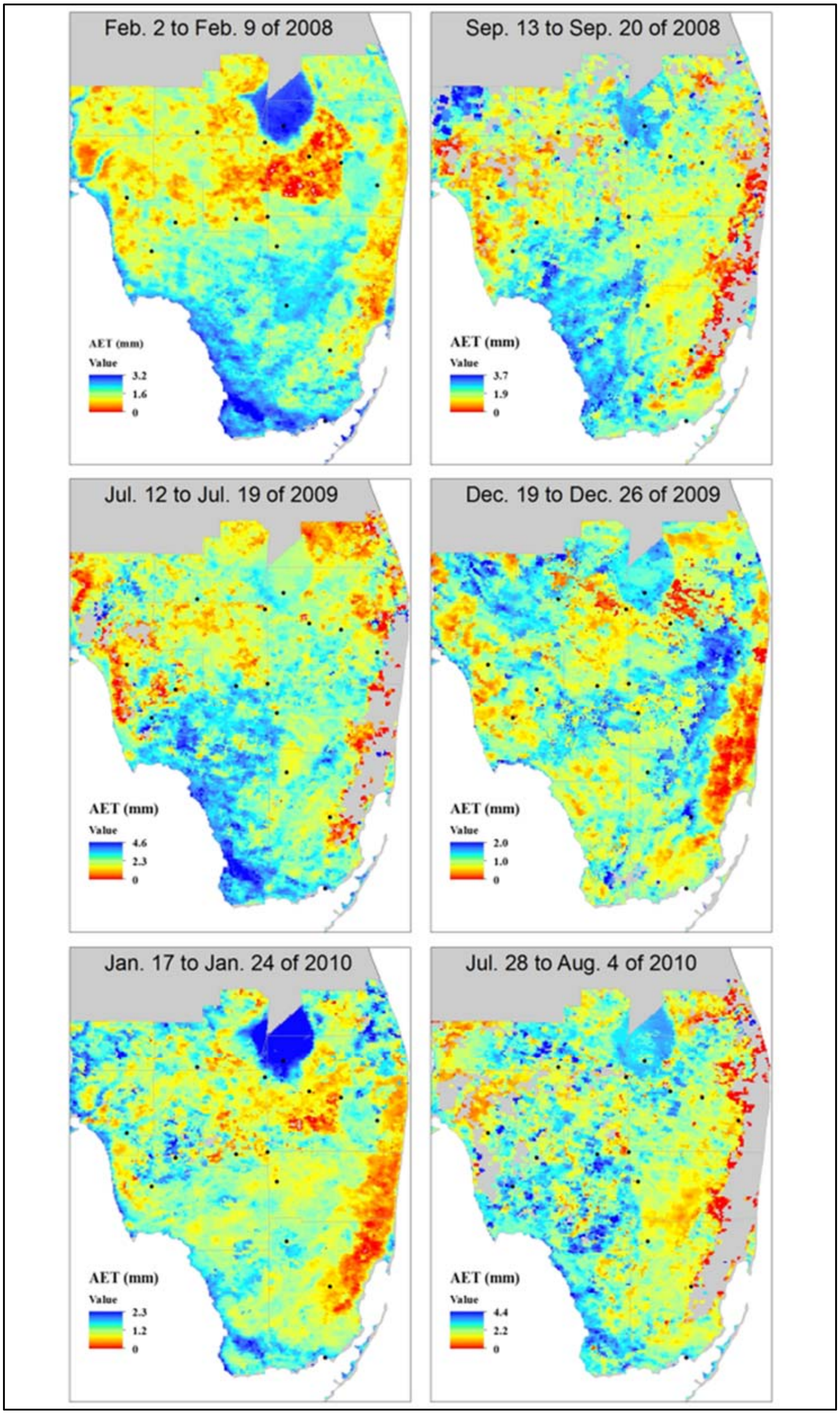

Figure 4.7. Control AET and Model AET and PET at Five Control Sites.

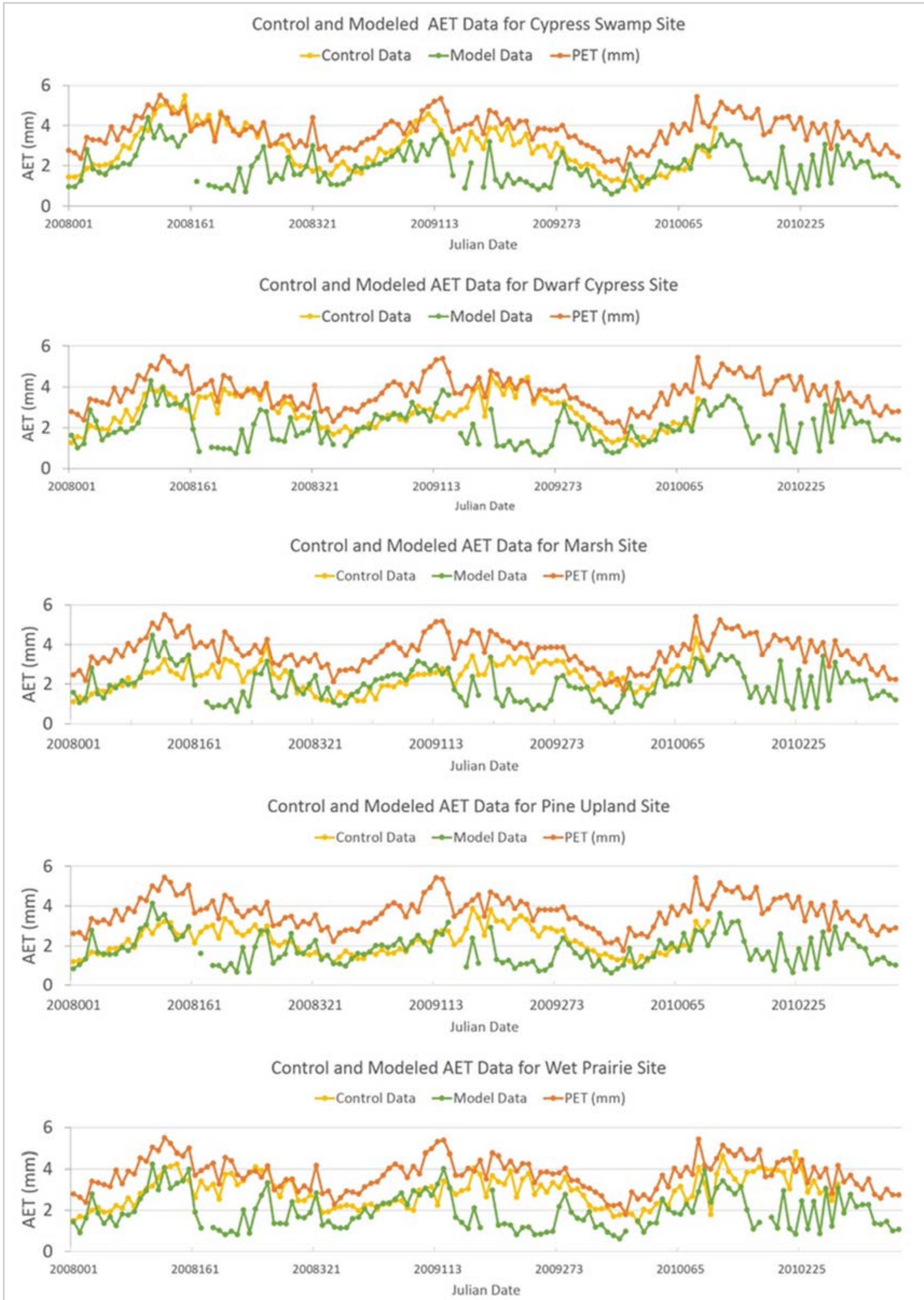

Figure 4.8. Comparison between Control and Model AET for Control Sites.

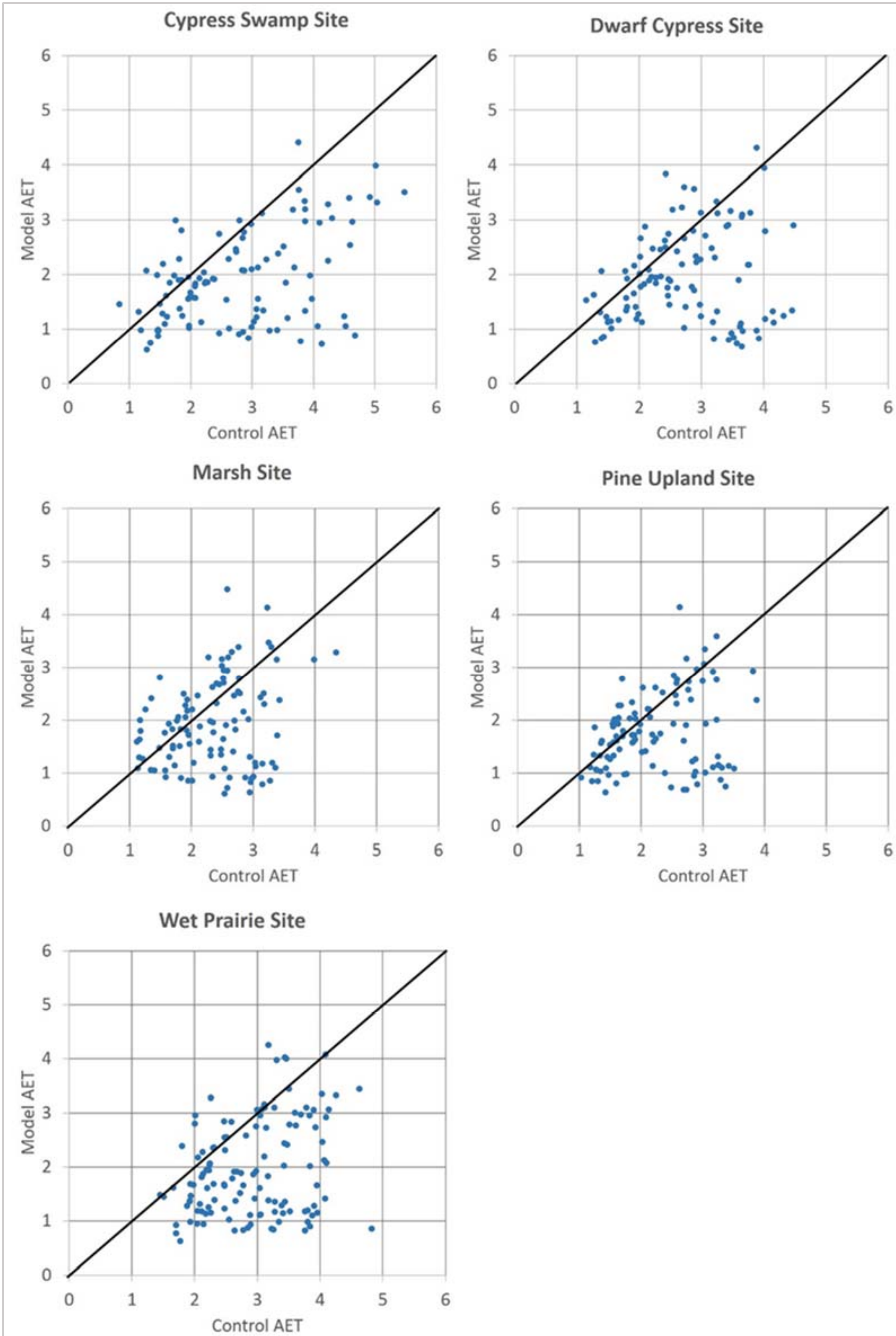

RMSE with a value of 0.983 mm while the Wet Prairie site shows the highest RMSE with a value of 1.384 mm.

Normality test results are summarized on Table 4.4. The Dwarf Cypress and Marsh site control data show strong signs of normality while none of the experimental data sets show strong signs of normality. All PET data sets show strong signs of being normally distributed. The results of Rank tests performed for each site are listed on Table 4.5 and histograms of the differences are provided in Appendix C. Again it is evident that the model is underestimating the AET values for each site with the majority of differences between model values and control values being negative. The Wet Prairie site showed the most disparity between positive and negative differences (19 positive, 144 negative) while the Marsh site showed the least disparity (40 positive, 64 negative). Table 4.6 shows the results of Pearson's (r), Kendall's (τ), and Spearman's (ρ) correlation tests performed on the model and control data. All tests show a slight positive correlation between the two data sets for all five sites. All three tests rank the Cypress Swamp site as having the highest correlation ($r(105) = 0.454$, $p < 0.0005$; $\tau = 0.280$, $p < 0.0005$; $\rho =0.374$, $p < 0.0005$) with a high statistical significance (p-value < 0.05). Furthermore, all three tests rate the Dwarf Cypress site as having the lowest correlation ($r(105) = 0.173$, $p = 0.083$; $\tau = 0.122$, $p =0.07$; $\rho = 0.130$, $p = 0.195$) but with a weak statistical significance (P-value > 0.5). Although the data may not show strong signs of normality both the normal correlation test (Pearson's) and the nonparametric tests (Kendall's and Spearman's) show similar results for the correlation of data at each of the five sites.

Table 4.3. Statistical Comparison between Control and Model AET for full Data.

Site	$Mean_c$ (mm)	STD_c (mm)	CV_c	$Mean_m$ (mm)	STD_m (mm)	CV_m	Bias (mm)	RMSE (mm)	$Bias/Mean_c$	$RMSE/Mean_c$
Cypress Swamp	2.835	1.077	37.9%	1.917	0.839	43.7%	-0.918	1.355	-32.4%	47.8%
Pine Upland	2.236	0.690	30.8%	1.798	0.753	41.8%	-0.438	0.983	-19.6%	44.0%
Dwarf Cypress	2.723	0.835	30.6%	1.988	0.840	42.2%	-0.734	1.329	-27.0%	48.8%
Marsh	2.352	0.674	28.6%	1.946	0.840	43.1%	-0.406	1.025	-17.3%	43.6%
Wet Prairie	2.923	0.765	26.1%	1.940	0.862	44.3%	-0.983	1.384	-33.6%	47.3%
Average	2.614	0.808	30.8%	1.918	0.827	43.0%	-0.696	1.215	-26.0%	46.3%

Table 4.4. Normality Test Results for Full Dataset. Data is considered normally distributed when $p > 0.05$.

Site	Control AET p-value	Normality	Experimental AET p-value	Normality	Experimental PET p-value	Normality
Cypress Swamp	0.010	No	0.000	No	0.724	Yes
Pine Upland	0.004	No	0.002	No	0.707	Yes
Dwarf Cypress	0.052	Yes	0.001	No	0.612	Yes
Marsh	0.117	Yes	0.002	No	0.708	Yes
Wet Prairie	0.008	no	0.000	no	0.636	Yes

Table 4.5. Rank Test Results for Full Dataset. The rank test performed consisted of subtracting the control AET values from the model AET values (i.e. $AET_m - AET_c$).

Site	Positive Differences	Negative Differences	Result
Cypress Swamp	17	86	Underestimation
Pine Upland	35	66	Underestimation
Dwarf Cypress	23	78	Underestimation
Marsh	40	64	Underestimation
Wet Prairie	19	104	Underestimation

Table 4.6. Results of Correlation Tests between Full Data Control AET and Model AET.

Site	r	σ_r	τ	σ_τ	ρ	σ_ρ
Cypress Swamp	0.454	< 0.0005	0.280	< 0.0005	0.374	< 0.0005
Pine Upland	0.263	0.008	0.200	0.003	0.237	0.017
Dwarf Cypress	0.173	0.083	0.122	0.070	0.130	0.195
Marsh	0.248	0.011	0.125	0.059	0.166	0.093
Wet Prairie	0.291	0.001	0.177	0.004	0.251	0.005

Data were separated into Dry Season (data between November and April) and Wet Season (data between May and October) sets to evaluate the accuracy of the model during each season and the effect each season has on the overall accuracy of the model.

Dry season model data shows a much better agreement with control data than that of the complete dataset across all five sites (Fig. 4.9). Model AET vs. Control AET plots (Fig. 4.10) again show underestimation of values by the model, but in general there is a much better agreement with control values. Basic statistical information for each site's AET data is provided in Appendix B and a comparison between "Dry" control AET and "Dry" model AET is given in Table 4.7. The average "Dry" control AET across the five sites has an average mean value of 2.14 mm while the average mean for the modeled values is 1.93 mm. The average bias is -0.213 mm which is -9.4% of the average control mean. The Pine Upland site shows the lowest bias value with -0.042 mm while the Wet Prairie site has the largest bias at -0.414 mm. The average RMSE across the five "Dry" control sites is 0.602 mm, constituting 28.1% of the average control mean. Again, the Pine upland site shows the lowest RMSE with a value of 0.463 mm while the Wet Prairie site shows the highest RMSE with a value of 0.701 mm.

Normality tests for the "Dry" data are summarized on Table 4.8 and histograms of the data are provided in Appendix C. None of the control data sets show strong signs of normality. Experimental data sets for the Cypress Swamp, Dwarf Cypress, and Marsh sites show signs of normality, while the Pine Upland and Wet Prairie sites show no strong signs of normality. Again, all PET data sets show signs of being normally distributed. The results of Rank tests performed for each site for the "Dry" periods are listed on Table 4.9 and histograms of the differences are provided in Appendix C. The Cypress Swamp, Dwarf Cypress, and Wet Prairie sites still show more negative differences than positive ones, meaning that control values are still being underestimated. But, the disparity between negative differences and positive differences is much less than that seen for the complete dataset. The Pine Upland and marsh site show equal or near equal numbers of positive and negative differences. Table 4.10 shows the results of correlations tests performed on the model and control "Dry" datasets. All tests show a much stronger positive correlation between the two data sets for all five sites. All three tests rank the Dwarf Cypress site as having the highest correlation ($r(59) = 0.791$, $p < 0.0005$; $\tau = 0.566$, $p < 0.0005$; $\rho = 0.753$, $p < 0.0005$) with a high statistical significance (P-value < 0.05). Furthermore, all three tests rate the Marsh site as having the lowest correlation ($r(59) = 0.568$, $p < 0.0005$; $\tau = 0.393$, $p < 0.0005$; $\rho = 0.549$, $p < 0.0005$) (Pearson's = 0.568, Kendall's = 0.393, Spearman's = 0.549) with a strong statistical significance (P-value < 0.05). Again, although the data may not show strong signs of normality, both the normal correlation test (Pearson's) and the nonparametric tests (Kendall's and Spearman's) show similar results for the correlation of "Dry" data at each of the five sites.

Table 4.7. Statistical Comparison between Control and Model AET for Dry Data.

Site	$Mean_c$ (mm)	STD_c (mm)	CV_c	$Mean_m$ (mm)	STD_m (mm)	CV_m	Bias (mm)	RMSE (mm)	$Bias/Mean_c$	$RMSE/Mean_c$
Cypress Swamp	2.302	0.943	40.8%	1.944	0.761	39.0%	-0.357	0.697	-15.5%	30.3%
Pine Upland	1.816	0.513	28.2%	1.774	0.674	37.8%	-0.042	0.463	-2.3%	25.5%
Dwarf Cypress	2.209	0.631	28.4%	2.003	0.718	35.7%	-0.206	0.494	-9.3%	22.3%
Marsh	2.013	0.617	30.6%	1.968	0.753	38.1%	-0.045	0.655	-2.2%	32.6%
Wet Prairie	2.360	0.549	23.2%	1.946	0.775	39.7%	-0.414	0.701	-17.5%	29.7%
Average	2.140	0.651	30.2%	1.927	0.736	38.1%	-0.213	0.602	-9.4%	28.1%

Figure 4.9. Dry Season Control AET, Model AET, and PET values at Control Sites.

Figure 4.10. Dry Season Comparison between Control and Modeled AET Data.

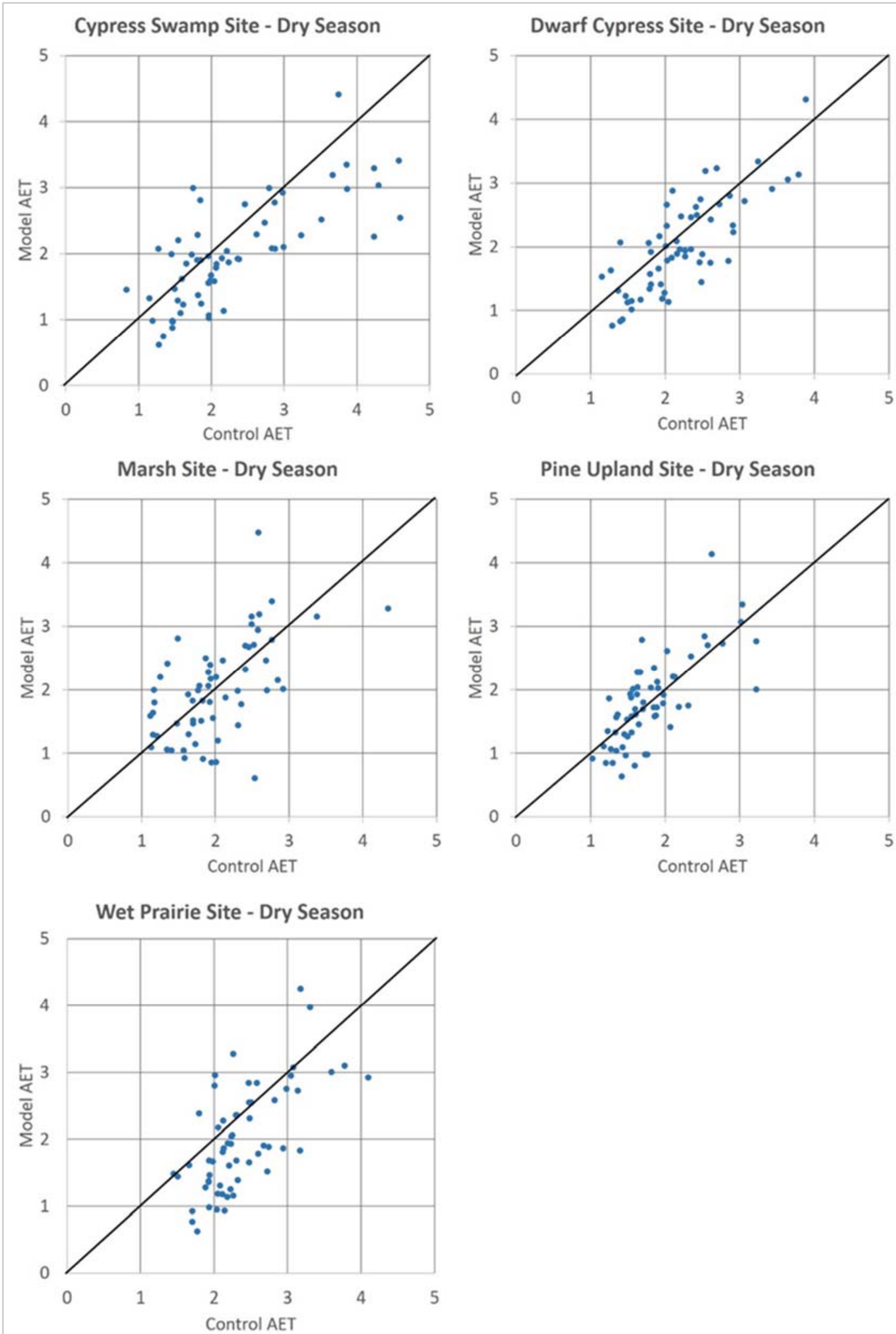

Wet season model data shows a clear disagreement with control data across all five sites (Fig. 4.11). Model AET vs. Control AET plots (Fig. 4.12) show a severe underestimation of values by the model and a much worse agreement than that seen in "Dry" season data. Basic statistical information for each site's AET data are given in Appendix B and a comparison between "Wet" control AET and "Wet" model AET is given in Table 4.11.

Table 4.8. Normality Test Results for Dry Season Data. Data is considered normally distributed when $p > 0.05$.

Site	Control AET p-value	Normality	Experimental AET p-value	Normality	Experimental PET p-value	Normality
Cypress Swamp	< 0.0005	No	0.06	Yes	0.084	Yes
Pine Upland	< 0.0005	No	0.018	No	0.060	Yes
Dwarf Cypress	0.04	no	0.095	Yes	0.050	Yes
Marsh	0.003	No	0.101	Yes	0.163	Yes
Wet Prairie	< 0.0005	No	0.032	No	0.053	Yes

Table 4.9. Rank Test Results for Dry Season Dataset. The rank test performed consisted of subtracting the control AET values from the model AET values (i.e. $AET_m - AET_c$).

Site	Positive Differences	Negative Differences	Result
Cypress Swamp	17	44	Underestimation
Pine Upland	30	30	Equal
Dwarf Cypress	19	39	Underestimation
Marsh	31	29	Overestimation
Wet Prairie	15	45	Underestimation

Table 4.10. Results of Correlation Tests between Dry Season Control AET and Model AET.

Site	r	σ_r	τ	σ_τ	ρ	σ_ρ
Cypress Swamp	0.754	< 0.0005	0.568	< 0.0005	0.738	< 0.0005
Pine Upland	0.734	< 0.0005	0.542	< 0.0005	0.722	< 0.0005
Dwarf Cypress	0.791	< 0.0005	0.566	< 0.0005	0.753	< 0.0005
Marsh	0.568	< 0.0005	0.393	< 0.0005	0.549	< 0.0005
Wet Prairie	0.654	< 0.0005	0.466	< 0.0005	0.642	< 0.0005

The average "Wet" control AET across the five sites has an average mean value of 3.19 mm while the average mean for the modeled values is 1.91 mm. The average bias is -1.281 mm which is -39.6% of the average control mean. The Marsh site shows the lowest bias value with -0.871 mm while the Cypress Swamp site has the largest bias at -1.654 mm. The average RMSE across the five "Wet" control sites is 1.725 mm, constituting 53.9% of the average control mean. Again, the Marsh site shows the lowest RMSE with a value of 1.409 mm while the Cypress Swamp site shows the highest RMSE with a value of 2.013 mm.

Normality tests for the "Wet" data are summarized on Table 4.12 and histograms of the data are provided in Appendix C. The control data for the Dwarf Cypress and the Marsh site show signs of normality while the Cypress Swamp, Pine Upland, and Wet Prairie data do not show strong signs of normality. None of the experimental data show strong signs of normality and the PET data for all five sites show strong signs of being normally distributed. The results of Rank tests performed for each site for the "Wet" periods are listed on Table 4.13 and histograms of the differences are given in Appendix C. All sites show more negative differences than positive. Table 4.14 shows the results of correlations tests performed on the model and control "Wet" datasets. All tests show weak or no correlation between the control and model datasets and only the Wet Prairie site has a consistent statistically significant correlation value (r(46) = 0.434, p = 0.004). All other sites have so significant statistical correlation and show practically the same correlations a randomly generated set of points would show. All the tests show that the model does not successfully recreate the excepted AET values during the wet season.

Table 4.11. Statistical Comparison between Control and Model AET for Wet Data.

Site	$Mean_c$ (mm)	STD_c (mm)	CV_c	$Mean_m$ (mm)	STD_m (mm)	CV_m	Bias (mm)	RMSE (mm)	$Bias/Mean_c$	$RMSE/Mean_c$
Cypress Swamp	3.543	0.808	22.7%	1.889	0.918	48.4%	-1.654	2.013	-46.7%	56.8%
Pine Upland	2.784	0.471	16.8%	1.824	0.834	45.5%	-0.960	1.448	-34.5%	52.0%
Dwarf Cypress	3.381	0.556	16.4%	1.973	0.957	48.3%	-1.409	1.954	-41.7%	57.8%
Marsh	2.795	0.453	16.1%	1.924	0.925	47.9%	-0.871	1.409	-31.2%	50.4%
Wet Prairie	3.443	0.533	15.4%	1.934	0.948	48.8%	-1.509	1.800	-43.8%	52.3%
Average	3.189	0.564	17.5%	1.909	0.916	47.8%	-1.281	1.725	-39.6%	53.9%

Figure 4.11. Wet Season Control AET, Model AET, and PET values at Control Sites.

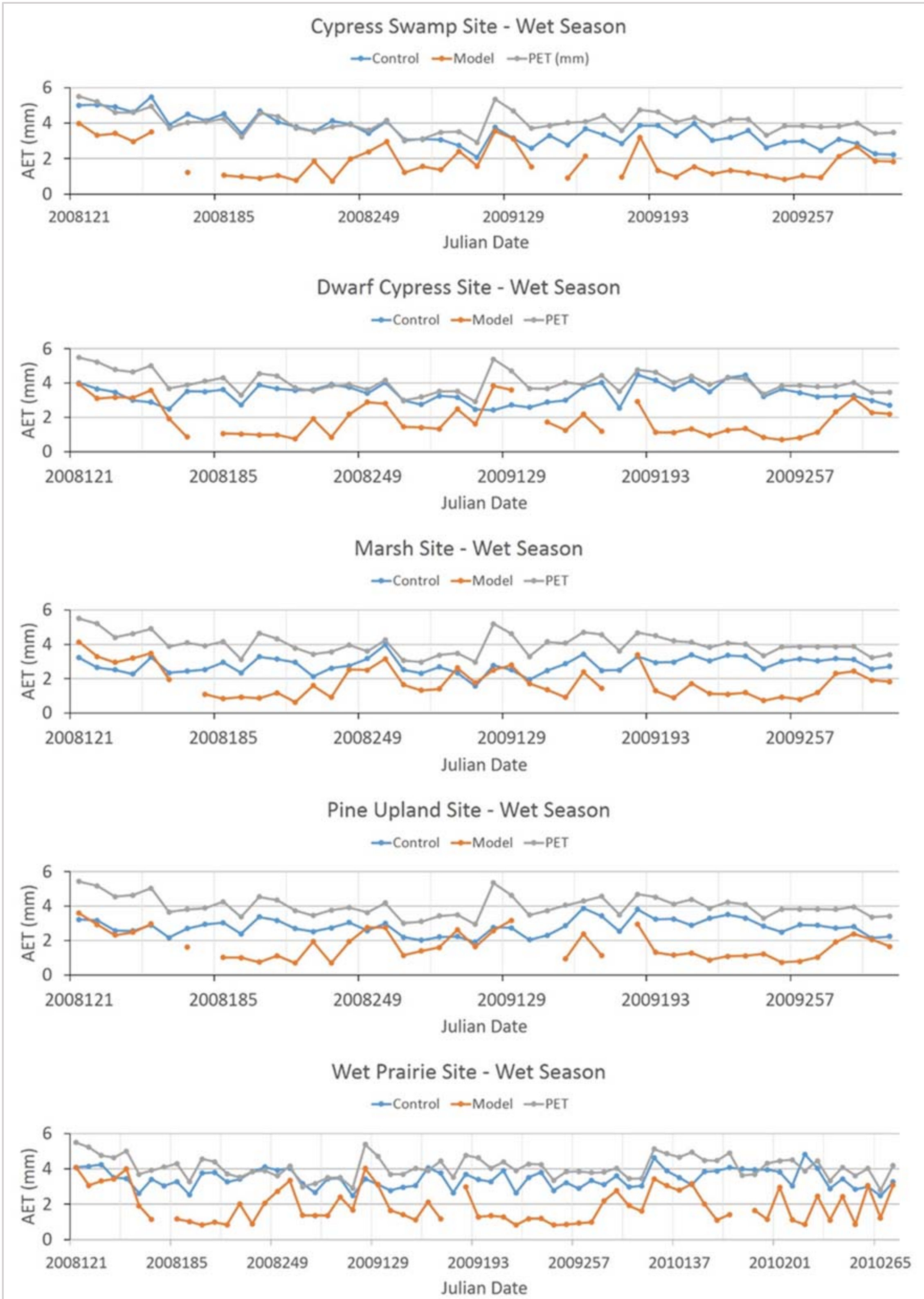

Figure 4.12. Wet Season Comparison between Control and Modeled AET Data.

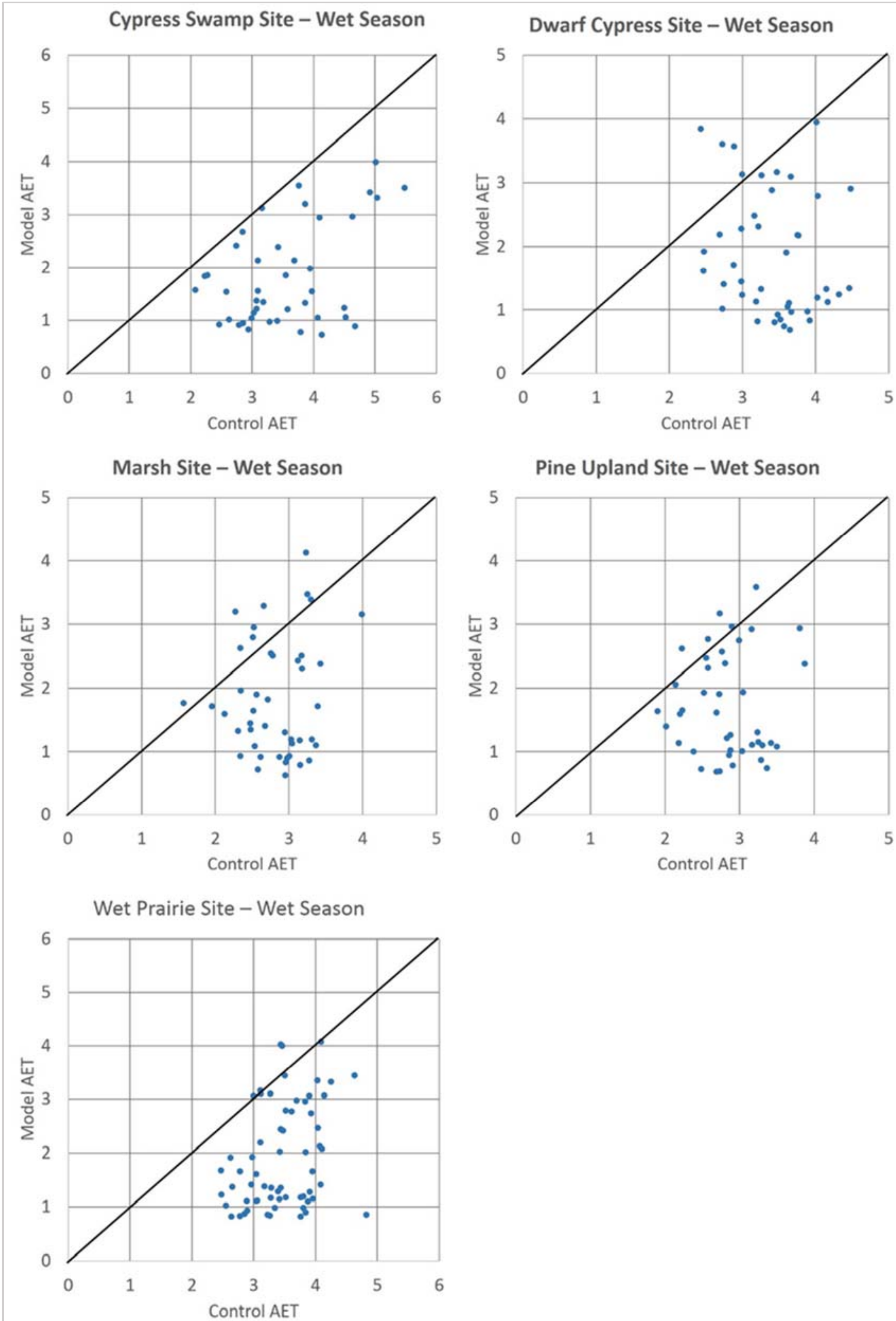

Table 4.12. Normality Test Results for Wet Season Data. Data is considered normally distributed when $p > 0.05$.

Site	Control AET p-value	Normality	Experimental AET p-value	Normality	Experimental PET p-value	Normality
Cypress Swamp	0.010	No	0.001	No	0.844	Yes
Pine Upland	0.004	No	0.008	No	0.670	Yes
Dwarf Cypress	0.052	Yes	0.001	No	0.638	Yes
Marsh	0.117	Yes	0.002	No	0.691	Yes
Wet Prairie	0.008	no	0.000	No	0.697	Yes

Table 4.13. Rank Test Results for Wet Season Dataset. The rank test performed consisted of subtracting the control AET values from the model AET values (i.e. $AET_m - AET_c$).

Site	Positive Differences	Negative Differences	Result
Cypress Swamp	0	42	Underestimation
Pine Upland	5	36	Underestimation
Dwarf Cypress	4	39	Underestimation
Marsh	9	35	Underestimation
Wet Prairie	4	59	Underestimation

Table 4.14. Results of Correlation Tests between Wet Season Control AET and Model AET.

Site	r	σ_r	τ	σ_τ	ρ	σ_ρ
Cypress Swamp	0.434	0.004	0.208	0.520	0.283	0.069
Pine Upland	0.032	0.843	-0.034	0.753	-0.067	0.676
Dwarf Cypress	-0.201	0.196	-0.141	0.184	-0.226	0.144
Marsh	0.114	0.462	-0.019	0.856	-0.013	0.934
Wet Prairie	0.308	0.014	0.219	0.011	0.315	0.012

Comparisons between control AET and modeled PET were carried out for the wet season data due to the poor performance of the model and the propensity for AET rates to reach PET rates during the wet season. As before, rank tests (Table 4.15) and correlation tests (Table 4.16) were performed to see how closely control AET data approached the calculated PET values for each site during the wet season. We see that PET is predominately larger than the control AET (i.e. PET – Control AET > 0 for the majority of data pairs) but that these two datasets are better correlated than Model and Control AET. This correlation between PET and control AET can further be seen in Figure 4.13.

Table 4.15. Rank Test Results for Wet Season Dataset. The rank test performed consisted of subtracting the PET values from the model AET values (i.e. PET – AET_c).

Site	Positive Differences	Negative Differences	Result
Cypress Swamp	32	14	Overestimation
Pine Upland	46	0	Overestimation
Dwarf Cypress	42	4	Overestimation
Marsh	46	0	Overestimation
Wet Prairie	58	8	Overestimation

Table 4.16. Results of Correlation Tests between Wet Season Control AET and Model PET.

Site	r	σ_r	τ	σ_τ	ρ	σ_ρ
Cypress Swamp	0.706	< 0.0005	0.507	< 0.0005	0.695	< 0.0005
Pine Upland	0.647	< 0.0005	0.559	< 0.0005	0.728	< 0.0005
Dwarf Cypress	0.391	0.007	0.380	< 0.0005	0.504	< 0.0005
Marsh	0.463	0.001	0.326	0.001	0.446	0.002
Wet Prairie	0.559	< 0.0005	0.400	< 0.0005	0.562	< 0.0005

Figure 4.13. Wet Season Comparison between modeled PET and Control AET Data.

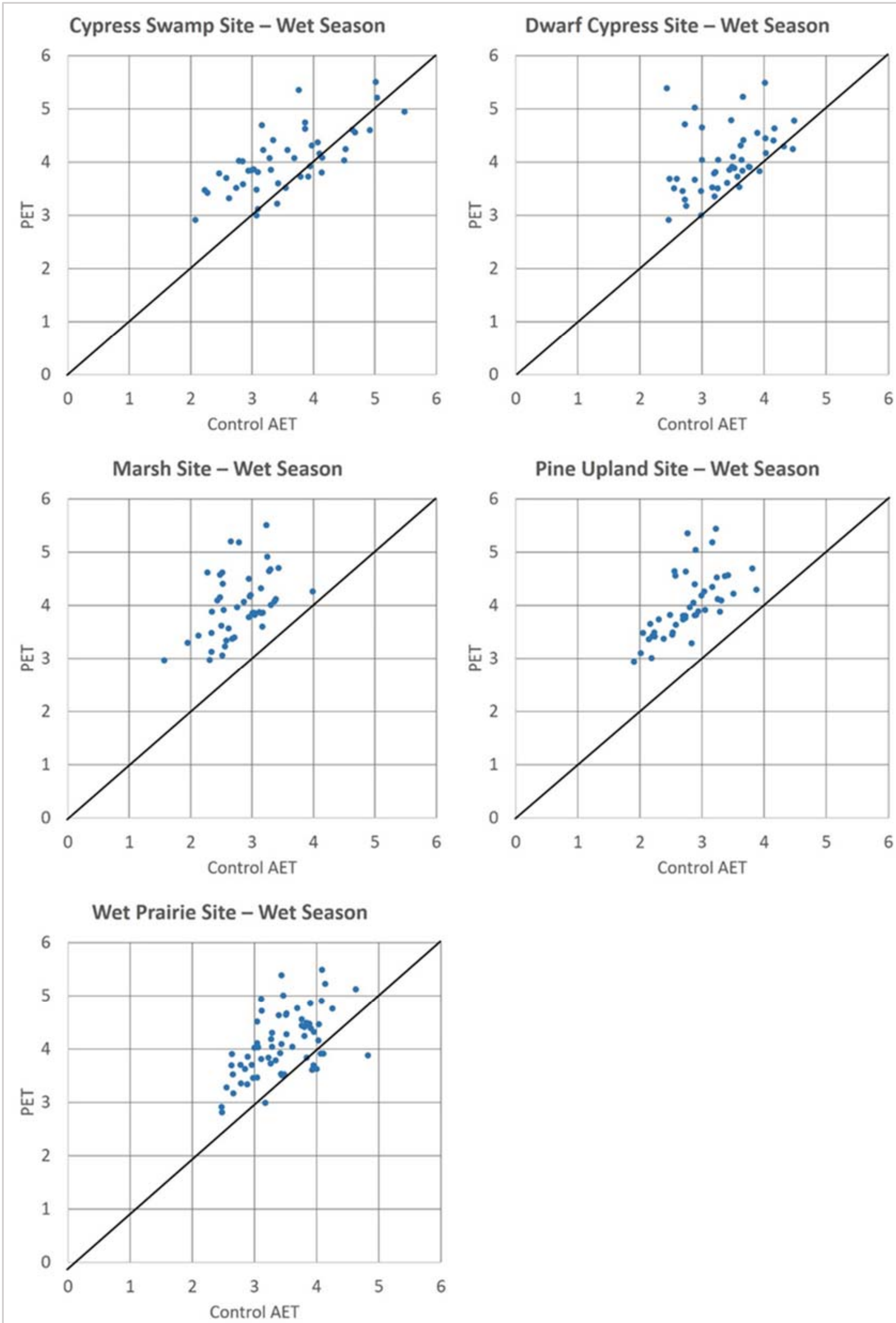

CHAPTER 5: DISCUSSION

5.1. Summary of Results, Hypothesis, and Goals.

The main objective of this study was to validate the applicability of using the "simple method" in conjunction with the SSEB method to produce AET estimates for the South Florida region. This is the first time these models have been used in tandem to produce AET estimates for South Florida. The model utilizes solar radiation data from 15 South Florida sites to calculate PET values using the "simple model". These values are then interpolated to create a surface of PET values which stretches over the South Florida region. MODIS temperature images are used to create Etf maps using the SSEB approach. The PET surface and Etf maps are then multiplied together to create final AET maps of the study area. The model data was compared to USGS eddy covariance tower data at five different sites located inside Big Cypress National Preserve. The comparison data used stretch from January 1st, 2008 to December 31st 2010.

The model showed varying degrees of success depending on the time of year. There was a clear distinction between certain parts of each year. MODIS temperature data for hotter, wetter months like August and September had a higher instance of missing and low value pixels than images taken during cooler, dryer months (December, January). Hence, the data were separated into "Dry" (data from November to April of each year) and "Wet" (data from May to October of each year) sets to see how each distinct season affected the overall trends seen in the complete dataset.

Dry months experienced closer agreement between model and control data with an average RMSE and bias across the five sites of 0.602 mm and -0.213 mm respectively. Furthermore, control and model AET values showed significant correlation at all five sites with the lowest correlation occurring at the Marsh site (r(59) = 0.568) and the highest occurring at the Dwarf Cypress Swamp (r(59) = 0.791). Control and modeled AET values experienced little agreement during Wet season months. The average RMSE and bias for the five control sites were 1.725 and -1.281 respectively. No site showed a significant correlation between control and modeled AET values. Wet season control values did show a stronger correlation with PET values, demonstrating that as expected, AET tends to be high and close to the PET values during wet season.

The first major question this study set out to answer was whether the combination of these two methods was applicable to the South Florida study area. By "applicable" it was meant that the procedure is not severely limited by the geography or any other variable associated with the calculation process. It was hypothesized that surface temperature and solar radiation would be sufficient variables to accurately calculate Actual Et values for the study area. The results show that these two variables can provide reasonable values of AET during dry periods of the year. But, poor quality and missing temperature data during extended periods of cloud cover mostly experienced during the wetter parts of the year, lead to critically underestimated AET values. Extended cloud cover periods occurred frequently during the wet seasons of the 3 year period. Cloud cover was the main source of missing and underestimated temperature data. The missing and low temperature pixels values translated to low or missing Etf values which in turn resulted in missing or severely underestimated AET values. Derived PET and Etf values using this model provide satisfactory estimates of AET when cloud cover was not continuously present for long periods of time as seen for most 8-day periods occurring during the dry season.

This analysis also asked whether the SSEB/Simple Method approach would be useful for the Everglades study area. By “useful”, it was meant that the procedure will provide comparable results to those obtained by more standard methods (Florida Water Management Data) while still maintaining its simplicity and ease of use. It was hypothesized that the Actual Et values derived from the SSEB/simple model approach would have a significant correlation to control values provided by USGS, with a correlation coefficient (R) of at least 0.7. Again, the utility of the model is affected by the season of the year. Dry periods showed high correlation values between control and modeled AET values. Three of the control sites showed a correlation value (R) higher than 0.7 (Dwarf Cypress, Pine upland, and Cypress Swamp), while the remaining two sites (Marsh and Wet Prairie) showed a correlation value higher than 0.5. Data obtained for each site during wet periods show very little correlation between control and modeled data. All five sites show correlations lower than 0.5 during wet season and control values show stronger correlations to experimental PET than to experimental AET. These results again confirm the tendency of the model to perform much better during dry periods than during wet periods of the year.

It must be noted that the validation sites were all located in a wetland environment and there were no validation sites within urban or agricultural regions. This is important since the k-coefficient (k = 0.53) used in the Simple Equation corresponds to a wetland environment. Hence, the PET values calculated in the current study may not be representative of the PET values of urban or agricultural regions. A new k-coefficient may be needed to better represent the PET values seen in these regions. A larger number of validation sites, covering both agricultural and urban areas, are needed to assess the accuracy of the current model when predicting both PET and AET rated at urban and agricultural regions. Unfortunately, no long term, easily accessible AET monitoring sites were found within urban or agricultural to provide validation data for the current study. Hence, further study is needed to validate the accuracy of the Simple-Model/SSEB methodology for urban and agricultural environments.

The study also aimed to answer how many ground based stations are sufficient to provide accurate evapotranspiration values for the Everglades study area. The study only had 15 available stations from which to collect solar radiation, hence it was expected that these 15 sites would be enough to create reliable PET maps of the study region. In practice, the 15 sets of solar radiation data were enough to create the PET maps needed to calculate AET maps. That said, the interpolation method (Baysian-Kriging method) had a tendency of underestimating high PET values and overestimating low values. This “narrowing” of values is seen in the majority of interpolated PET maps and it is most pronounced when either the lowest and/or highest PET value used to create the interpolation is an outlier. Because of this narrowing effect on interpolated PET values it is not recommended to use less sources of solar radiation data than the 15 used in this study. A quick test using only 9 stations reproduced similar surfaces as those created with 15 stations, but it is recommended to use as many sources of data as possible in order to optimize the output of the interpolation method. This is because Kriging interpolation works best with a normally distributed set of data, which is tough to achieve with 15 or fewer data points. It is anticipated that the narrowing effect experienced is due to the small number of data points being interpolated and that a much larger set of data points would reduce this effect.

5.2. Comparison to Previous Studies and Challenges Experienced.

Several previous studies have provided ET estimates for the South Florida region. In general, annual ET for South Florida is estimated to be about 137 cm by the SFWMD (Abtew, 2003). All previous studies reviewed show the strong seasonal pattern seen in this study (German, 2000; Douglas, 2009; Abtew, 2004; Bidlake 1996), where the highest ET rates are measured during wet season months and lower ET rates are measured in dry season months. The method tested in this study does not provide useful ET estimates for wet season months, making the calculation of yearly estimates not feasible. Hence a direct comparison between yearly ET rates provided by this model and others is not possible. Instead of yearly ET comparison, dry season ET comparisons are made. Abtew (1996) used Lysimeters to calculate ET of a marsh site from 1993 to 1994. The average ET of dry season months (Nov. to Apr.) were 3.16 mm/day in 1993 (Jan. estimate not included) and 2.74 mm/day in 1994. The lowest dry season ET of the study period corresponded to January of 1994 (1.9 mm/day) and the highest ET corresponded to April of 1993 (4.8 mm/day). Douglas (2009) conducted a broader study relying on several methods, including the Priestly-Taylor and Penman-Monteith methods, to calculate ET for a wide range of site across Florida. Among the sites were several marsh sites inside Everglades National Park and a few pine forest sites in Northern Florida. The marsh sites showed an average ET of 3.0 mm/day and the Pine forest sites had an average ET of 2.05 mm/day. Estimates from Lysimeter sites (sawgrass and cattail) carried out from 1996 to 1999 give dry season ET average estimates ranging from 1.42 mm/day (Jan. cattail) to 4.9 mm/day (Apr. Sawgrass) (Mao, 2002). Dry season ET estimates ranging from about 1.5 mm/day to about 4.5

mm/day are seen in the majority of ET studies of wetland regions across Florida (German, 2000; Douglas, 2009; Abtew, 2004; Bidlake 1996).

The ET estimates calculated in this study fall within the range seen in the aforementioned studies. In general the estimates calculated through the Simple/SSEB method fall towards the low end of the range. For example, the marsh site had a dry season average of 1.97 mm/day over the observation period which is lower than the average seen at similar sites in Abtew's and Douglas's studies. Similarly, the Pine Upland site had an average dry season of 1.77 mm/day, which again is lower that the ET estimates of previous studies. The control values provided by Shoemaker (2011) – 2.01 mm/day for the Marsh site and 1.82 mm/day for the Pine Upland site - show that the low dry season ET estimates are not necessarily due to poor model performance, but that the dry seasons ET rates experienced during the study period were lower than those of previous study periods. The average experimental dry season ET across all five sites was 1.92 mm/day which falls within the range of ET values observed in previous studies (German, 2000; Abtew, 1996; Douglas, 2009). The average control dry season AET across all five sites was 2.14 mm/day. These averages show that the model does tend to slightly underestimate the AET values for all five sites.

A second interesting feature of the experimental AET data is evident when looking at the dry season averages (Table 5.1). The averages for dry season AET are relatively close to one another, and the higher the control AET value is, the more severe the model underestimation becomes. The most probable reason for this feature in the experimental

Table 5.1. Mean Control and Experimental AET values for five control sites.

Site	Control AET (mm)	Experimental AET (mm)
Cypress Swamp	2.30	1.94
Pine Upland	1.82	1.77
Dwarf Cypress	2.21	2.00
Marsh	2.01	1.97
Wet Prairie	2.36	1.95
Average	2.14	1.93

data is the "narrowing" of estimated PET values due to the Bayesian-Kriging interpolation method utilized. Steep, or relatively steep, changes in solar radiation (and consequently PET) estimates are not well represented when only 15 data points are used to create the interpolated surfaces used as part of the final AET calculation. In a way, the surfaces are "too smooth" and are unable to accurately represent areas of unusually high or low PET. Even with this smoothing effect in place, the error parameters (coefficient of variation, RMSE, Bias/$Mean_{obs}$, RMSE/$Mean_{obs}$) calculated for dry season experimental AET values fall within errors usually seen in remote sensing based methods, which range from 15% to 40% (Allen, 2011; Kustas, 1996).

More specifically, Allen (2011) states that AET estimates through remote sensing methods can expect errors (defined as one standard deviation away from the true mean) between 10% and 30%. The metric in this study that provides the most similar definition of error as defined by Allen is RMSE/$Mean_{con}$, which also gives an estimate of how far away the experimental values fall from the true values (in this case taken to be the control value). The average RMSE/$Mean_{con}$ of the five control sites was 28.1%, meaning that on average the experimental values were about 30% away from the control value. In a similar study to that carried out in this study, Jiang (2009) used daily LST data to provide daily AET estimates in the South Florida region. His results showed a range for RMSE/$Mean_{con}$ from 23.1% to 45% across 11 sites, with an average of 30.8%, which again is similar to the RMSE/$Mean_{con}$ observed across the five sites used in this study for dry season months. In general, the Simple/SSEB method provided AET estimates in line with previous studies using relatively simple techniques which do not require the technical expertise, large equipment and maintenance costs, nor time that other methods require (Abtew, 2004; Enku, 2011; Douglas, 2009; Courault, 2005).

The calculation of AET estimates carried out in this study experienced common challenges faced by similar wetland AET estimation studies. First and foremost, prolonged periods of cloud cover experienced during wet season months had a serious effect on the LST data provided by the MODIS sensor. This lead to a serious underestimation of Etf, and consequently AET, estimates. Jiang (2009) was also faced with the problem of clouded out remotely sensed images and applied a model where missing pixels were approximated by using neighboring pixels and pixels from previous observations. This can work, as Jiang (2009) showed, but not when a large portion of the observation area is clouded out for a long time (the better part of 8 days in this study). In this situation, there are just not enough pixels to use as reference to estimate the missing pixel values. The ability to acquire useful LST data under cloudy conditions would definitely improve the AET estimates provided by this study and it remains a major challenge for any methodology that relies on remote sensing to provide useful AET estimates for the South Florida or any region.

The second major challenge faced by this study was the lack of a comprehensive and coordinated source of meteorological data, specifically solar radiation data, for the South Florida region. The SFWMD DBHYDRO database provided the study with 15 solar radiation data sources, which proved sufficient for methodology carried out in this study. But, the final AET estimated could have benefited from a much larger number of solar radiation data sources. As previously mentioned, the interpolation technique used to create the PET surfaces works best with a large set of data (50 or more points). Finding fifty or more sources of quality, long-running solar radiation measurements in the South Florida region proved impossible. Another noticeable issue with the availability of solar radiation data has to do with the distribution of weather stations providing useful data. Figure 3.4 shows the unsymmetrical distribution of stations providing solar radiation data, with most of the stations located on the northern edge of the study area and very few stations located on the southern edge. The lack of stations providing solar radiation data from areas inside Everglades National Park is evident and speaks to the great challenge of installing and maintaining monitoring equipment within such a large and often inaccessible area. That said, a more expansive and comprehensive network of basic weather monitoring stations would alleviate one of the major challenges faced by AET estimation studies in the South Florida region.

CHAPTER 6: CONCLUSION AND RECOMMENDATIONS

6.1. Conclusion

The Simple-Method/SSEB model tested in this study provided mixed results. On one hand, AET estimates provided by the model had good agreement with control EC values during dry season months. For these dry months, the model proved to be both applicable and useful (as defined at the outset of this study) and provided AET values that may help wetland recovery assessments. On the other hand, AET estimates for wet season months were severely underestimated and should not be used for any restoration assessment. The main source of error for wet month AET estimates came from poor LST data from the MODIS sensor, which suffered from many prolonged periods (the majority or the whole 8-day observation period) of cloud cover.

The model shows promise as a quick and simple monitoring tool for wetland recovery but needs improvement. It is notable that the simplicity of the model, which relies only on temperature and solar radiation data, can produce comparable results to more complex methods when the input data used is of good quality. Furthermore, this study demonstrated the model's ability to successfully cover a study area as large as the South Florida region. The model's ability to cover such a vast study area is a clear benefit that saves on time and on equipment costs. Unfortunately, the underestimation of AET values during wet season months limits the model's use and prevents it from providing accurate weekly estimates over a full year time span. Weekly, accurate estimates seem feasible for dry season months.

The close agreement between model and control AET values during dry season months show that the model can work given good quality input data. The poor performance of the model during wet season months does not necessarily discredit the ability of the model to predict accurate AET values, but it certainly hinders its usage. As it stands, the model is best suited for shorter term studies conducted during the dry months of the year. It may also be well suited for multi-year comparisons of dry season AET rates. Hence, the model works best for assessing short term (months during dry season) changes experienced by a wetland due to restoration efforts. Long term effects can be explored by comparing dry season AET rates from year to year and noting any overall increase or decrease of AET rates from one year to the next.

6.2. Recommendations

Several aspects of the Simple-Model/SSEB approach tested in this study can benefit from further refinement. First and foremost, better methods of gathering LST data are needed to replace the poor quality data that abounds during wet season months. Second, a larger network of solar radiation monitoring stations would help create more accurate PET maps for the South Florida region. Finally, Etf calculation may benefit from the introduction of new parameters (not just temperature) in order to increase the accuracy of final AET estimates. The following section elaborates on these main recommendations and gives possible solutions to make the procedure tested in this study more robust and practical to use.

First, a better estimation of wet season AET rates in necessary for this model to truly achieve the goals set out at the beginning of the study. To do so, the low quality 8-day temperature data provided by MODIS during certain parts of the year must be overcome. The missing and underestimated LST data from MODIS were the main source of error for the final AET values. The 8-day composite temperature images are created by averaging the “clear sky” pixels from 8 single day temperature images. Defining a “clear sky” pixel is a rather complex endeavor detailed in Ackerman (2010), but in simple terms, a clear sky pixel is free from most, if not all, cloud contamination. In order to have a missing pixel in the 8-day composite image the majority (or all) of the single day images must have that pixel missing as well (i.e. clouded out). But, there is a chance that a clear sky pixel exists within one of the 8 single day images.

The single day LST data can provide one method of overcoming poor 8-day LST images. Single day LST images may be used instead of the 8-day average LST images to calculate the corresponding Etf, in the hopes that one clear image is more representative of the actual LST’s for an 8-day period than an average that includes days with missing LST data. Finding this clear single day temperature requires looking into the “clear_sky_days” layer of the MODIS image (See Table 3.1). This layer provides a number for every pixel that, when converted to binary, tells which days/nights had clear sky temperature values. The pixel values can be extracted using ArcMap software and then single day temperature images that have clear sky pixels can be downloaded using the same process described in the methodology section (in this case the MODIS product being downloaded is MOD11A1 instead of MOD11A2). These single day clear sky temperature values are then used to calculate the Etf for the pixel of interest.

This procedure was tested for a few 8-day periods that exhibited missing and underestimated pixels. Unfortunately, this procedure did not produce better Etf values than the original method. First, many of the pixel labeled as “clear day” were only clear during the nighttime. The binary flag provided by the “clear-sky” layer returns as “clear day” if either the day or night pixel is clear. Many of the 8-day periods investigated had all 8 days clouded out for a given pixel even though the “clear_sky_days” flag returned a clear flag for one day (or more) within the specific period. The positive flag was due to the pixel having a “clear” temperature value at night. Another issue afflicting the process of finding single day temperatures to substitute for 8-day average temperatures is how different days accounted for “clear sky” data for different pixels.

For example, if one is looking to substitute temperature values for five different pixels within the same 8-day period, it may be necessary to look at five different single day images. This means processing five extra images in order to obtain new Etf values. This might be feasible for a small amount of pixels over a small number of 8-day periods, but it makes trying to replace hundreds of pixels (common for the wet season images) over several months’ worth of images rather unmanageable. For now, the clearest solution for this problem is the acquisition of better temperature data. More complete data may be available from other satellite based sensors such as LandSat (Allen, 2005). For now, this study shows that calculated PET values give a better estimation of the control AET values than the modeled AET during the wet months of the year. Hence, looking at PET values during wetter months can at least give an idea of the AET rates for the study region.

Dry season AET results, which showed that the model can provide useful estimates, can also be improved by increasing the number of solar radiation data sources. The solar radiation data provided by SFWMD were of good quality, have been actively collected for a long period of time, and are easily accessible online. So, it would be of great benefit to future studies to have more stations providing such quality solar radiation. As mentioned before, having access to more than the 15 stations used in this study would allow for better

PET surface interpolations. Just as beneficial would be for those solar radiation stations to cover a wider range of the study site. For this study, the majority of solar radiation stations were located towards the northern edge of the study site. Only four stations were available to cover the entire South and Southeastern edges of the study area. In other words, only a few stations were used to represent the solar radiation being received for a large expanse of the study site, an expanse that covered most of Everglades National Park. The lack of coverage in these areas led to the underrepresentation of solar radiation variability within them, leading to less accurate PET estimates. So, adding stations to provide better, more even coverage of the study site would be just as beneficial to the final PET estimates (and consequently the AET estimates) as adding more solar radiation stations.

Improvements to the Etf estimation procedure can also help improve the accuracy of final AET estimates. Aside from correcting the aforementioned LST data issues, the Etf estimates could benefit from incorporating factors other than just LST into their calculation. This is currently being done in other studies that incorporate more complex techniques of calculating T_h and T_c, (Senay, 2013; Savoca, 2013). The approaches being tested may increase the accuracy of the final AET estimates, but they do so at the expense of simplicity. Whether these improvements in accuracy are worth sacrificing the simplicity of the model is a question that is still open to debate. The use of other remote sensing platforms which can provide higher resolution data and/or compliment the data provided by MODIS would also benefit final AET estimates accuracy. Lastly, ground based atmospheric temperature measurements (not remotely sensed) may help fill in data gaps found in the MODIS LST images; but, land surface temperature values and atmospheric temperature readings may not produce similar ETf results.

All in all, this study showed that the combination of the “Simple” model and the SSEB method can work well together to provide AET estimates. The model is easy to use, can cover a large area, and can produce similar results to the more established Eddy Covariance method. The main issue keeping this model from being a viable way of calculating reliable, weekly AET estimates is a lack of quality LST data for wet periods of the year. Although limited, this model can be a quick and relatively simple way of obtaining AET estimates to assess the success of wetland restoration projects. By working within the current limitations of the model, a short term (months) continuous monitoring of a treated wetland area can be conducted; Long term monitoring of wetland AET can also be conducted by comparing specific periods of time (during dry season) from year to year.

REFERENCES

Abers, J. S. (2012). Part I and Part II. In J. S. Abers, *Wetland environments: A Global Perspective* (pp. 1-57, 59-132). Chichester: Wiley and Sons.

Abtew, W. (1996). Evapotranspiration measurements and modeling for three wetland systems in South Florida. *Journal of the American Water Resources Association, 32*, 465-473.

Abtew, W. (1996). Evapotranspiration Measurements and Modeling for Three Wetland Systems in South Florida. *J. of the American Water Resources Association, 32 (3)*, 465-473.

Abtew, W. (2004). *Evapotranspiration in the Everglades: Comparison of Bowen Ratio Measurements and Model Estimations.* West Palm Beach, Florida 33406: Environmental Resource Assesment Department, South Florida Water Management District.

Abtew, W., & Melesse, A. (2013). Ch 6: Evaporation and Evapotranspiration Estimation Methods. In W. Abtew, & A. Melesse, *Evaporation and Evapotranspiration: Measurements and Estimations* (pp. 63-91). Dordretcht: Springer.

Abtew, W., Obeysekera, J., & Iricanin, N. (2011). Pan evaporation and potential evapotranspiration trends in South Florida. *Hydrol. Process., 25*, 958–969.

Abtew, W., Obeysekera, J., Irizarry-Ortiz, M., Lyons, D., & Reardon, A. (2003). Evapotranspiration Estimation for South Florida. *Evapotranspiration Estimation for South Florida. World Water & Environmental Resources Congress 2003*, 1-9.

Ackerman, S., Frey, R., Strabala, K., Liu, Y., Gumley, L., Baum, B., & Menzel, P. (2010). *Discriminating clear-sky from cloud with MODIS algorithm theoretical basis document (MOD35).* Madison: Cooperative Institute for Meteorological Satellite Studies, University of Wisconsin.

Acreman, M., Fisher, J., Stratford, C., Mould, D., & Mountford, J. (2007). Hydrological Science and Wetland Restoration: Some case studies from Europe. *Hydrol. Earth Syst. Sci., 11(1)*, 158-169.

Allen, R. G., Jensen, M. E., Wright, J. L., & Burman, R. D. (1989). Operational Estimates of Reference Evapotranspiration. *Agron. J., 89*, 650–662.

Allen, R., Pereira, L., Howell, T., & Jensen, M. (2011). Evapotranspiration information reporting: I. Factors governing measurement accuracy. *Agricultural Water Management, 98*, 899-920.

Allen, R., Pereira, L., Raes, D., & Smith, M. (1998). *Crop Evapotranspiration.* Rome, Italy: Food and Agriculture Organization of the United Nations.

Allen, R., Tasumi, M., & Trezza, R. (2007). Satellite-Based Energy Balance for Mapping Evapotranspiration with Internalized Calibration (METRIC)-Model. *Journal of Irrigation and Drainage Engineering, Vol. 133(4)*, 380.

Allen, R., Tasumi, M., Morse, A., & Trezza, R. (2005). A Landsat-based energy balance and evapotranspiration model in Western US water rights regulation and planning. *Irrigation and Drainage Systems, 19*, 251-268.

Arthington, A. (2012). Wetlands, Threats, and Water Requirements. In A. Arthington, *Freshwater Ecology Series, Volume 4 : Environmental Flows : Saving Rivers in the Third Millennium* (pp. 243-258). Berkeley: University of California Press.

Bastiaanssen, W., Menenti, M., Feddes, R., & Holtslag, A. (1998a). A remote sensing surface energy balance algorithm for land (SEBAL) 1. Formulation. *Journal of Hydrology 212-213*, 198-212.

Bastiaanssen, W., Noordman, E., Pelgrum, H., Davids, G., Thoreson, B., & Allen, R. (2005). SEBAL Model with Remotely Sensed Data to Improve Water-Resources Management under Actual Field Conditions. *Journal of Irrigation and Drainage Engineering, 131*, 85-93.

Bastiaanssen, W., Pelgrum, H., Wang, J., Ma, Y., Moreno, J., Roerink, G., & van der Wal, T. (1998b). A remote sensing surface energy balance algorithm for land (SEBAL) 2. Validation. *Journal of Hydrology 212-213*, 213-229.

Bedford, B. (1999). Cumulative effects on wetland landscapes: links to wetland. *WETLANDS, Vol. 19, No. 4*, 775-788.

Bendix, J., & Hupp, C. (2000). Hydrological and geomorphological impacts on riparian plant communities. *Hydrol. Process., 14*, 2977–2990.

Bidlake, W., Woodham, W., & Lopez, M. (1996). *Evapotranspiration from Areas of Native Vegetation in West-Central Florida.* Reston, VA: U.S. Geological Survey.

Bunn, S., & Arthington, A. (2002). Basic Principles and Ecological Consequences of Altered Flow Regimes for Aquatic Biodiversity. *Environmental Management Vol. 30, No. 4*, 492-507.

Cammalleri, C., Ciraolo, G., La Loggia, G., & Maltese, A. (2012). Daily evapotranspiration assessment by means of residual surface energy balance modeling: A critical analysis under a wide range of water availability. *Journal of Hydrology, 452-453*, 119-129.

Clark, I. (1987). *Practical Geostatistics.* London: Elsevier Applied Science.

Clewell, A., & Lea, R. (1989). Creation and restoration of forested wetland vegetation in the southeastern United States. *Wetland Creation and Restoration: The Status of the Science*, 195–232.

Cole, C., & Brooks, R. (2000). Patterns Of Wetland Hydrology In The Ridge And Valley Province, Pennsylvania, Usa. *WETLANDS, Vol. 20, No. 3*, 438–447.

Coll, C., Wan, Z., & Galve, J. (2009). Temperature-based and radiance-based validations of the V5 MODIS land surface temperature product. *J. Geophys. Res., 114*.

Cooper, D., & Merritt, D. (2012). *Assessing the water needs of riparian and wetland vegetation in the western United States.* Fort Collins: United States Department of Agriculture.

Courault, D., Seguin, B., & Olioso, A. (2005). Review on estimation of evapotranpiration from remote sensing data: From empirical to numerical modeling approaches. *Irrigation and Drainage Systems, 19*, 223-249.

Cowdery, T., Lorenz, D., & Arntson, A. (2008). *Hydrology Prior to Wetland and Prairie Restoration in and around the Glacial Ridge National Wildlife Refuge, Northwestern Minnesota, 2002–5.* Reston, Virginia: U.S. Geological Survey.

Davidson, T., Mackay, A., Wolski, P., Mazebedi, R., Murray-Hudson, M., & Todd, M. (2012). Seasonal and spatial hydrological variability drives aquatic biodiversity in a flood-pulsed, sub-tropical wetland. *Freshwater Biology, 57*, 1253–1265.

Davis, D. (2013, September 18). *EPA*. Retrieved from http://permanent.access.gpo.gov/gpo701/threats.pdf

Delclaux, F., & Coudrain, A. (2005). Optimal evaporation models for simulation of large lake levels: application to lake Titicaca, South America. *Geophysical Research Abstracts, Vol. 7*, 53.

Douglas, E., Jacobs, J., Sumner, D., & Ray, R. (2009). A comparison of models for estimating potential evapotranspiration for Florida land cover types. *Journal of Hydrology, 373*, 366-376.

Enku, T., van der Tol, C., Gieske, A., & Rientjes, T. (2011). Ch 8: Evapotranspiration Modeling Using Remote Sensing and Empirical Models in the Fogera Floodplain, Ethiopia. In *Nile River Basin: Hydrology, Climate and Water Use* (pp. 163-178). Dordrecht: Springer.

Faulkner, S., Patrick, W., & Gambrell, R. (1989). Field Techniques for Measuring Wetland Soil Parameters. *Soil Science Society of America journal*, 883-890.

Fisher, J., Whittaker, R., & Malhi, Y. (2011). ET come home: Potential evapotranspiration in geographical ecology. *Global Ecology and Biogeography, 20*, 1-18.

German, E. R. (2000). *Regional Evaluation of Evapotranspiration* . Tallahassee: U.S. GEOLOGICAL SURVEY.

Glenn, P., Doody, T., Guerschman, J., Huete, A., King, E., McVicar, T., . . . Zhang, Y. (2011). Actual Evapotranspiration estimation by ground and remote sensing methods: The Australian experience. *Hydrological Processes, 25*, 4103-4116.

Gurnell , A., Hupp, C., & Gregory, S. (2000). Linking hydrology and ecology. *Hydrological Processes*, 2813-2815.

Immerzeel, W. W., & Droogers, P. (2008). Calibration of a distributed hydrological model based on satellite evaporation. *Journal of Hydrology, 349*, 411- 424.

Janssen, R., Goosen, H., Verhoeven, M., Verhoeven, J., Omtzigt, A., & Maltby, E. (2004). Decision support for integrated wetland management. *Environmental Modeling & Software 20*, 215-229.

Jia, Z., Liu, S., Xu, Z., Chen, Y., & Zhu, M. (2012). Validation of remotely sensed evapotranspiratin over the Hai River Basin, China. *Journal of Geophysical Research, Vol. 117*, 1-21.

Jiang, L., Islam, S., Guo, W., Jutla, A., Senarath, S., Ramsay, B., & Eltahir, E. (2009). A satellite-based Daily Actual Evapotranspiration estimation algorithm over South Florida. *Global and Planetary Change 67*, 62-77.

Konar, M., Todd, J., Muneepeerakul, R., Rinaldo, A., & Rodriguez-Iturbe, I. (2013). Hydrology as a driver of biodiversity: Controls on carrying capacity, niche. *Advances in Water Resources 51*, 317-325.

Kustas, W. P., & Norman, J. M. (1996). Use of remote sensing for evapotranspiration monitoring over land surfaces. *Hydrological Sciences Journal, 41(4)*, 495-516.

LePage, B. A. (2011). Wetlands: A Multidisciplinary Perspective. In *Wetlands: Integrating Multidisciplinary Concepts* (pp. 3-25). Philadelphia: Springer.

Liu, G., Liu, Y., Hafeez, M., Xu, D., & Vote, C. (2012). Comparison of two methods to derive time series of actual evapotranspiration using eddy covariance measurements in the southeastern Australia. *Journal of Hydrology, 454-455*, 1-6.

Makkink, G. F. (1957). Testing the Penman formula by means of lysimeters. *J. Inst. Water Eng, 11(3)*, 277-288.

Maltby, E., & Barker, T. (2009). Section II: Wetlands in the natural environment, how do wetlands work? In E. Maltby, & T. Barker, *The Wetlands Handbook : 2 Volume Set* (pp. 115-326). Oxford: Wiley.

Mao, L., Bergman, M., & Tai, C. (2002). Evapotranspiration Measurement And Estimation Of Three Wetland Environments In The Upper St. Johns River Basin, Florida. *Journal of the Americann Water Resource Association Vol. 38, No. 5*, 1271-1285.

Melesse, A., Abtew, W., & Dessalegne, T. (2009). Evaporation Estimation of Rift Valley Lakes: Comparison of. *Sensors, 9*, 9603-9615.

Melesse, A., Nangia, V., Wang, X., & McClain, M. (2007). Wetland Restoration response Analysis using MODIS and Groundwater Data. *Special Issue: Remote Sensing of Natural Resources and the Environment, SENSORS, 7*, 1916-1933.

Melesse, A., Oberg, J., Nangia, V., & Baumgartner, D. (2006). Spatiotemporal Dynamics of Evapotranspiration and Vegetation at the Glacial Ridge Prairie Restoration. *Hydrological Processes, 20(7)*, 1451-1464.

Miralles, D. G., Holmes, T., De Jeu, R., Gash, J. H., Meesters, A., & Dolman, A. J. (2010). Global land-surface evaporation estimated from satellite-based observations. *Hydrology and Earth System Sciences Discussions, 7*, 8479-8519.

Mitsch, W. G. (2000). *Wetlands.* New York: John Wiley & Sons.

Money, R., Wheeler, B., Baird, A., & Heathwaite, L. (2009). Ch 33: Replumbing Wetlands - Managing Water for the restoration of bogs and Fens. In M. Edward, & T. Barker, *The Wetlands Handbook : 2 Volume Set* (pp. 755-779). Oxford: Wiley.

Mu, Q., Heinsch, F. A., Zhao, M., & Running, S. (2007). Develeopment of a global evapotranspiration algorithm based on MODIS and global meteorology data. *Remote Sensing of Environment, 4*, 519-536.

Mu, Q., Zhao, M., & Running, S. (2011). Improvements to a MODIS global terrestrial evaporation algorithm. *Remote Sensing of Environment 115*, 1781-1800.

Oberg, J., & Melesse, A. (2005). Wetland Evapotranspiration Dynamics Vs. Ecohydrological Restoration: An Energy Balance and Remote Sensing Approach. *J. of American Water Resources Association 42(3)*, 565-582.

Oudin, L., Hervieu, F., Michel, C., Perrin, C., Andreassian, V., Anctil, F., & Loumagne, C. (2005). Which potential evapotranspiration input for a lumped rainfall–runoff model?: Part 2—Towards a simple and efficient potential evapotranspiration model for rainfall–runoff modelling. *Journal of Hydrology, Volume 303*, 290–306.

Price, C. (1990). Using Spatial Context in Satellite Data to Infer REgional Scale Evapotranspiration. *IEEE Transactions on Geoscience and Remote Sensing Vol. 28(5)*, 940-948.

Price, J., & Waddington, J. (2000). Advances in Canadian wetland hydrology and biogeochemistry. *Hydrological Processes 14*, 1579-1589.

Savoca, M., Senay, G. B., Maupin, M., Kenny, J., & Perry, C. (2013). *Actual evapotranspiration modeling using operational Simplified Surface Energy Balance (SSEBop) approach.* Reston, Virginia: U.S. Geological Survey.

Senay , G., Budde , M., Verdin , J., & Melesse, A. (2007). A Coupled Remote Sensing and Simplified Surface Energy Balance Approach to Estimate Actual Evapotranspiration from Irrigated Fields. *Sensors, 7(6)*, 979-1000.

Senay, G. B., Budde, M. E., & Verdin, J. P. (2011). Enhancing the Simplified Surface Energy Balance (SSEB) approach for estimating landscape ET; Validation with the METRIC model. *Agricultural Water Management, 98*, 606-618.

Senay, G., & James, V. (2003). Characterization of yield reduction in Ethiopia using a GIS-based crop water balance model. *Canadian Journal of Remote Sensing, 29*, 687-692.

Senay, G., Bohms, S., Singh, R., Gowda, P., Velpuri, N., Alemu, H., & Verdin, J. P. (2013). Operational Evapotranspiration Mapping Using Remote Sensing and Weather Datasets: A New Parameterization for the SSEB Approach. *Journal of the American Water Resources Association, 49(3)*, 577-591.

Senay, G., Budde, M., Verdin, J., & Melesse, A. (2007). A Coupled Remote Sensing and Simplified Surface Energy Balance Approach to Estimate Actual Evapotranspiration from Irrigated Fields. *Sensors, 7*, 979-1000.

Serrat-Capdevila, A., Scott, R., Shuttleworth, W. J., & Valdes, J. (2011). Estimating evapotranspiration under warmer climates: Insights from a semi-arid riparian system. *Journal of Hydrology, 399*, 1-11.

Shoemaker, B., Lopez, C., & Duever, M. (2011). *Evapotranspiration over spatially extensive plant communitiesin the Big Cypress National Preserve, Southern Florida, 2007-2010.* Reston, virginia: U.S. Geological Survey.

Shuttleworth, W. J. (1993). Ch 4: Evaporation. In W. J. Shuttleworth, *Maidment DR (ed) Handbook of Hydrology.* New York: McGraw-Hill, inc.

Taconet, O., Berdnar, R., & Vidal-Madjar, D. (1986). Evapotranspiration over an Agricultural Region Using a Surface Flux/Temperature Model Based on NOAA-A VHRR Data. *Journal of Climate and Applied Meteorology, Vol. 25*, 284.

Tang, R., Li, Z., & Chen, K. (2011). Validating MODIS-derived land surface evapotranspiration with in situ measurements at two AmeriFlux sites in a semiarid region. *Journal of Geophysical Research, 116*.

Tapley, B., Bettadpur, S., Reis, J., Thompson, P., & Watkins, M. (2004, July 23). GRACE Measurements of Mass Variability in the Earth System. *Science*, pp. 503-505.

Tapley, B., Bettadpur, S., Watkins, M., & Reigber, C. (2004). The gravity recovery and climate experiment: Mission overview and early results. *Geophysical Research Letters, 31*, DOI: 10.1029/2004GL019920.

Timmermans, W., Kustas, W., Anderson, M., & French, A. (2007). An intercomparison of the Surface Energy Balance Algorithm for Land (SEBAL) and the Two-Source Energy Balance (TSEB) modeling schemes. *Remote Sensing of Environment, 108*, 369-384.

Todd, J., Muneepeerakul, R., Pumo, D., Azaele, S., Miralles-Wilhelm, F., Rinaldo, A., & Rodriguez-Iturbe, I. (2010). Hydrological drivers of wetland vegetation community distribution within Everglades National Park, Florida. *Advances in Water Resources Vol. 33, Iss. 10*, 1279–1289.

Turner, R., & Lewis, R. (1997). Hydrologic restoration of coastal wetlands. *Wetlands Ecology and Management Vol. 4 no. 2*, 65-72.

U.S. Army Corps of Engineers. (2013, September 18). *About CERP: A Brief Overview*. Retrieved from http://www.evergladesplan.org/about/about_cerp_brief.aspx

van der Valk, A., Squires, L., & Welling, C. (1994). Assessing the Impacts of an Increase in Water Level on Wetland Vegetation. *Ecological Applications Vol. 4, No. 3*, 525-534.

Various. (2012). *MODIS Level 1B Product User's Guide.* Greenbelt, MD: NASA/Goddard Space Flight Center.

Venterink, O., Davidsson, T., Kiehl, K., & Leonardson, L. (2002). Impact of drying and re-wetting on N, P and K dynamics in a wetland soil. *Plant and Soil 243*, 119-130.

Wan, Z. (2006). *Collection-5 MODIS Land Surface Temperature Products User's Guide.* Santa Barbara: University of California.

Wan, Z. (2008). New refinements and validation of the MODIS Land-Surface Temperature/Emissivity products. *Remote Sensing of Environment, 112*, 59-74.

Wang, K., & Dickinson, R. (2012). A Review of Global Terrestrial Evapotranspiration: Observation, Modeling, Climatology, and Climatic Variability. *Reviews of Geophysics, 50*, 1-54.

Wang, K., & Liang, S. (2008). An Improved Method for Estimating Global Evapotranspiration Based on Satellite Determination of Surface Net Radiation, Vegetation Index, Temperature, and Soil Moisture. *Journal of Hydrometeorology, 9*, 712-727.

Wassen, M., Okruszko, T., Kardel, I., Chormanski, J., & Swiatek, D. (2006). Eco-Hydrological Functioning of the Biebrza Wetlands: Lessons for the Conservation and Restoration of Deteriorated Wetlands. In Various, *Ecological Studies 191 Wetlands: Functioning, Biodiversity Conservation, and Restoration* (pp. 285-310). Berlin: Springer.

Wetlands Definitions. (2013, Oktober 5). Retrieved from epa.gov: http://water.epa.gov/lawsregs/guidance/wetlands/definitions.cfm

Xu, C.-Y., & Singh, V. (2000). Evaluation and generalization of radiation-based methods for calculating evaporation. *Hydrological Processes 14*, 339-349.

Xu, C.-Y., & Singh, V. (2001). Evaluation and generalization of temperature-based methods for calculating evaporation. *Hydrol. Process., 15*, 305–319.

Zedler, J. (2000). Progress in wetland restoration ecology. *TREE vol. 15, no. 10*, 402-407.

Zhai, L., Feng, Q., Li, Q., & Xu, C. (2010). Comparison and modification of equations for calculating evapotranspiration (ET) with data from Gansu Province, Northwest China. *Irrig. and Drain., 59*, 477–490.

APPENDICES

Appendix A.

Figure A.1. Full Model Etf Data of Control Sites.

Figure A.2. Full Model PET Data of Control Sites.

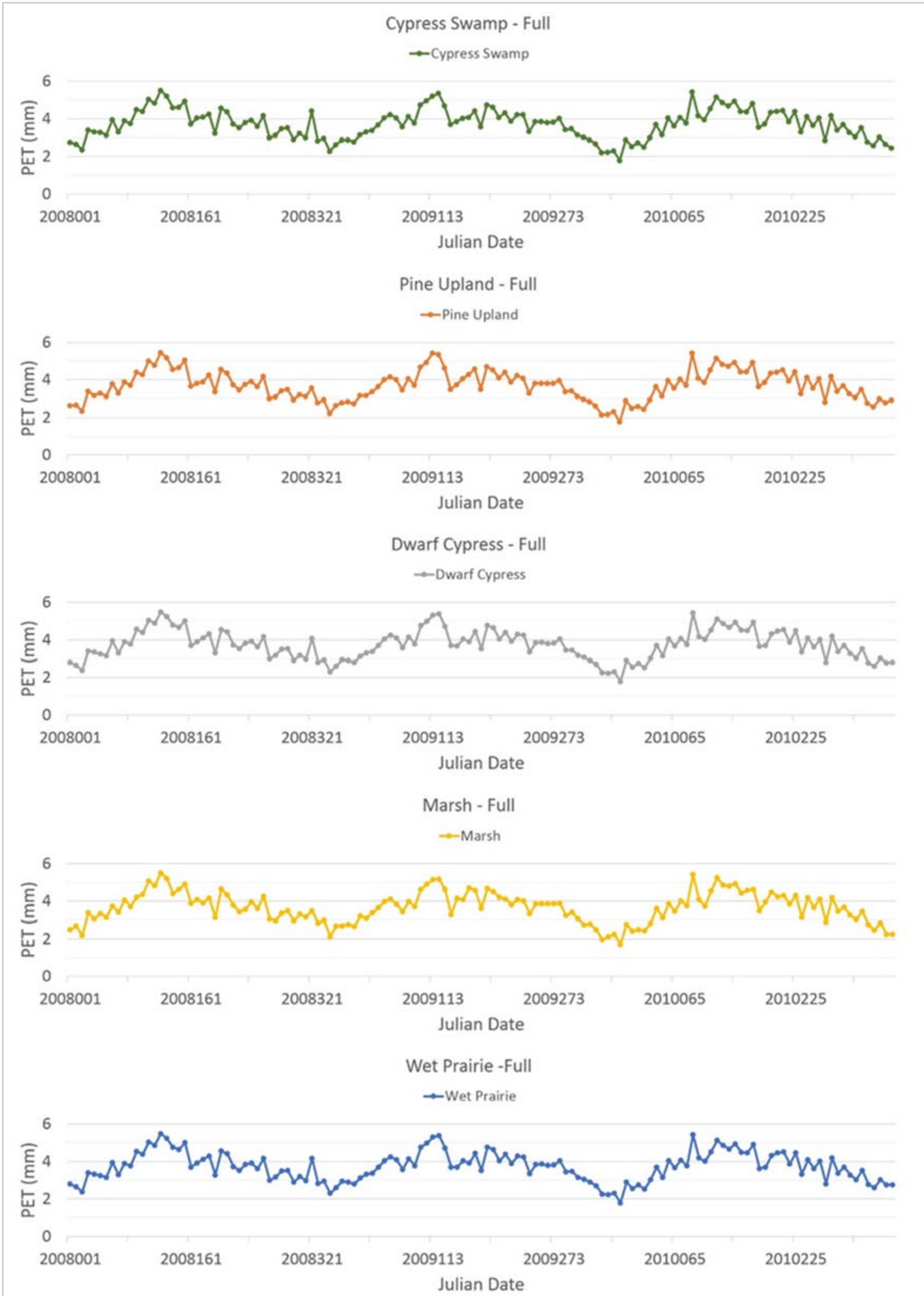

Appendix B. Basic Statistical Information of Validation Data Sets.

Table B.1. Control AET Full Data Set Statistics. Values are given in mm.

Control AET Full (N=105)		Cypress Swamp		Pine Upland		Dwarf Cypress		Marsh		Wet Prairie	
		Value	Std. Error	Value	Std. Error	Value	Std. Error	Value	Std. Error	Value	Std. Error
Mean		2.829	0.106	2.227	0.067	2.723	0.082	2.349	0.066	2.792	0.070
95% CI for Mean	Lower Bound	2.619		2.094		2.561		2.218		2.653	
	Upper Bound	3.038		2.359		2.884		2.480		2.930	
5% Trimmed Mean		2.801		2.209		2.714		2.341		2.783	
Median		2.834		2.143		2.687		2.431		2.726	
Variance		1.172		0.471		0.697		0.457		0.510	
Std. Deviation		1.082		0.686		0.835		0.676		0.714	
Minimum		0.834		1.027		1.152		1.118		1.448	
Maximum		5.483		3.872		4.481		4.343		4.252	
Range		4.650		2.845		3.328		3.225		2.804	
Interquartile Range		1.807		1.161		1.432		0.985		1.184	
Skewness		0.321	0.236	0.315	0.236	0.127	0.236	0.127	0.236	0.223	0.236
Kurtosis		-0.826	0.467	-0.913	0.467	-0.901	0.467	-0.284	0.467	-0.976	0.467

Table B.2. Modeled AET Full Data Statistics. Values are given in mm.

Model AET Full (N=126)		Cypress Swamp		Pine Upland		Dwarf Cypress		Marsh		Wet Prairie	
		Value	Std. Error	Value	Std. Error	Value	Std. Error	Value	Std. Error	Value	Std. Error
Mean		1.952	0.075	1.821	0.068	2.006	0.075	1.986	0.076	1.972	0.078
95% CI for Mean	Lower Bound	1.804		1.687		1.857		1.837		1.818	
	Upper Bound	2.101		1.955		2.155		2.136		2.126	
5% Trimmed Mean		1.922		1.790		1.976		1.960		1.929	
Median		1.883		1.724		1.913		1.890		1.848	
Variance		0.711		0.577		0.718		0.720		0.760	
Std. Deviation		0.843		0.760		0.847		0.848		0.872	
Minimum		0.618		0.635		0.682		0.605		0.629	
Maximum		4.411		4.139		4.313		4.477		4.255	
Range		3.792		3.504		3.631		3.872		3.625	
Interquartile Range		1.331		1.235		1.375		1.320		1.491	
Skewness		0.520	0.216	0.516	0.216	0.420	0.216	0.427	0.216	0.573	0.216
Kurtosis		-0.544	0.428	-0.326	0.428	-0.715	0.428	-0.546	0.428	-0.532	0.428

Table B.3. Modeled PET Full Data Statistics. Values are given in mm.

Model PET Full (N=137)		Cypress Swamp		Pine Upland		Dwarf Cypress		Marsh		Wet Prairie	
		Value	Std. Error	Value	Std. Error	Value	Std. Error	Value	Std. Error	Value	Std. Error
Mean		3.725	0.067	3.701	0.067	3.740	0.067	3.670	0.070	3.740	0.067
95% CI for Mean	Lower Bound	3.593		3.568		3.608		3.532		3.608	
	Upper Bound	3.857		3.833		3.872		3.807		3.872	
5% Trimmed Mean		3.722		3.696		3.736		3.670		3.736	
Median		3.750		3.716		3.724		3.719		3.723	
Variance		0.610		0.618		0.612		0.663		0.611	
Std. Deviation		0.781		0.786		0.782		0.814		0.782	
Minimum		1.785		1.761		1.792		1.704		1.792	
Maximum		5.509		5.439		5.488		5.507		5.493	
Range		3.724		3.678		3.697		3.803		3.700	
Interquartile Range		1.145		1.153		1.150		1.129		1.142	
Skewness		0.015	0.207	0.080	0.207	0.062	0.207	-0.044	0.207	0.052	0.207
Kurtosis		-0.512	0.411	-0.461	0.411	-0.521	0.411	-0.507	0.411	-0.522	0.411

Table B.4. Control AET Dry Season Data Set Statistics. Values given in mm.

Control AET Dry (N=59)		Cypress Swamp		Pine Upland		Dwarf Cypress		Marsh		Wet Prairie	
		Value	Std. Error	Value	Std. Error	Value	Std. Error	Value	Std. Error	Value	Std. Error
Mean		2.272	0.122	1.792	0.063	2.209	0.082	2.001	0.080	2.345	0.068
95% CI for Mean	Lower Bound	2.029		1.666		2.045		1.841		2.209	
	Upper Bound	2.516		1.918		2.374		2.162		2.481	
5% Trimmed Mean		2.217		1.756		2.176		1.963		2.316	
Median		1.969		1.667		2.097		1.922		2.231	
Variance		0.876		0.233		0.398		0.380		0.272	
Std. Deviation		0.936		0.483		0.631		0.616		0.521	
Minimum		0.834		1.027		1.152		1.118		1.448	
Maximum		4.594		3.224		3.884		4.343		4.096	
Range		3.760		2.198		2.732		3.225		2.647	
Interquartile Range		1.259		0.505		0.744		0.873		0.594	
Skewness		1.047	0.311	1.168	0.311	0.708	0.311	1.023	0.311	1.024	0.311
Kurtosis		0.262	0.613	1.159	0.613	0.335	0.613	2.293	0.613	1.282	0.613

Table B.5. Modeled AET Dry Season Data Statistics. Values given in mm.

Model AET Dry (N=66)		Cypress Swamp		Pine Upland		Dwarf Cypress		Marsh		Wet Prairie	
		Value	Std. Error	Value	Std. Error	Value	Std. Error	Value	Std. Error	Value	Std. Error
Mean		1.956	0.094	1.783	0.084	2.002	0.089	1.983	0.093	1.958	0.095
95% CI for Mean	Lower Bound	1.768		1.616		1.825		1.797		1.768	
	Upper Bound	2.144		1.950		2.180		2.168		2.148	
5% Trimmed Mean		1.926		1.746		1.979		1.955		1.922	
Median		1.910		1.721		1.909		1.954		1.848	
Variance		0.584		0.460		0.523		0.567		0.600	
Std. Deviation		0.764		0.678		0.723		0.753		0.775	
Minimum		0.618		0.635		0.762		0.605		0.629	
Maximum		4.411		4.139		4.313		4.477		4.255	
Range		3.792		3.504		3.551		3.872		3.625	
Interquartile Range		0.943		0.841		1.119		1.030		1.180	
Skewness		0.648	0.295	0.853	0.295	0.574	0.295	0.637	0.295	0.666	0.295
Kurtosis		0.402	0.582	1.144	0.582	0.212	0.582	0.528	0.582	0.189	0.582

Table B.6. Modeled PET Dry Season Data Statistics. Values are given in mm.

Model PET Dry (N=68)		Cypress Swamp		Pine Upland		Dwarf Cypress		Marsh		Wet Prairie	
		Value	Std. Error	Value	Std. Error	Value	Std. Error	Value	Std. Error	Value	Std. Error
Mean		3.395	0.099	3.353	0.097	3.411	0.098	3.295	0.101	3.411	0.098
95% CI for Mean	Lower Bound	3.198		3.159		3.215		3.094		3.215	
	Upper Bound	3.591		3.546		3.606		3.496		3.607	
5% Trimmed Mean		3.367		3.320		3.382		3.265		3.383	
Median		3.251		3.168		3.209		3.178		3.218	
Variance		0.662		0.641		0.652		0.691		0.655	
Std. Deviation		0.814		0.801		0.808		0.831		0.810	
Minimum		1.785		1.761		1.792		1.704		1.792	
Maximum		5.431		5.430		5.431		5.418		5.433	
Range		3.646		3.669		3.640		3.715		3.640	
Interquartile Range		1.237		1.089		1.241		1.124		1.248	
Skewness		0.517	0.291	0.637	0.291	0.562	0.291	0.508	0.291	0.552	0.291
Kurtosis		-0.336	0.574	0.109	0.574	-0.210	0.574	-0.167	0.574	-0.244	0.574

Table B.7. Control AET Wet Season Data Set Statistics. Values given in mm.

Control AET Wet (N=46)		Cypress Swamp		Pine Upland		Dwarf Cypress		Marsh		Wet Prairie	
		Value	Std. Error	Value	Std. Error	Value	Std. Error	Value	Std. Error	Value	Std. Error
Mean		3.543	0.119	2.784	0.069	3.381	0.082	2.795	0.067	3.364	0.071
95% CI for Mean	Lower Bound	3.303		2.644		3.216		2.661		3.221	
	Upper Bound	3.783		2.924		3.547		2.929		3.507	
5% Trimmed Mean		3.526		2.773		3.374		2.802		3.365	
Median		3.417		2.783		3.454		2.768		3.401	
Variance		0.652		0.222		0.309		0.205		0.233	
Std. Deviation		0.808		0.471		0.556		0.453		0.482	
Minimum		2.075		1.902		2.429		1.569		2.472	
Maximum		5.483		3.872		4.481		3.985		4.252	
Range		3.408		1.970		2.052		2.417		1.780	
Interquartile Range		1.096		0.705		0.797		0.661		0.745	
Skewness		0.390	0.350	0.187	0.350	0.066	0.350	-0.097	0.350	-0.026	0.350
Kurtosis		-0.371	0.688	-0.389	0.688	-0.797	0.688	0.449	0.688	-0.904	0.688

Table B.8. Modeled AET Wet Season Data Statistics. Values given in mm.

Model AET Wet (N=60)		Cypress Swamp		Pine Upland		Dwarf Cypress		Marsh		Wet Prairie	
		Value	Std. Error	Value	Std. Error	Value	Std. Error	Value	Std. Error	Value	Std. Error
Mean		1.949	0.120	1.863	0.109	2.010	0.125	1.990	0.122	1.987	0.126
95% CI for Mean	Lower Bound	1.709		1.645		1.759		1.745		1.736	
	Upper Bound	2.189		2.081		2.261		2.235		2.239	
5% Trimmed Mean		1.919		1.840		1.981		1.966		1.938	
Median		1.848		1.820		1.979		1.825		1.775	
Variance		0.863		0.712		0.944		0.900		0.948	
Std. Deviation		0.929		0.844		0.972		0.949		0.974	
Minimum		0.683		0.651		0.682		0.631		0.824	
Maximum		3.987		3.614		3.944		4.132		4.074	
Range		3.304		2.963		3.261		3.502		3.249	
Interquartile Range		1.863		1.496		1.824		1.629		1.790	
Skewness		0.444	0.309	0.267	0.309	0.333	0.309	0.301	0.309	0.498	0.309
Kurtosis		-1.125	0.608	-1.106	0.608	-1.259	0.608	-1.166	0.608	-1.009	0.608

Table B.9. Modeled PET Wet Season Data Statistics. Values are given in mm.

Model PET Wet (N=69)		Cypress Swamp		Pine Upland		Dwarf Cypress		Marsh		Wet Prairie	
		Value	Std. Error	Value	Std. Error	Value	Std. Error	Value	Std. Error	Value	Std. Error
Mean		4.050	0.071	4.044	0.073	4.064	0.073	4.039	0.073	4.063	0.073
95% CI for Mean	Lower Bound	3.908		3.899		3.919		3.893		3.918	
	Upper Bound	4.192		4.188		4.209		4.184		4.208	
5% Trimmed Mean		4.040		4.035		4.056		4.029		4.055	
Median		4.032		3.962		4.018		4.069		4.024	
Variance		0.351		0.364		0.366		0.367		0.363	
Std. Deviation		0.592		0.603		0.605		0.605		0.602	
Minimum		2.848		2.814		2.804		2.886		2.811	
Maximum		5.509		5.439		5.488		5.507		5.493	
Range		2.661		2.625		2.684		2.621		2.681	
Interquartile Range		0.790		0.881		0.873		0.909		0.856	
Skewness		0.257	0.289	0.236	0.289	0.255	0.289	0.161	0.289	0.254	0.289
Kurtosis		-0.269	0.570	-0.467	0.570	-0.434	0.570	-0.455	0.570	-0.400	0.570

Appendix C. Histograms, Q-Q plots, and Rank Tests.

Figure C.1. Histograms - Full Control AET Data.

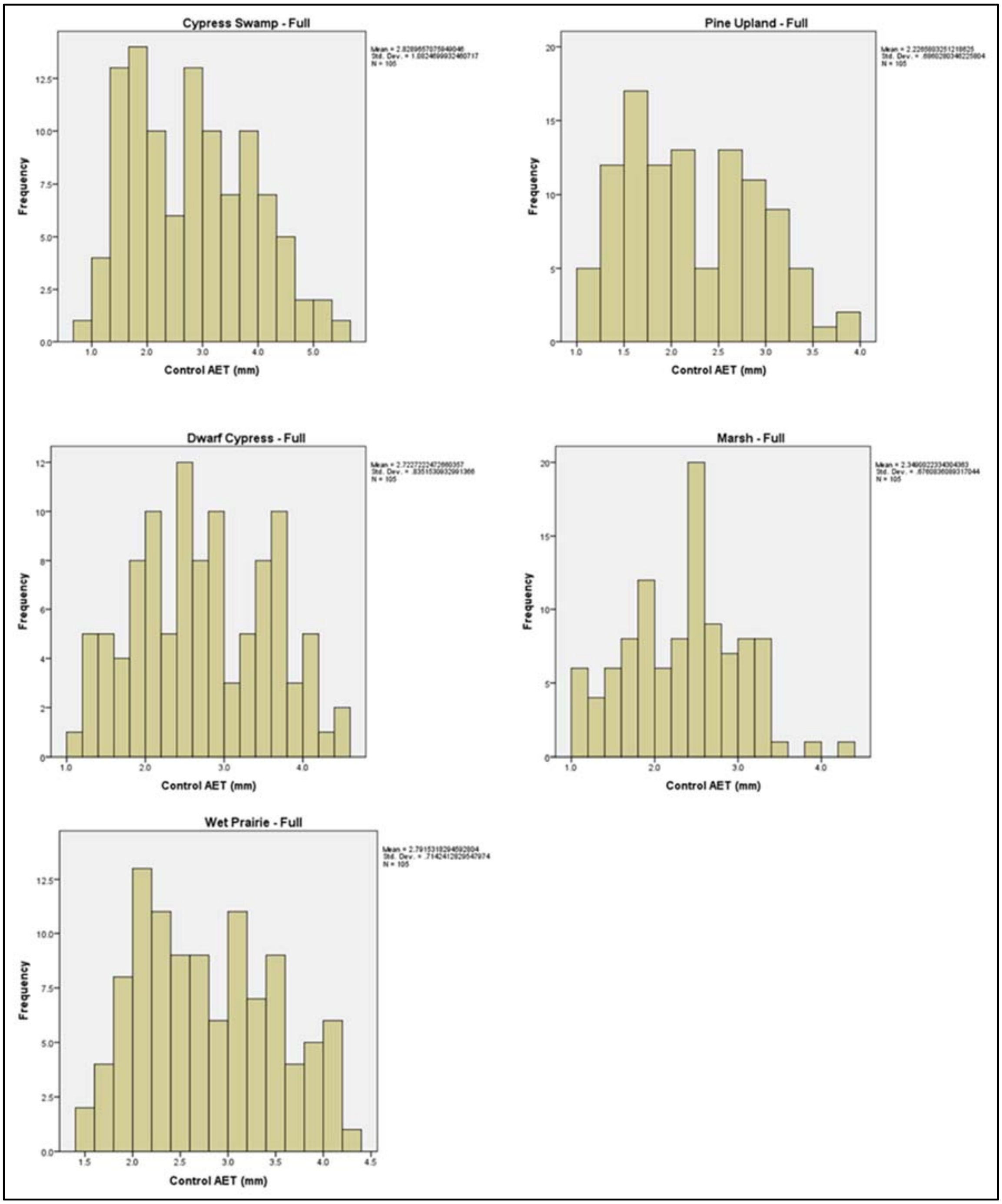

Figure C.2. Q-Q Plots - Full Control AET Data.

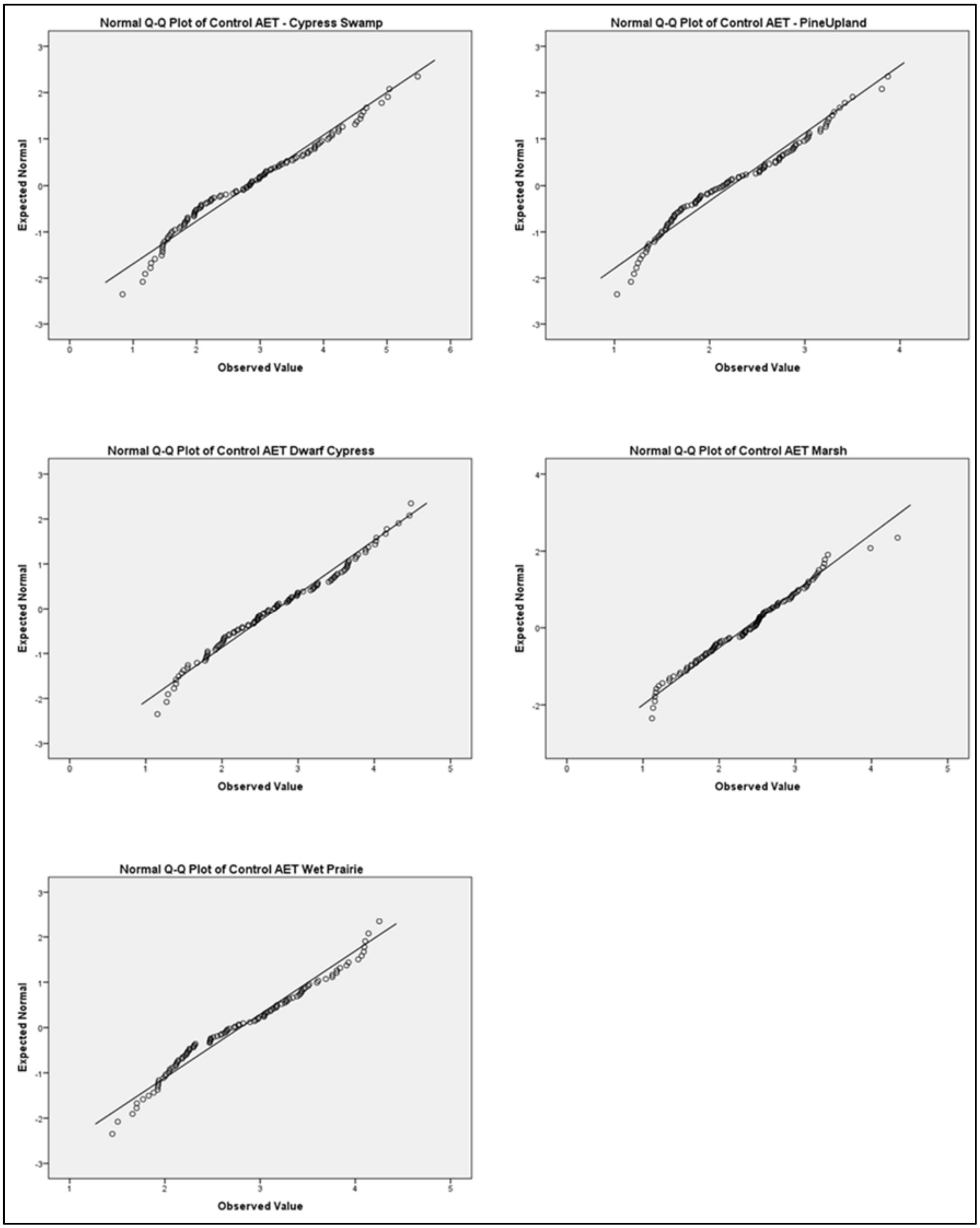

Figure C.3. Histograms – Full Model AET Data.

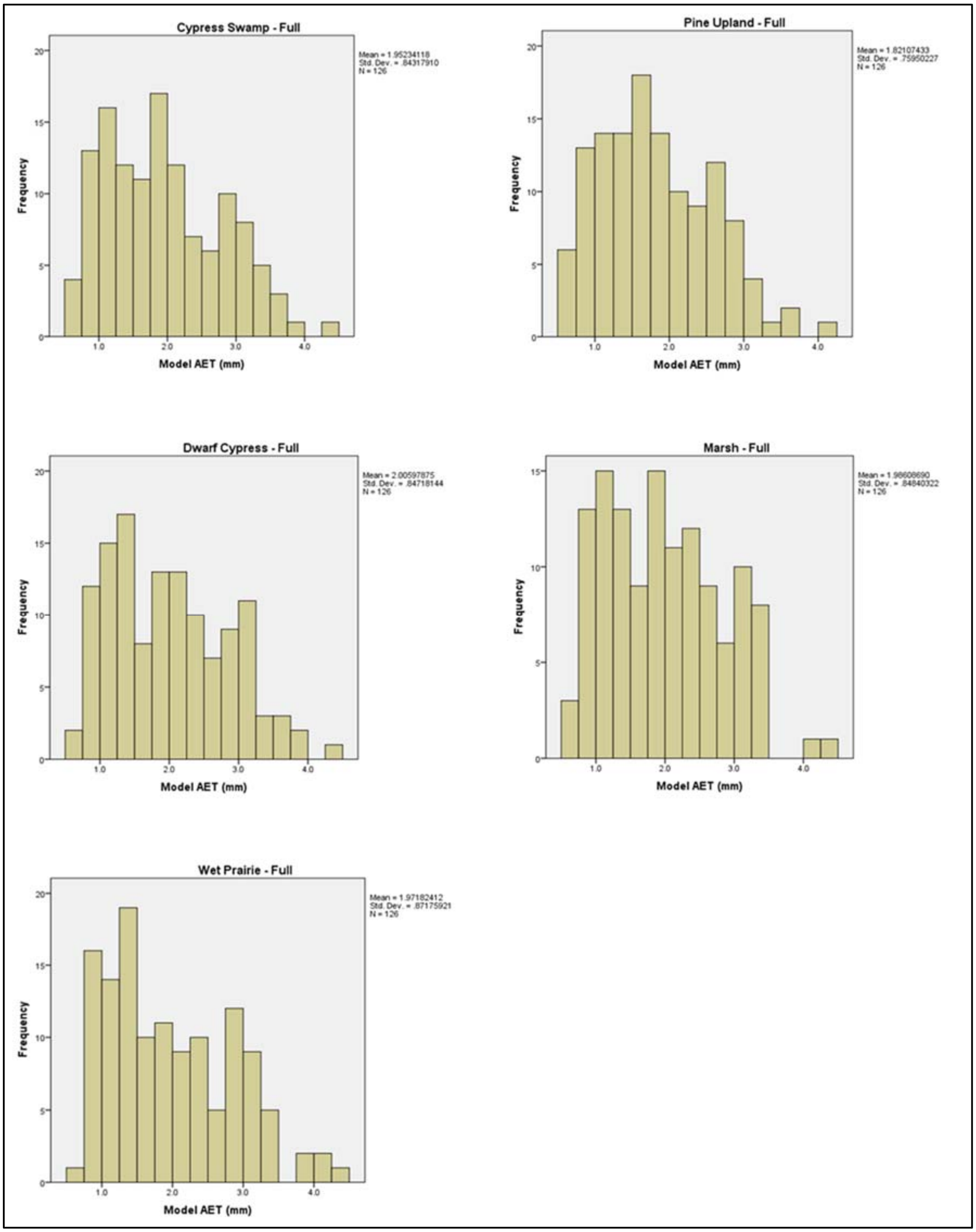

Figure C.4. Q-Q plots - Full Model AET Data.

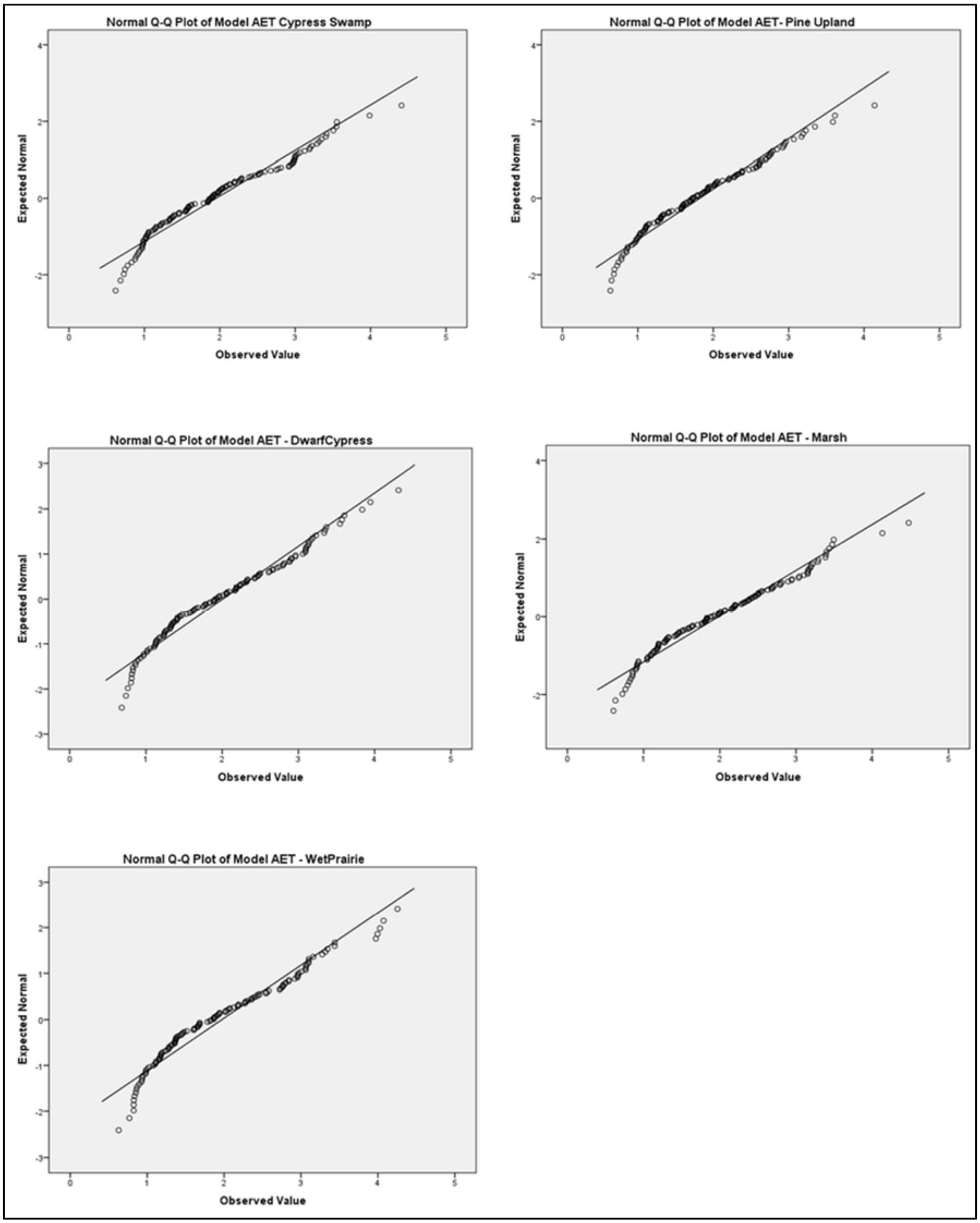

Figure C.5. Histograms – Full Model PET Data.

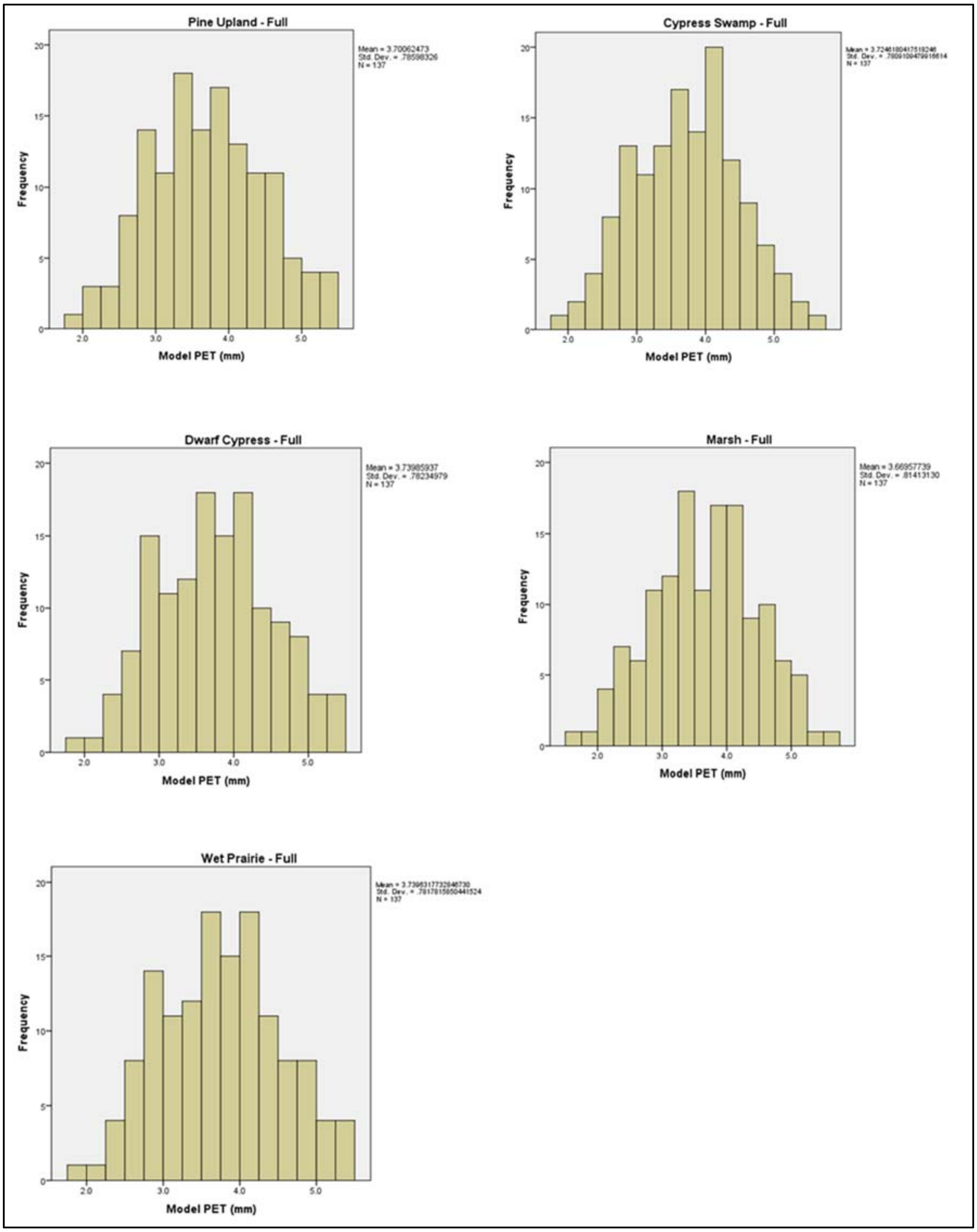

Figure C.6. Q-Q plots - Full Model PET Data.

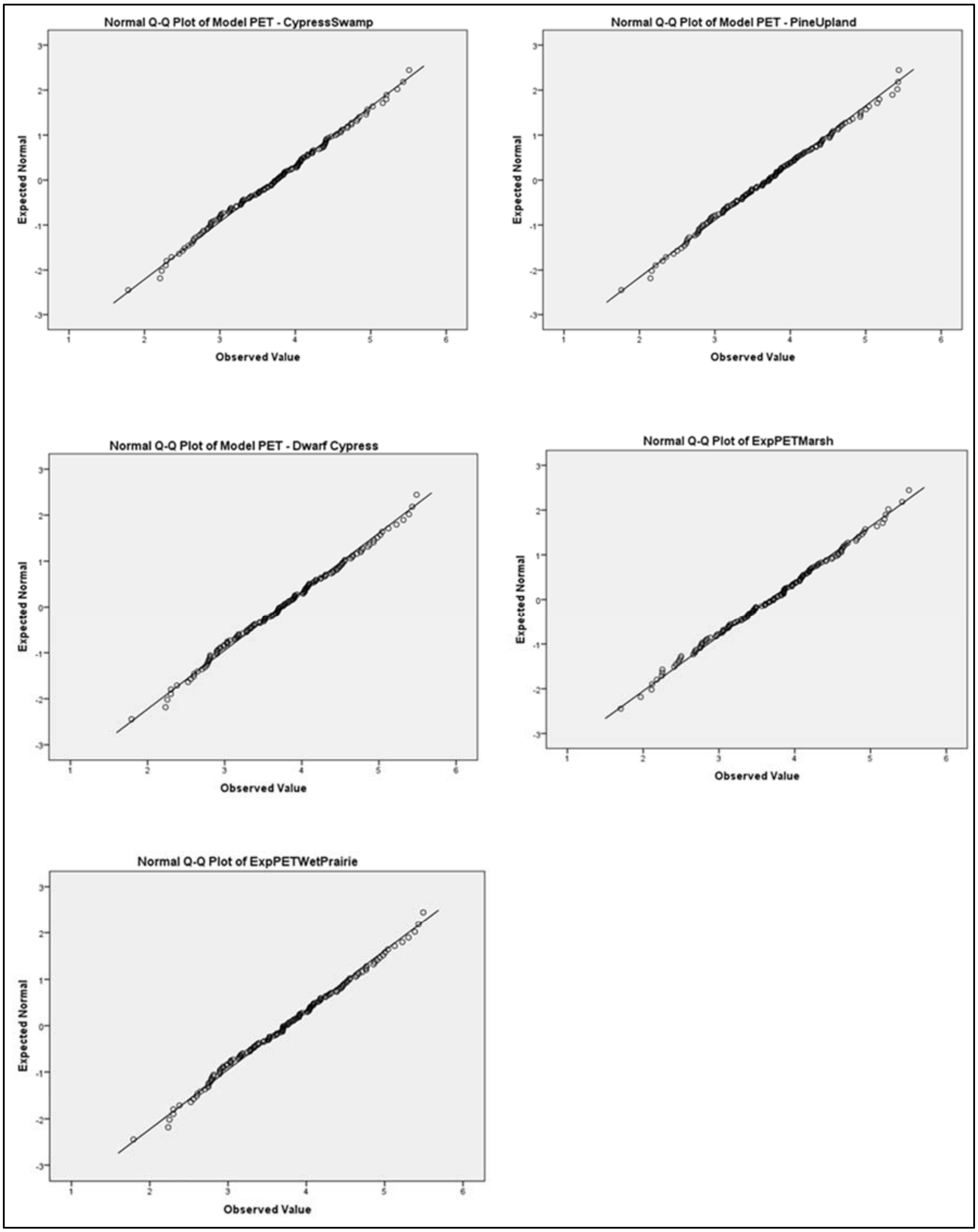

Figure C.7. Histograms – Dry Season Control AET Data.

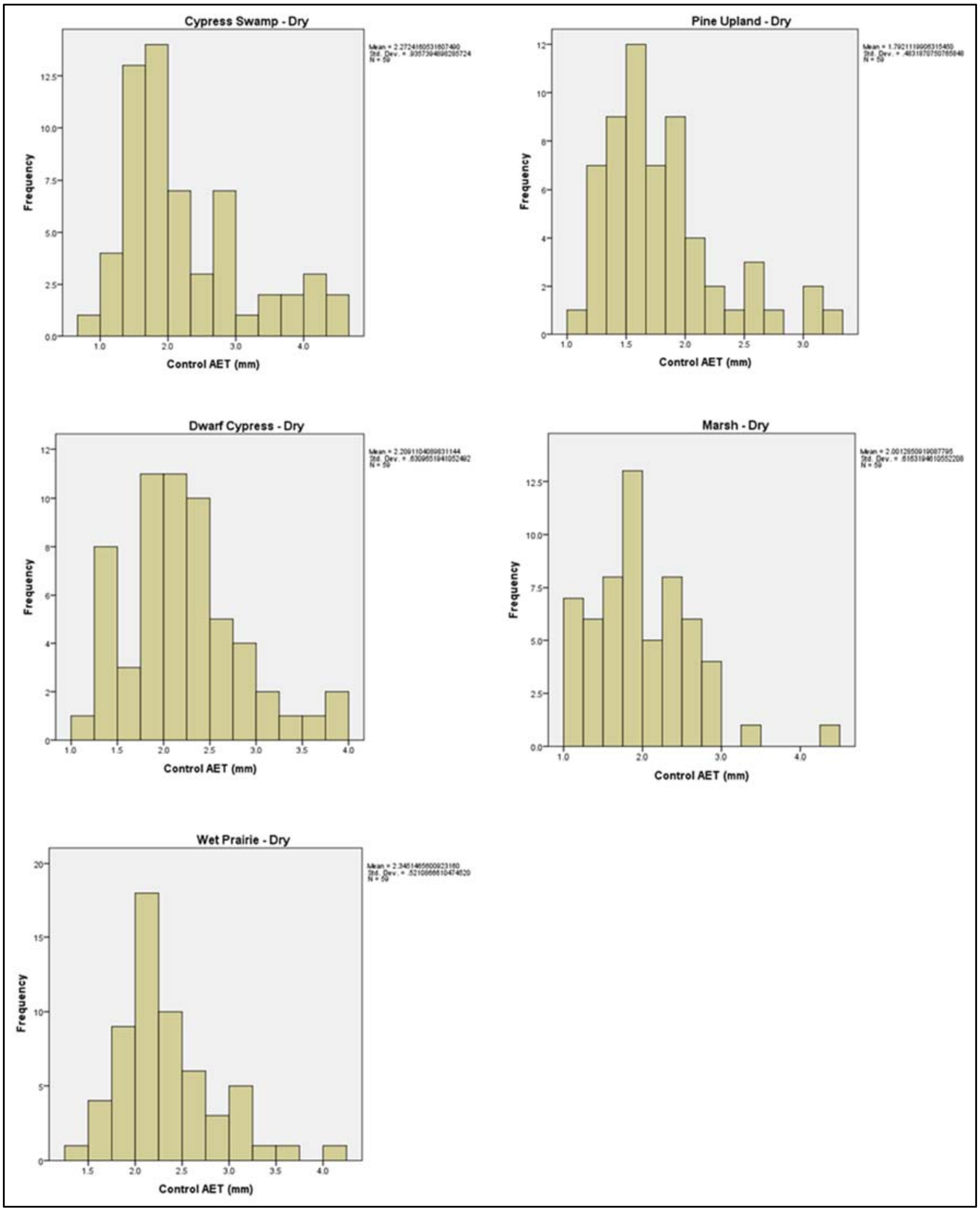

Figure C.8. Q-Q Plots – Dry Season Control AET Data.

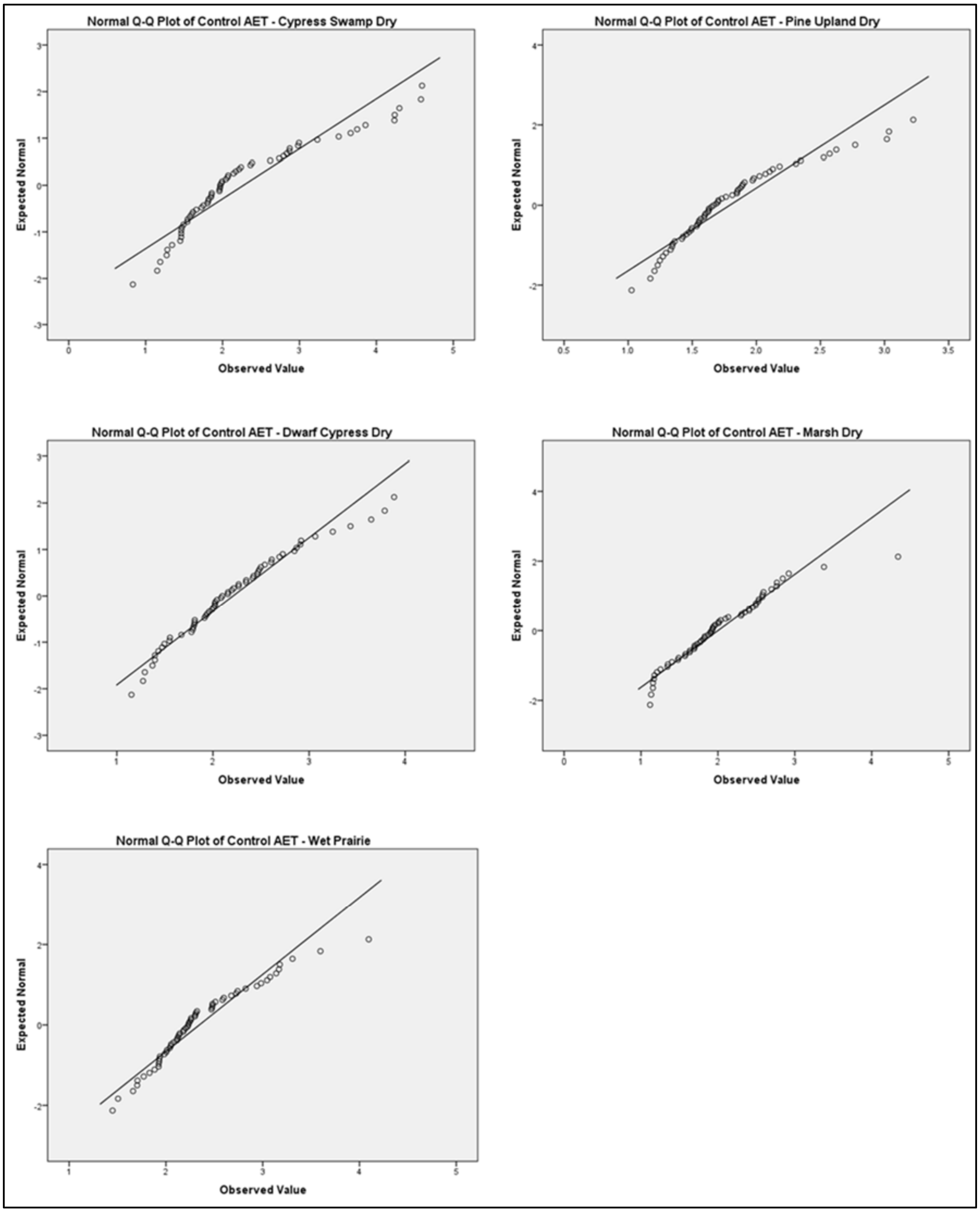

Figure C.9. Histograms – Dry Season Model AET Data.

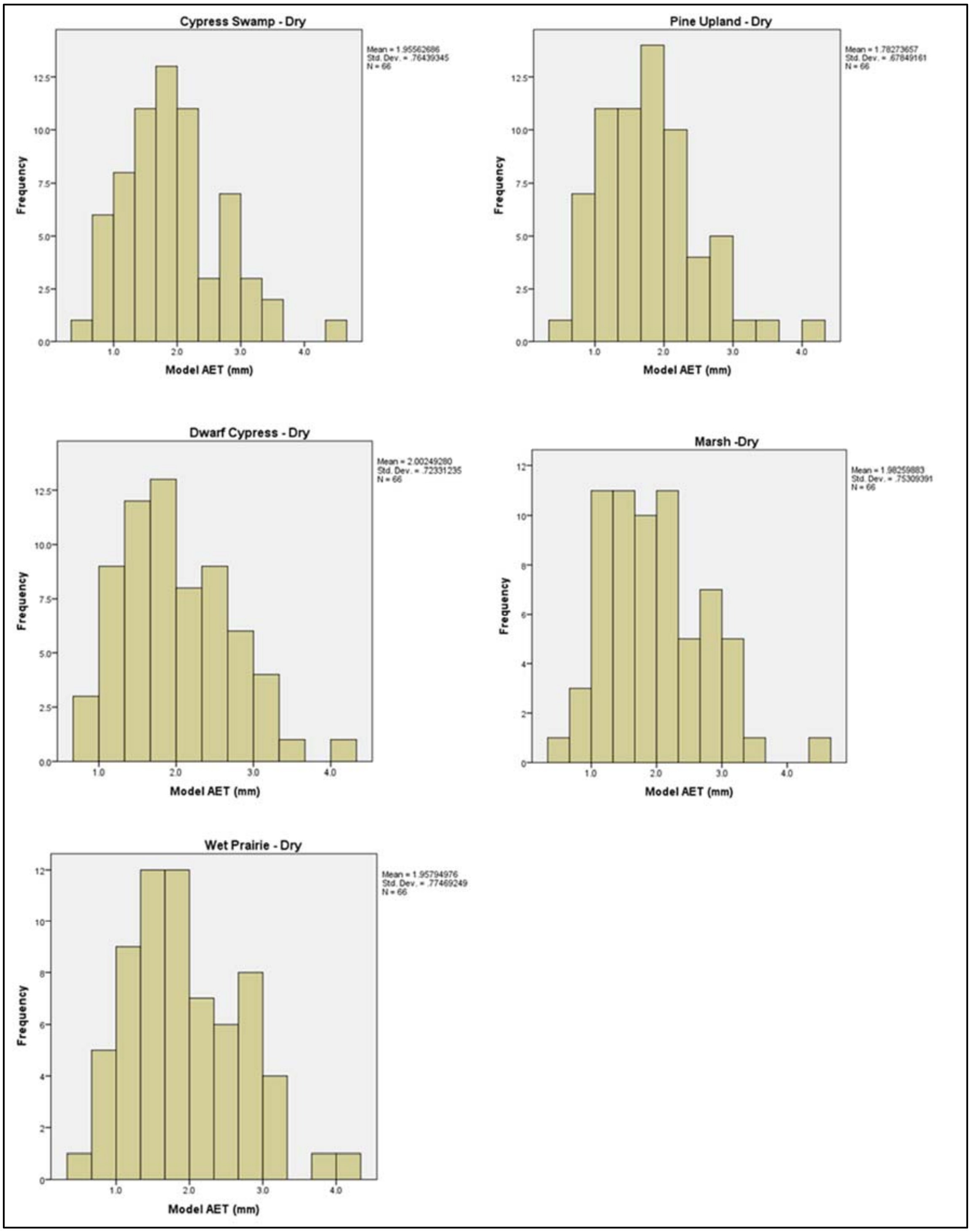

Figure C.10. Q-Q Plots – Dry Season Model AET Data.

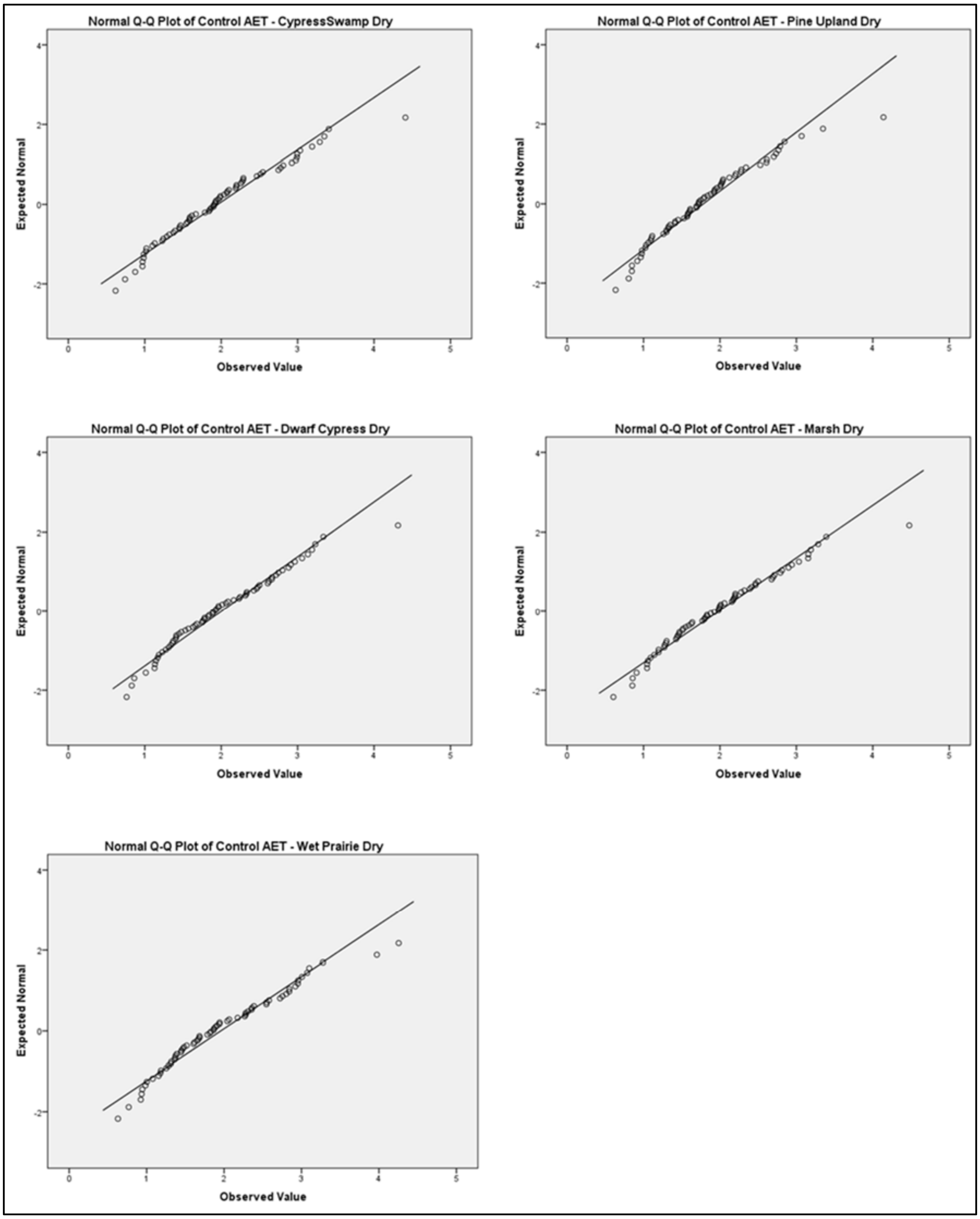

Figure C.11. Histograms – Dry Season Model PET Data.

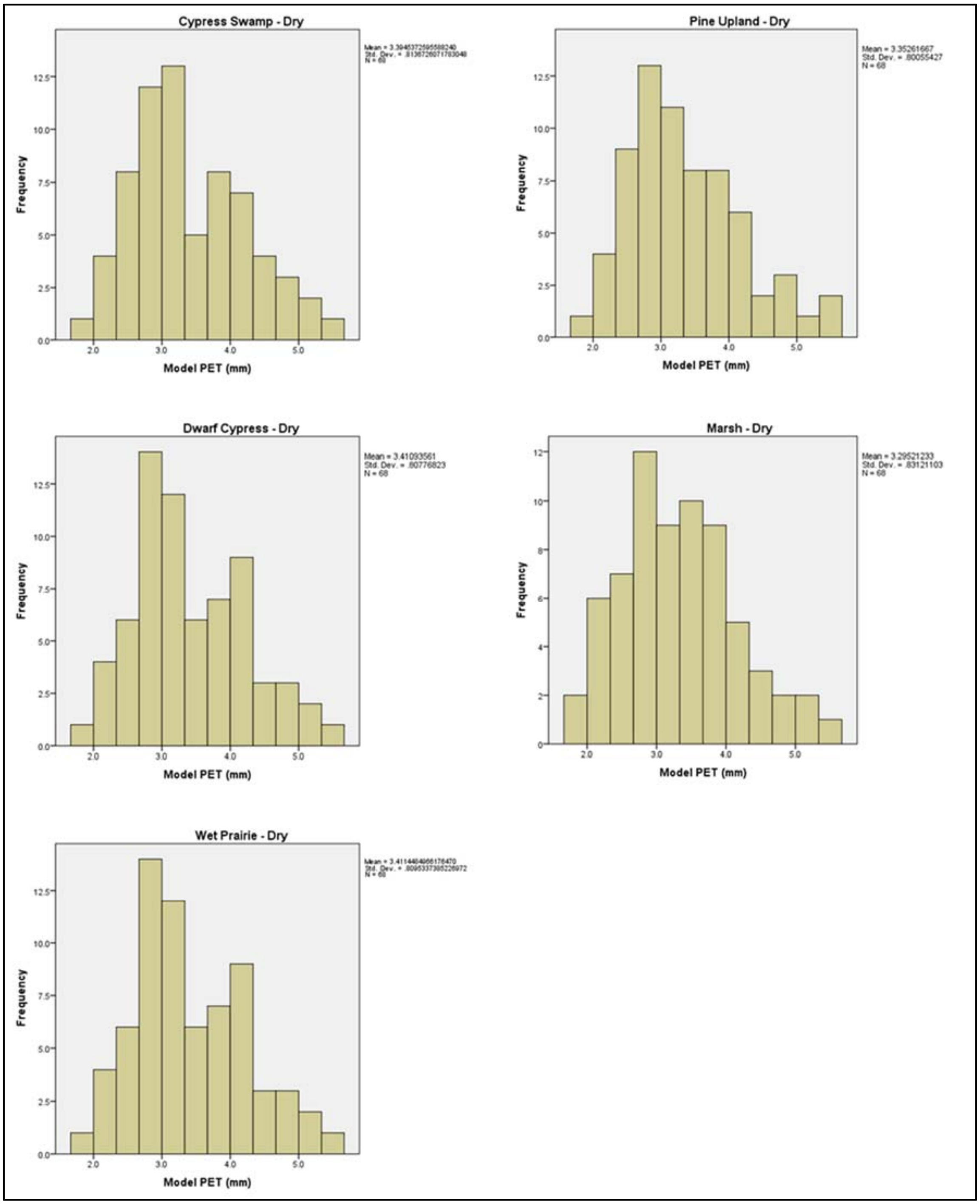

Figure C.12. Q-Q Plots – Dry Season Model PET Data.

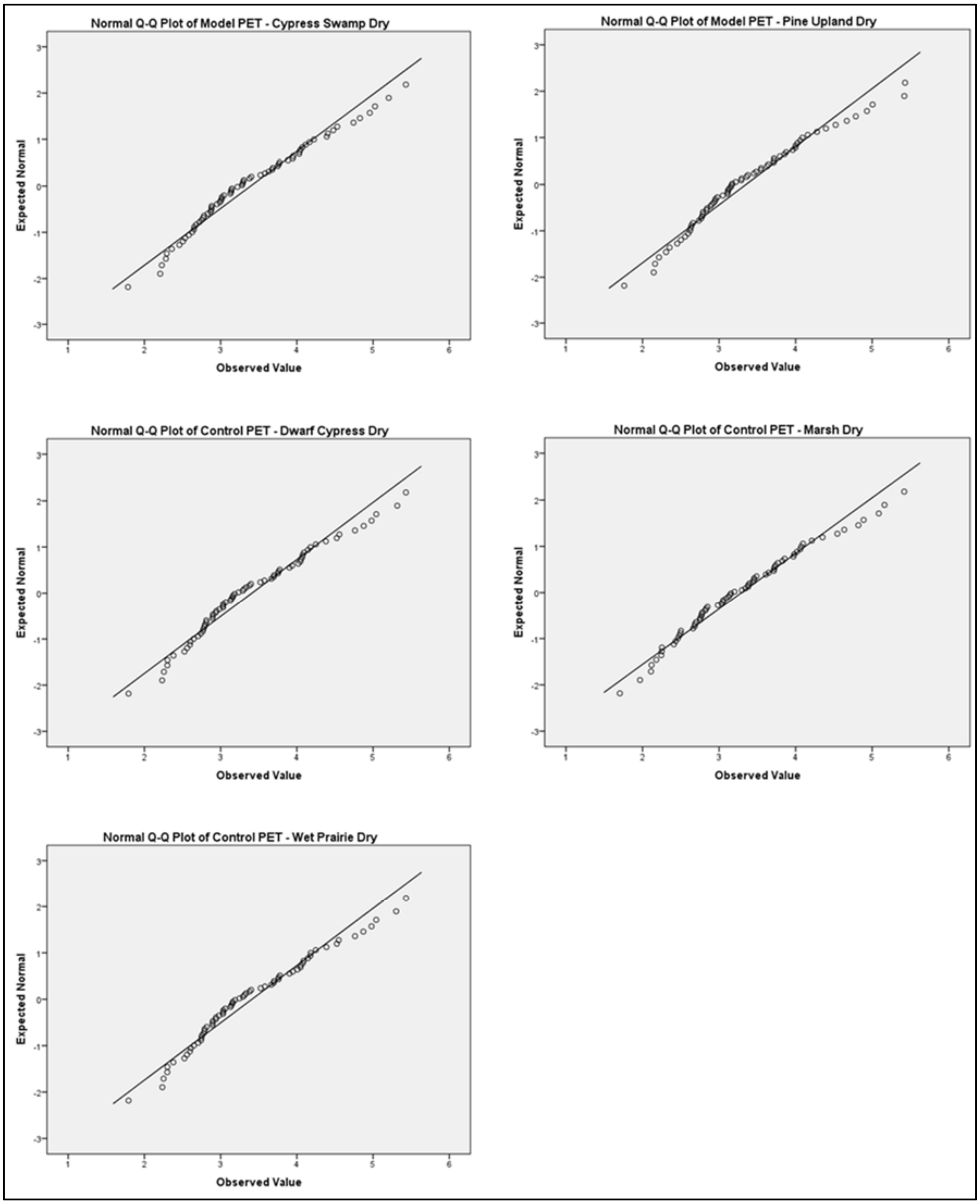

Figure C.13. Histograms – Wet Season Control AET Data.

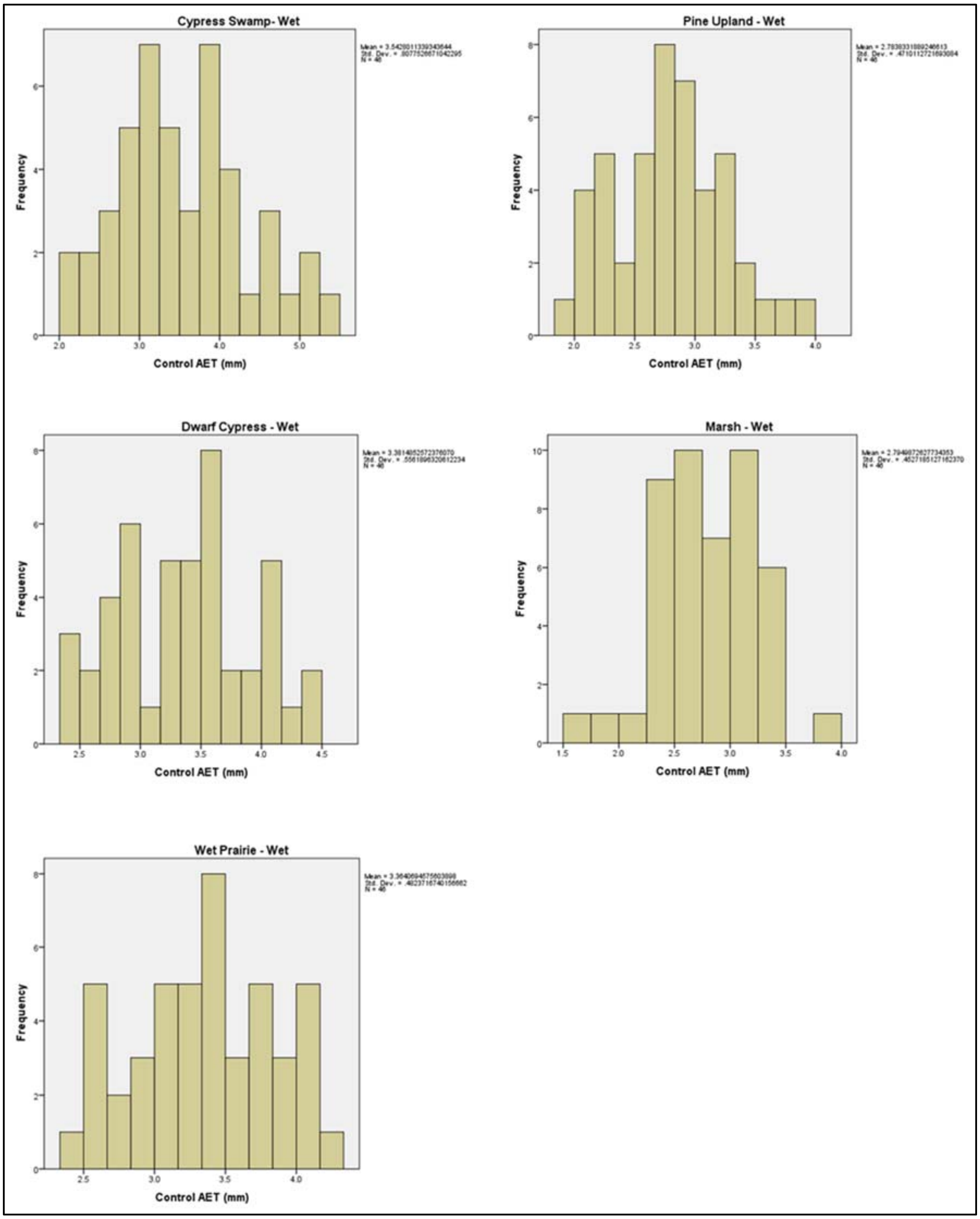

Figure C.14. Q-Q Plots – Wet Season Control AET Data.

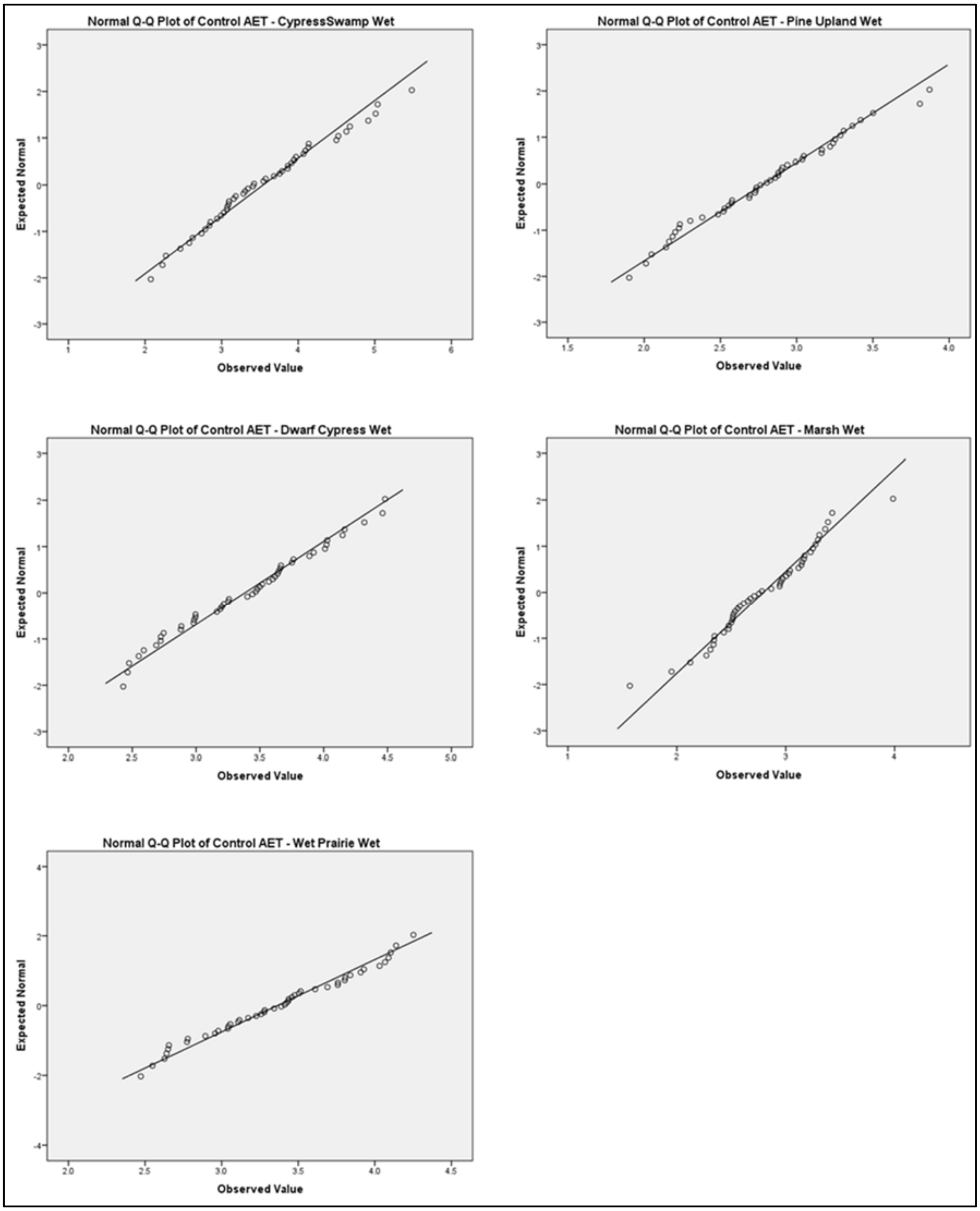

Figure C.15. Histograms – Wet Season Model AET Data.

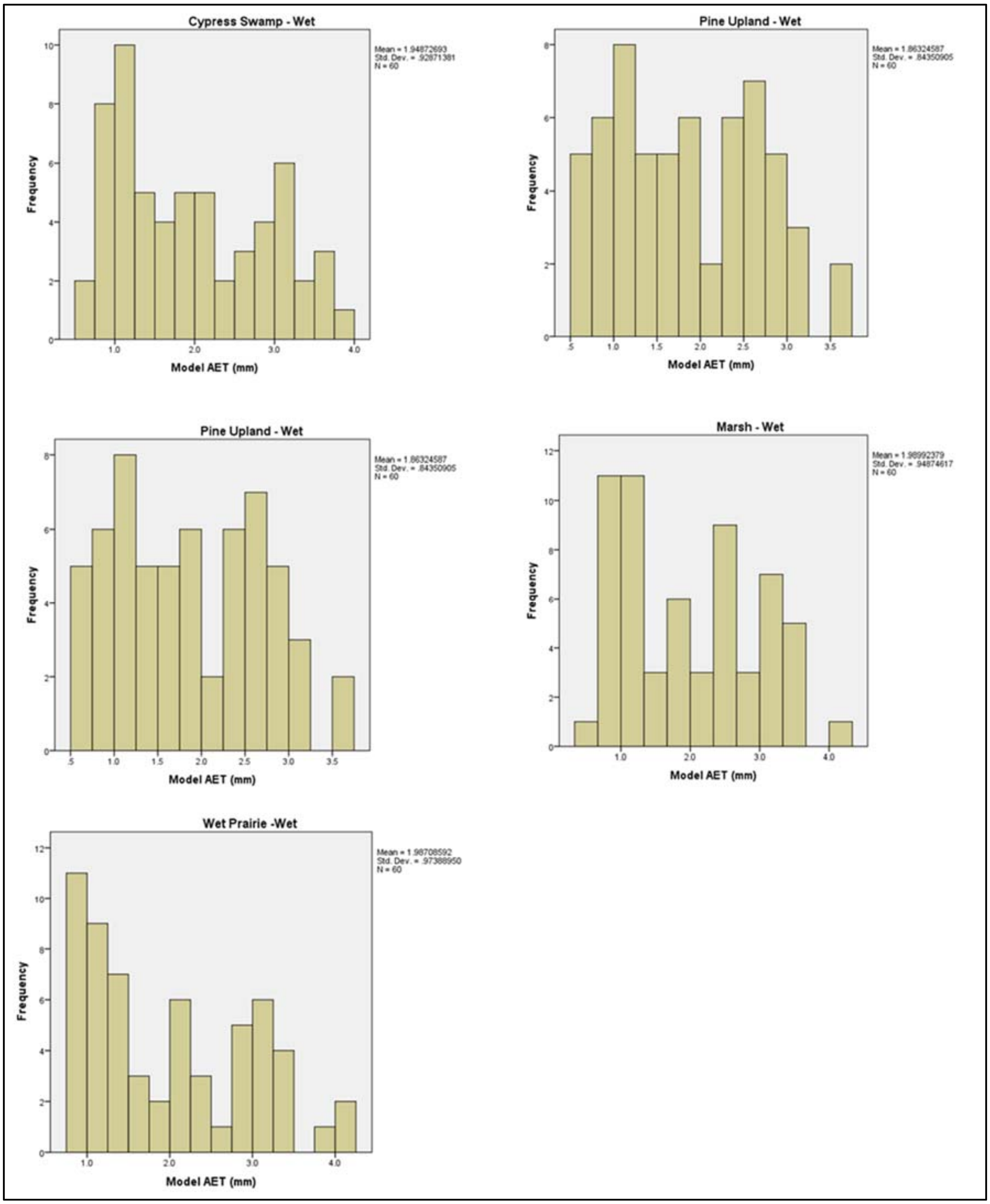

Figure C.16. Q-Q Plots – Wet Season Model AET Data.

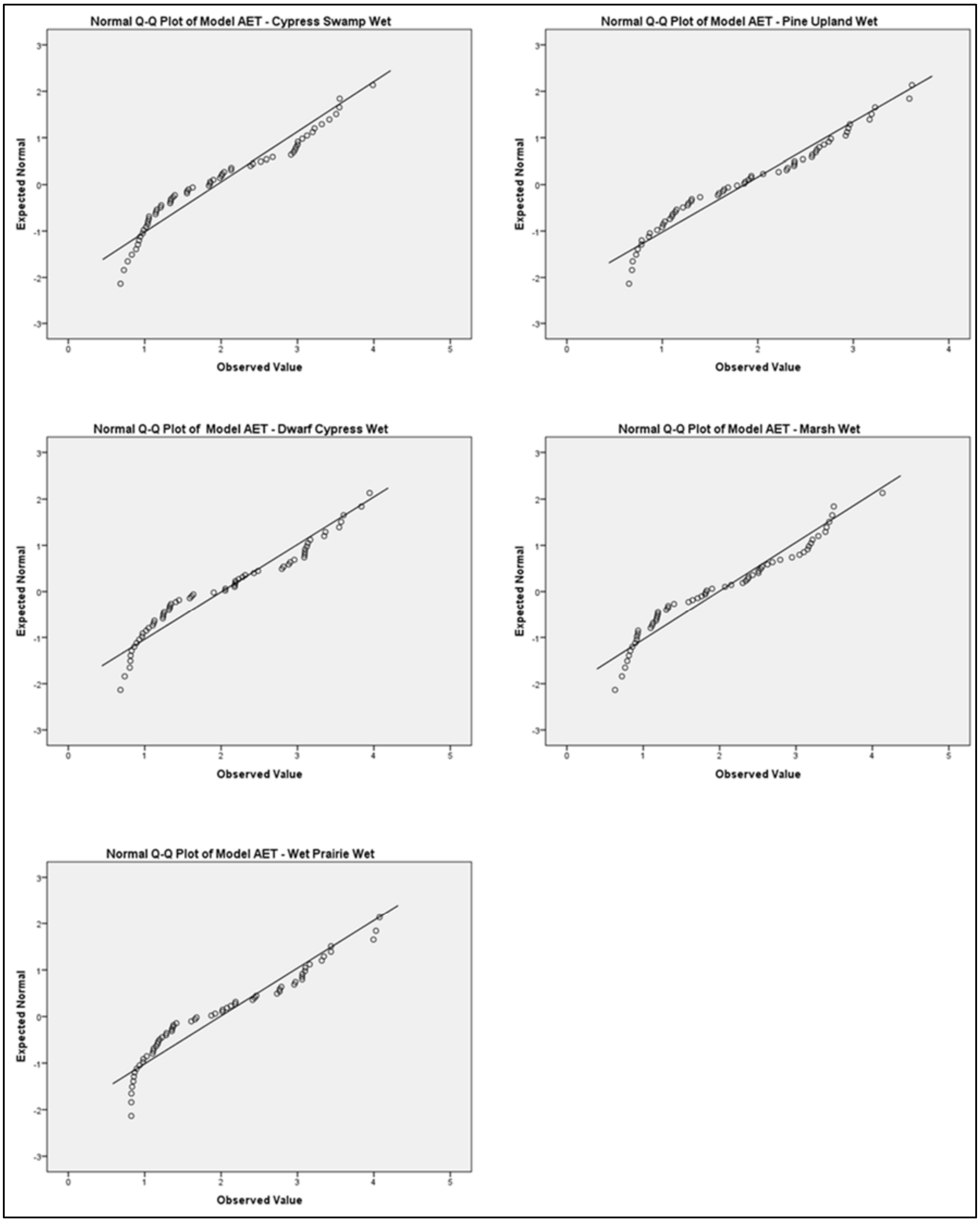

Figure C.17. Histograms – Wet Season Model PET Data.

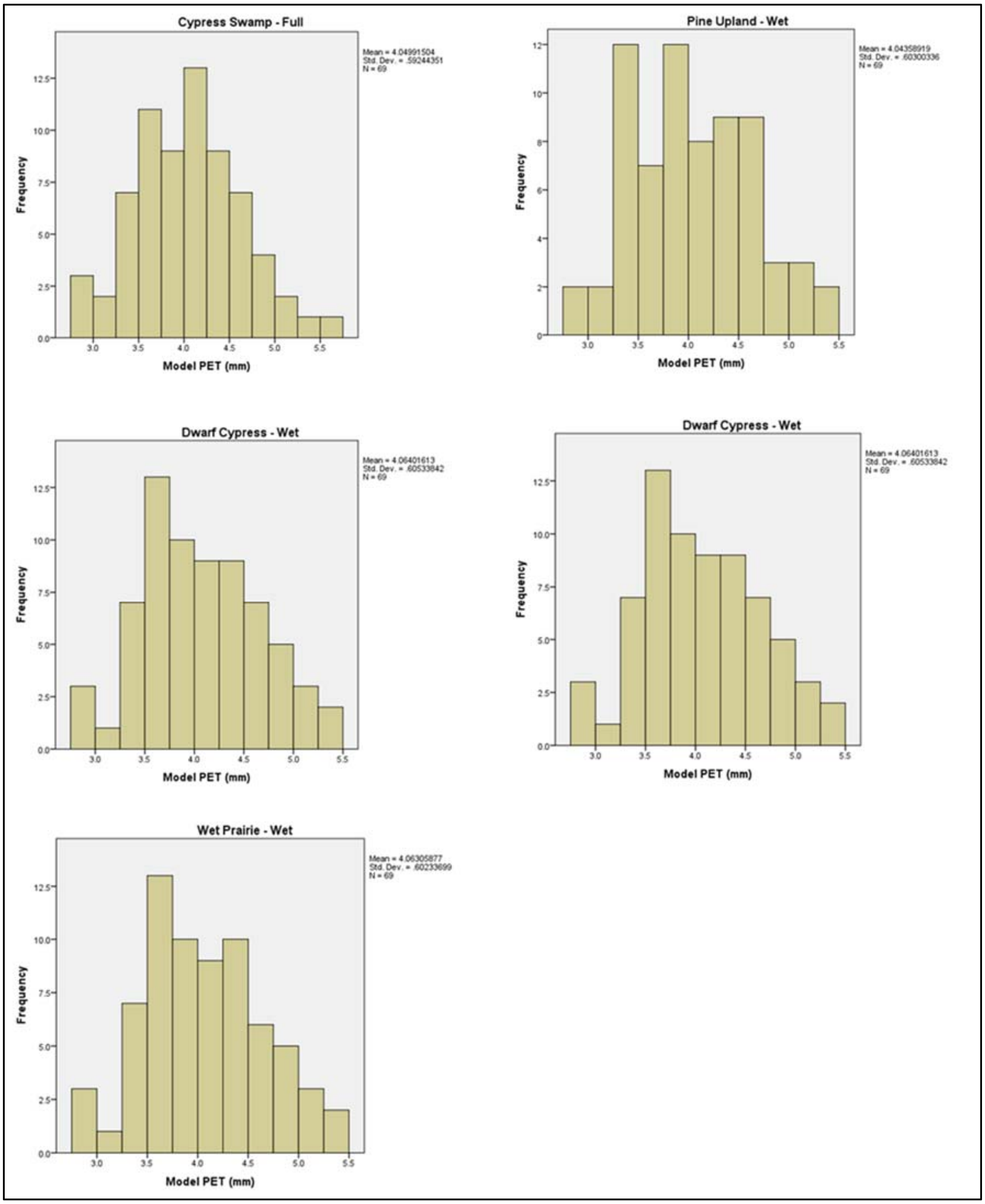

Figure C.18. Q-Q Plots – Wet Season Model PET Data.

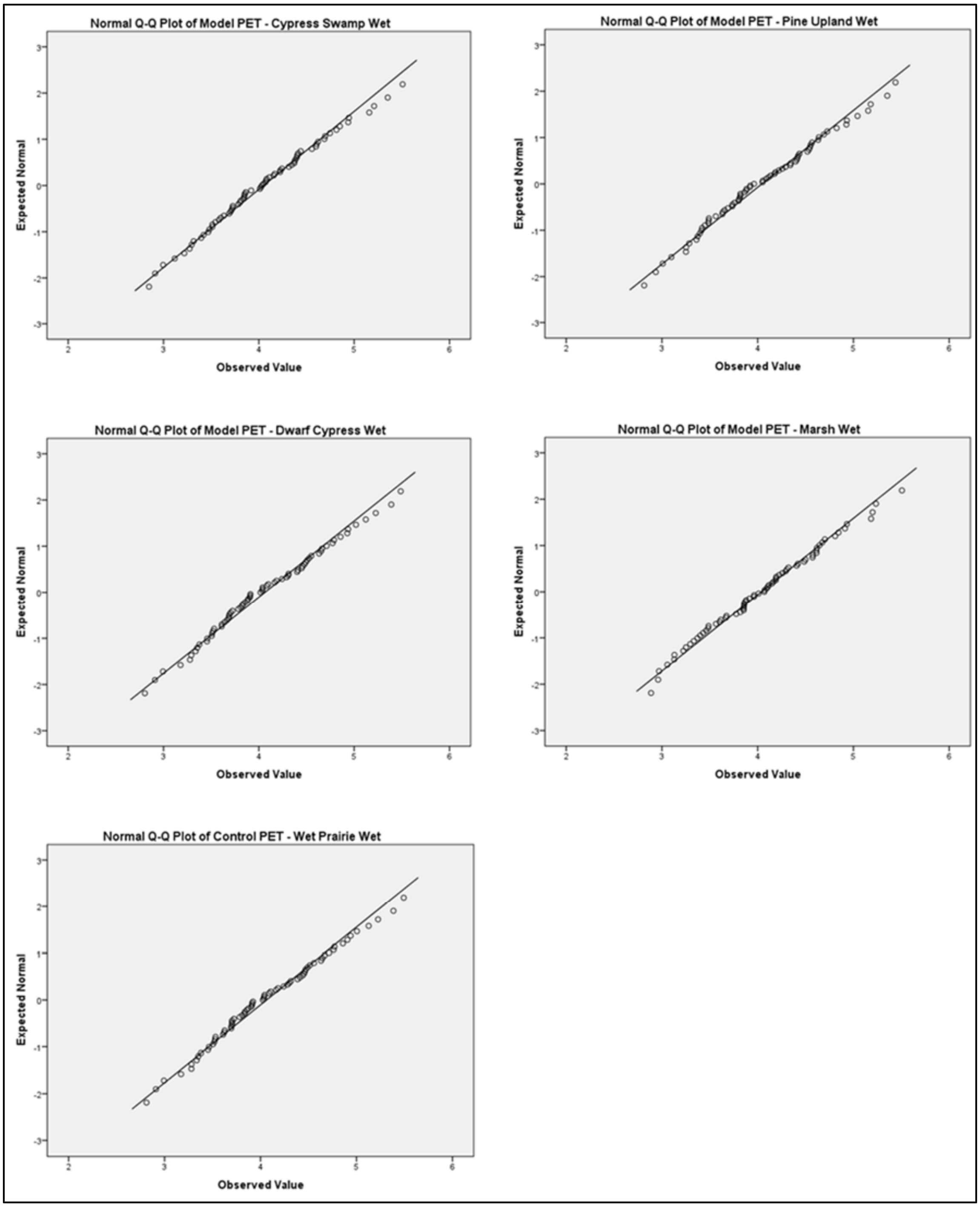

Figure C.19. Rank Tests between Control and Modeled AET – Full Dataset.

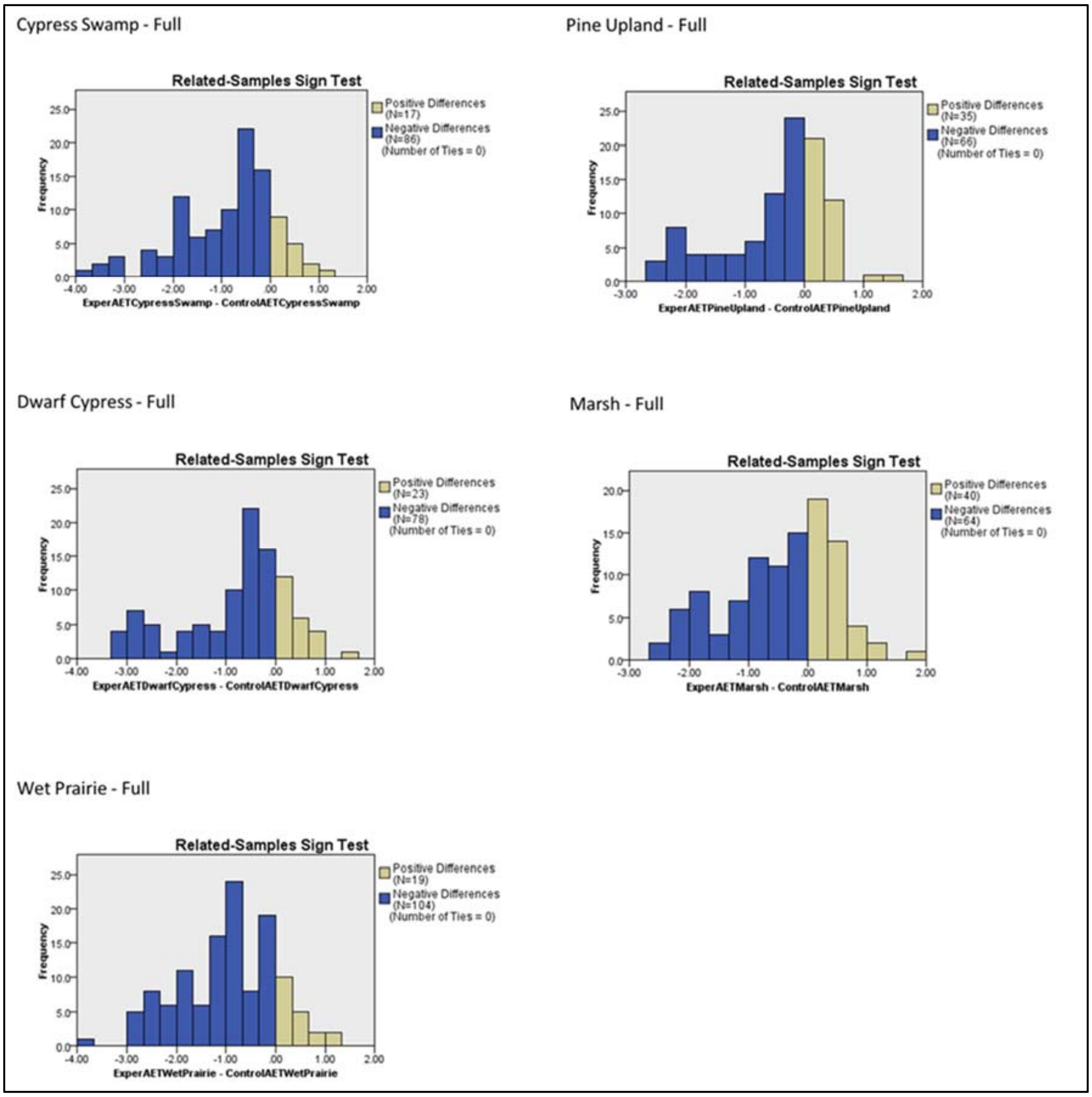

Figure C.20. Rank Tests between Control and Modeled AET – Dry Season Dataset.

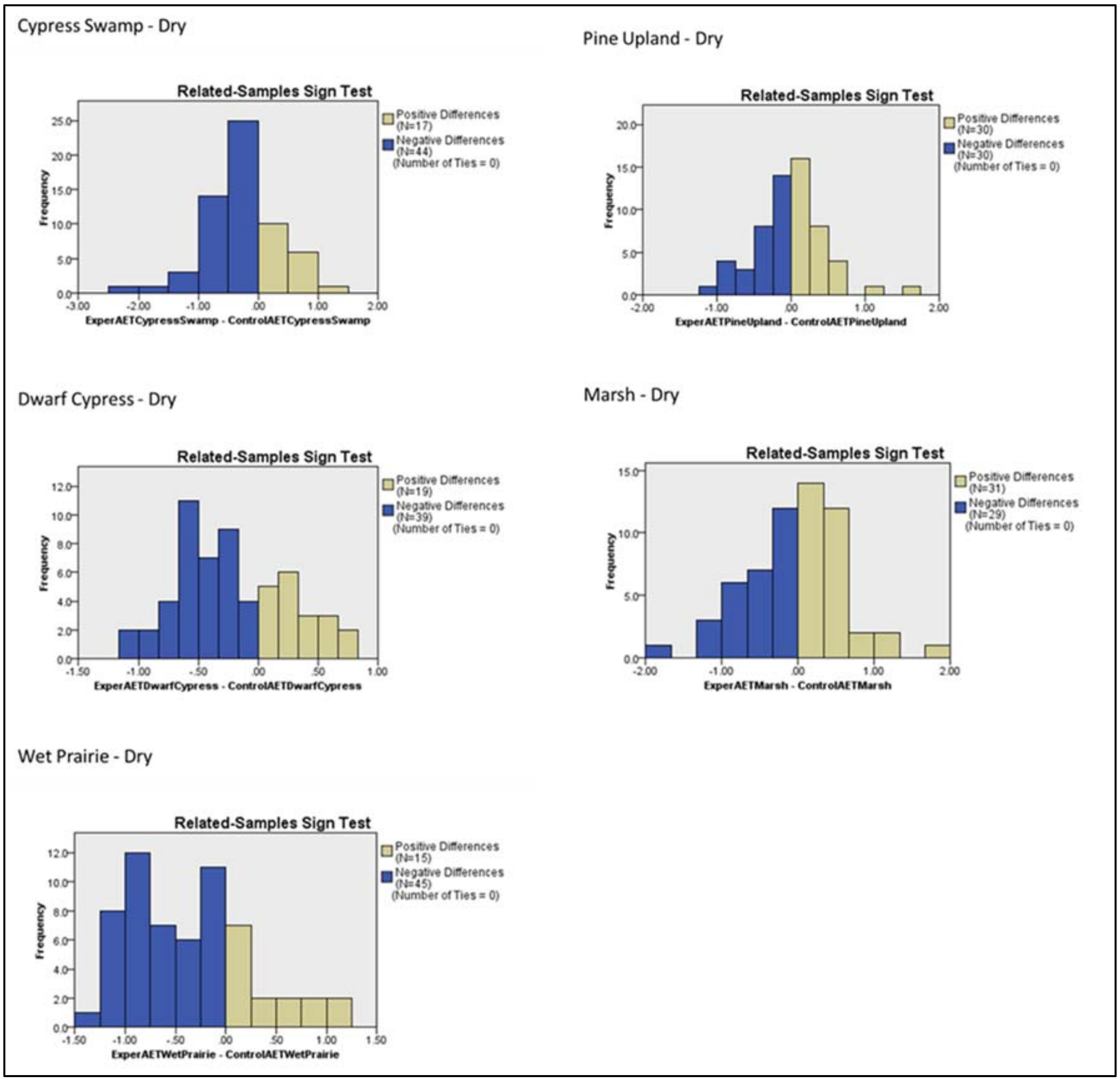

Figure C.21. Rank Tests between Control and Modeled AET – Wet Season Dataset.

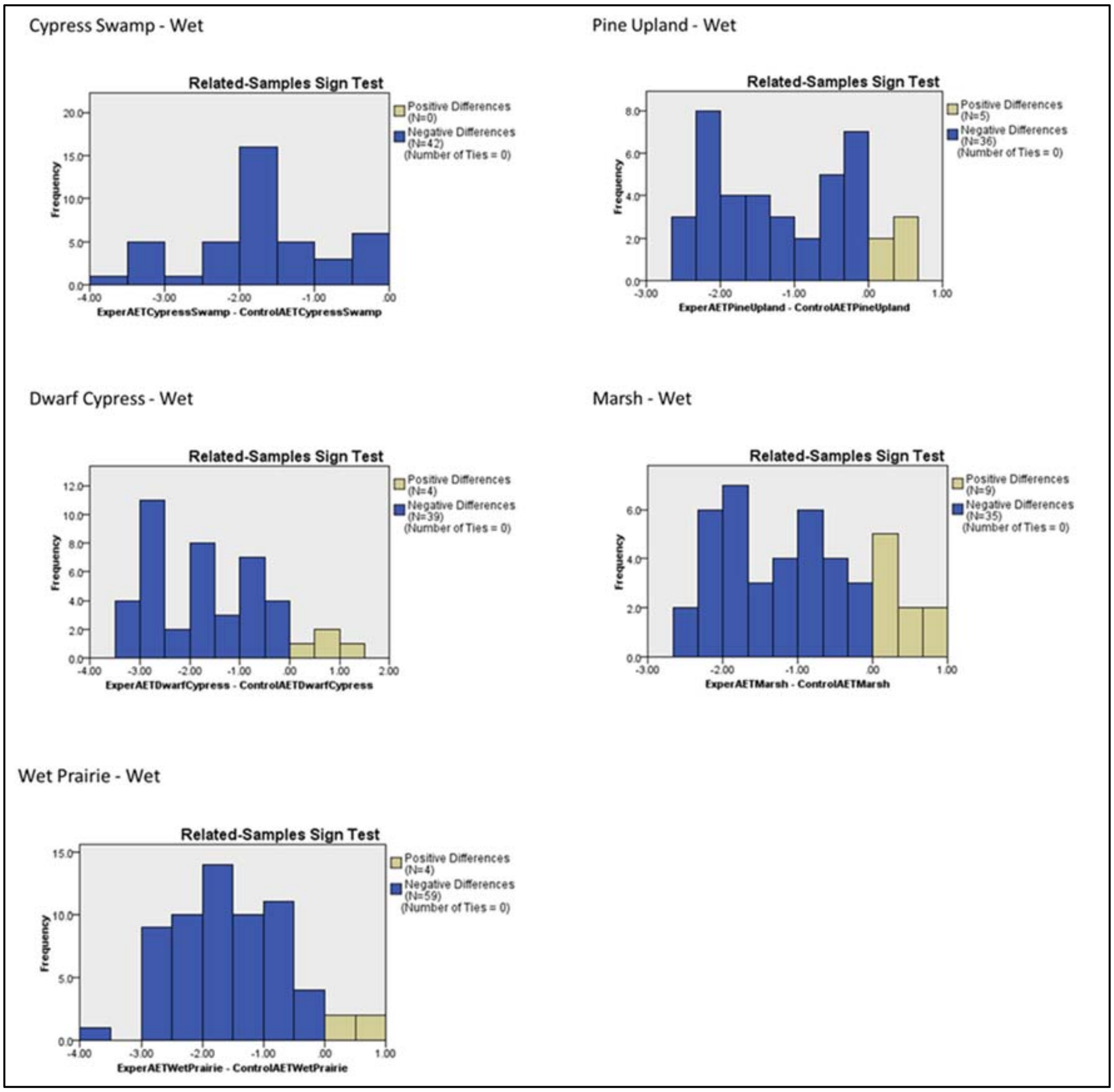

Figure C.22. Rank Tests between Control AET and Modeled PET – Wet Season Dataset.